SIRTUIN 2 IN THE CNS: EXPRESSION, FUNCTIONAL ROLES, ACTION MECHANISM AND MUTATION-INDUCED ALTERATION OF MOLECULAR/CELL BIOLOGICAL PROPERTIES

LI WENBO

(*B.Sc., Zhejiang University, Hangzhou, China*)

A THESIS SUBMITTED

FOR THE DEGREE OF DOCTOR OF PHILOSOPHY

DEPARTMENT OF ANATOMY

YONG LOO LIN SCHOOL OF MEDICINE

NATIONAL UNIVERSITY OF SINGAPORE

2008

ACKNOWLEDGEMENTS

I sincerely thank **Associate Professor Liang Fengyi**, Department of Anatomy, Yong Loo Lin School of Medicine, National University of Singapore (NUS), for his critical supervision and active support during my PhD study. His insights in grasping the best direction of projects, originality in analyzing the experimental data and dedication to scientific research impressed me and will surely benefit my future endeavors.

I am also grateful to my co-supervisor **Associate Professor Xiao Zhicheng** and **Dr. Hu Qidong**, Department of Clinical Research, Singapore General Hospital, for valuable discussions about my projects and kind support in providing cell culture materials and techniques.

My special appreciation is to **Professor Ling Eng Ang** for his insights into the significance of research projects and his encouragement from time to time.

My sincere acknowledgement and gratitude are also devoted to those colleagues in our research group that I have worked with and benefited from: Dr. Zhang Bin, Dr. Tang Junhong, Dr. Cao Qiong, Dr. Guo Anchen, Ms. Wu Chun, Ms. Guo Jing, Mr. Xia Wenhao, Mr. Meng Jun, Ms. Tang Jing, Dr. Tran Manh Hung, Ms. Luo Xuan and Ms. Pooneh Memar Ardestani.

I wish to thank Ms. Chan Yee Gek and Ms. Wu Ya Jun who provided perfect support in the confocal and electron microscopy studies. I am also grateful to Ms. Ng Geok Lan and Ms. Yong Eng Siang for their technical assistance; to Mdm Ang Lye Gek Carolyne, Mdm Teo Li Ching Violet and Mdm Diljit Kour d/o Bachan Singh for

their assistance.

I would like to express my gratitude to all the colleagues, students and staff members of Department of Anatomy, Yong Loo Lin School of Medicine for their generous help. In particular, I would like to thank Dr. Guo Chunhua for his accompaniment and sharing of research and life experiences; I am also grateful to Ms. Loh Wan Ting for her kind help in research work and providing experimental materials; furthermore, the thankfulness is given to Mr. Feng Luo, Mr. Guo Kun and Mr. Jiang Boran for instructions on facility using as well as help in my experiments.

I would like to thank NUS for granting me graduate student scholarship and president's graduate fellowship to support my life and study in Singapore. This work was supported by research grants from Singapore Biomedical Research Council (BMRC/01/1/21/19/179 04/1/21/19/305 and 06/1/21/19/460) and National Medical Research Council (0946/2005) (to A/P Liang FY).

Finally, I must always be grateful to my parents and sister, who are my support for study and life at all times, whose love and support accompanied me during the up-and-downs in my 23 years of life as a student. This thesis for PhD degree would be dedicated to them.

TABLE OF CONTENTS

Tables

Figures

LIST OF ABBREVIATIONS

Ab	antibody
ABC	avidin-biotin complex
AD	Alzheimer's disease
ALS	amyotrophic lateral sclerosis
AP	alkaline phosphate
BCIP	5-bromo-4-chloro-3´-indolylphosphate
bFGF	bovine fibroblast growth factor
bp	base pair
BSA	bovine serum albumin
CBD	corticobasal degeneration
cDNA	complementary DNA
CNP	2', 3'-cyclic nucleotide-3'-phosphodiesterase
CNS	central nervous system
CR	calorie restriction
cRNA	complementary RNA
DAB	3. 3'-diaminobenzidine tetrahydrochloride
DAPI	4',6-diamidino-2-phenylindole
DMEM	dulbecco's modified Eagle's medium
DMSO	dimethyl sulfoxide
DNA	deoxyribonucleic acid
DTT	dithiothreitol

EDTA	ethylenediaminetetraacetic acid
EGFP	enhanced green fluorescent protein
EM	electron microsopy
FBS	fetal bovine serum
FOXO	Forkhead box class O
FTDP-17	frontotemporal dementias with Parkinsonism linked to chromosome 17
GD3	Ganglioside GD3
GFAP	glial fibrillary acidic protein
HA	hemagglutinin
HAT	histone acetyltransferases
HD	Huntington's disease
HDAC	histone deacetylase
HEPES	4-(2-Hydroxyethyl) piperazine-1-ethanesulfonic acid
HIC1	hypermethylated in cancer 1
HMG	high-mobility-group family proteins
HMSN	inherited motor and sensory neuropathies
hNter	the 37-residue N terminus domain of hSIRT2
ICC	immunocytochemistry
IHC	immunohistochemistry
IPTG	isopropyl-1-thio-β-D-galactopyranoside
JN	juxtanodin

kDa	kilodalton
mAb	monocolonal antibody
MAG	myelin associated glycoprotein
MBP	myelin basic protein
MOG	myelin-oligodendrocyte glycoprotein
MS	multiple sclerosis
MW	molecular weight
mRNA	messager RNA
NAD	nicotinamide
NAM	nicotinamide adenine dinucleotide
NBT	nitro-blue tetrazolium
NDAC	NAD-dependent deacetylase
NF	neurofilament
NP-40	nonidet P-40
NGS	normal goat serum
OLP	primary cultured oligodendrocyte precursor cells
ORF	open reading frame
pAb	polyclonal antibody
PBS	phosphate buffered saline
PCR	polymerase chain reaction
PD	Parkinson’s disease
PDGF	platelet-derived growth factor

PDL	poly-D-lysine
PLP	proteolipid protein
PML4	promyelocytic leukemia protein 4
PSP	progressive supranuclear palsy
PVDF	polyvinylidene diluoride
RNA	ribonucleic acid
RPD	potassium dependency protein
RT	room temperature
SDS-PAGE	sodium dodecyl sulphate polyacrylamide gel electrophoresis
SNP	single nucleotide polymorphisms
siRNA	small interference RNA
SIR2	Silent information regulator-2
T3	triiodothyronine
T4	thyroxine
TBS	tris buffered saline
TEMED	N,N,N'N'-tetramethylethylene diamine
Tris	2-amino-2-(hydroxymethyl)-1,3-propanediol
TSA	Trichostatin A
WB	Western blotting
X-gal	5-Bromo-4-chloro-3-indoyl-β-D-galactopyranoside

LIST OF PUBLICATIONS

Articles

1. **Li W**, Zhang B, Tang J, Cao Q, Wu Y, Wu C, Guo J, Ling EA, Liang F. Sirtuin 2, a mammalian homolog of yeast silent information regulator-2 longevity regulator, is an oligodendroglial protein that decelerates cell differentiation through deacetylating alpha-tubulin. ***The Journal of Neuroscience.*** 2007, 7th March; 27(10):2606-16
2. Liang F, Zhang B, Tang J, Guo J, **Li W**, Ling EA, Chu H, Wu Y, Chan YG, Cao Q. RIM3gamma is a postsynaptic protein in the rat central nervous system. ***Journal of Comparative Neurology.*** 2007, 1st August; 503(4):501-10
3. **Li W**, Tang J, Ling EA, Zhang B, Liang F. Solubility loss-dependent cytoplasmic aggregation of SIRT2 mutants/variants, and the protective effect of human SIRT2 N-terminus. (Submitted)

Abstracts for conferences

1. **Li W**, Liang F. Specific Sirtuin-2 mutations trigger aggregate formation and reduce solubility of the protein when overexpressed in cultured cells. Proceedings of the SFN 37th Annual Meeting, 3-7th November, 2007, San Diego, California, USA
2. Liang F, Tang J, **Li W**. Developmental expression of Sirtuin-2 in the rat CNS. Proceedings of the SFN 37th Annual Meeting. 3-7th November, 2007, San Diego, California, USA

3. **Li W**, Liang F. Overexpression of specifically mutated forms of SIRT2 triggers aggregates formation. Annual Meeting for Singapore Microscopy Society. 20th April 2007, Singapore

4. Liang F, Zhang B, Tang J, Guo A, **Li W**, Cao Q. Developmental expression of juxtanodin in the rat CNS. Proceedings of the SFN 35th Annual Meeting. 12-16th November, 2005, Washington, D.C., USA

Oligodendrocytes, the myelin-forming cells in the Central Nervous System (CNS) of vertebrates, mature through a highly regulated but precisely timed differentiation process. The mechanisms underlying this differentiation process are under extensive investigations in the past decades.

Silent information regulator-2 (SIR2) proteins regulate lifespan of diverse organisms. In mammals, SIR2 are represented by seven members SIRT1-7, which are also collectively called Sirtuins. In the nervous system, though implicated to be important by many evidences, Sirtuins are still largely mysterious in their expression patterns, functional roles and action mechanisms. In addition, polymorphisms or mutations of Sirtuins are well documented, but the significance of these variations for health and diseases of the host cell or organism is essentially unknown.

The current study, on the first hand, shows that Sirtuin 2 (SIRT2) is an oligodendroglial cytoplasmic protein enriched in the outer and juxtanodal terminal loops in the myelin sheath. Among cytoplasmic proteins of OLN-93 oligodendrocytes, α-tubulin was the main substrate of SIRT2 deacetylation. In cultured primary oligodendrocyte precursors (OLPs), SIRT2 emergence accompanied elevated α-tubulin acetylation and OLP differentiation into the pre-maturity stage. siRNA knockdown of SIRT2 increased OLPs' α-tubulin acetylation, myelin basic protein (MBP) expression and cell arbor complexity. SIRT2 overexpression had opposite effects, and counteracted the cell arborization-promoting effects of overexpressed juxtanodin (JN). Specific SIRT2 mutations concomitantly reduced its deacetylase activity and inhibition on OLP arborization.

On the other hand, our study showed that overexpression of specific rSIRT2 mutants induced formation of prominent cytoplasmic aggregates containing both the mutated rSIRT2 and native cellular proteins including 2', 3'-cyclic nucleotide-3'-phosphodiesterase (CNP) and ubiquitin. But deacetylase activity loss could not account for the aggregate formation because siRNA knockdown of endogenous rSIRT2 did not replicate similar phenomenon, nor did overexpression of some enzymatically defective rSIRT2 mutants. By contrast, the current study identified solubility decrease as a direct result of SIRT2 mutations, which are inversely correlated to the aggregate formation propensities of rSIRT2 mutant proteins. Stabilization of the microtubule network or knockdown of innate histone deacetylase 6 (in 293T cells) reduced the number of aggregate-positive cells caused by rSIRT2 mutants. Furthermore, the results showed that a unique 37-residue N terminus domain of hSIRT2 (hNter) endowed mutated hSIRT2 or rSIRT2 a protection from solubility loss and aggregation; this domain also inhibits the solubility decreases after mutation.

These results firstly demonstrated a counterbalancing role of SIRT2 against a facilitatory effect of tubulin acetylation on oligodendroglial differentiation. Secondly, these results suggested contribution of solubility decrease to aggregate formation or cytotoxicity of specific SIRT2 mutants. Also, the 37aa hNter domain may be a crucial evolutionary improvement from rat to human, enhancing normal protein solubility and function. It calls for further investigations to test the role of SIRT2 in myelinogenesis, oligodendroglial differentiation and myelin-axon interaction. Future studies will also be necessary and important to understand Sirtuins' polymorphisms and mutations in

the context of brain aging, neurodegenerative diseases and dys- or demyelination as well as the exact role of hNter domain in relation to evolution.

CHAPTER 1
INTRODUCTION

1. Oligodendrocytes in the central nervous system

1.1 Cell types in the nervous system

The nervous system can be divided into Central Nervous System (CNS) or Peripheral Nervous System (PNS) based on their distinctiveness in anatomical distribution and function. Both at the cellular level consist of nerve cells (neurons) and glial cells (glia). Neurons are the main signaling units of the nervous system, and typically defined by four morphologically distinct regions: the nerve cell body, the axons, the dendrites and presynaptic terminals. Each of these four regions bears distinctly different functions in the generation and maintenance of information communication in the nervous system. Among these four regions, axons are specialized branches extending from neurons, which are long and tubular processes acting like antennas to convey signals to target cells. When neurons need to transmit signals, electrical signals have to be generated and propagated through axons. These electrical signals called action potentials are usually rapid, transient, all-or-none nerve pulse.

The other main class of cells in nervous system is glia. Firstly described by Virchow in 1846, gial cells were classically thought to be the connective tissue of brain at that time. They represent a large majority of cells in nervous system and greatly outnumber neurons by 10 to 50 times in vertebrate CNS. In addition to traditional supportive roles, findings in recent years have demonstrated the active participation of gila in the physiology of the brain and the adverse consequences of their dysfunction (Baumann and Pham-Dinh, 2001). There are four main glial cell

types in the nervous system: astrocytes, microglia, oligodendrocytes and Schwann cells. As the most numerous glial cells, astrocytes are largely supportive cells in the nervous system that are star-shaped and bear long processes. These cells may play roles in nourishing neurons, and some astrocytes can employ the endothelial cells of blood vessel to form tight junctions, creating the protective blood brain barrier in between blood and brain. Meanwhile, astrocytes can help to maintain or regulate concentrations of some ions or transmitters to protect neurons and guarantee normal neuronal functions (Kandel et al., 2001). Microglias are phagocytic cells residing in the nervous system, which can be activated after injury, infection or disease. Though these cells function in nervous system, it is still debated as whether microglias are physiologically and embryologically related to the other cell types of the nervous system because they arise from macrophages outside. Upon activation, microglia will extend processes stouter and more branched and may serve as antigen presenting cells in the nervous system. They are proposed to be activated in a series of diseases ranging from multiple sclerosis (MS) to Parkinson's disease (PD) and Alzheimer's disease (AD) (Kandel et al., 2001).

Oligodendrocytes and Schwann cells are two types of insulating cells, which function in different parts of nervous system. Oligodendrocytes exist in CNS whereas Schwann cells occur in PNS. Both of them work to wrap around axons in a spiral with their extended and specialized membranous processes. These processes around axons are called myelin sheath and this insulation process was named myelination (Kandel et al., 2001). By myelination, nerve impulses generated in excited neurons propagate

more rapidly along the shaft of myelinated axons.

1.2 Oligodendrocytes

Oligodendrocytes are specialized cells to fulfill the myelination function in the CNS. The term oligodendrocytes, or its interchangeable synonym oligodendroglia that was named by Rio Hortega (Hortega, 1921), are initially used to describe cells in the CNS that show few processes in material stained by metallic impregnation techniques. Oligodendrocytes are generated from multipotent neuroepithelial cells (Chandran et al., 1998), and their specialized myelin-forming function was endowed by a precisely regulated differentiation process. Along lineage progression, the sequential and timed expression of developmental regulators as well as gradual morphological differentiation divides the whole lineage into several distinct genotypic and phenotypic stages (Baumann and Pham-Dinh, 2001).

1.2.1 Differentiation of oligodendrocytes

The end-point of oligodendrocyte differentiation is to be functionally complete cells to form myelin sheaths around multiple axons that facilitates saltatory nerve conductions (Baumann and Pham-Dinh, 2001; Franklin, 2002). Oligodendrocytes experienced several distinct stages of differentiation till maturation in order to produce all the specific constituents of myelin sheaths and fulfill the myelination function. These stages can be generally divided into precursors, pre-oligodendrocytes, pre-maturity oligodendrocytes (immature oligodendrocytes), non-myelinating mature

oligodendrocytes and myelinating mature oligodendrocytes. Different stages are characterized by different proliferative capacities, migratory abilities and morphologies (Barry et al., 1996; Baumann and Pham-Dinh, 2001). The progression from precursors to myelinating oligodendrocyte entails a sequence of events, including cell cycle exit, cytoskeletal changes and synthesis of myelin components.

On the one hand, oligodendrocytes undergo striking changes in shapes during lineage progression. They develop from mono- or bipolar to multipolar morphology as shown in **Figure 1.1**. The eventual outcome is that the myelinating oligodendrocytes appear to be highly branched and complex (sometimes with wooly or hairy fine processes or even form lamellipodia structure) that they are able to extend their membranes to complete the myelination by wrapping around axons (Pfeiffer et al., 1993). On the other hand, a series of molecules are sequentially expressed in a timed fashion. The precursors of oligodendrocytes originated from distinct locations of CNS during late embryonic development. These cells can be stained by the monoclonal antibody (mAb) A2B5, which recognizes several gangliosides (Eisenbarth et al., 1979; Fredman et al., 1984). A2B5 immunoreactivity was accompanied by the expression of platelet-derived growth factor receptor α (PDGFRα, Hall et al., 1996). The mRNA of DM-20 coding a PLP (proteolipid protein) isoform can also be detected in this stage (Timsit et al., 1995). Some other markers are also used to observe early stage oligodendrocytes, such as NG2 proteoglycan (Nishiyama et al., 1996). When the cells further differentiate, they enter the second stage—pre-oligodendrocytes. The gene expressions in these cells are significantly

changed in comparison to precursor cells. Most cells in this stage cannot be identified by A2B5 immunoreactivity, PDGFRα or DM-20 expression. But they are immuno-positive to a mAb O4, which designates that these cells remain in their proliferative status, whereas the positivity of another mAb O1 is usually considered as the exit of proliferation (Sommer and Schachner, 1981; Tang et al., 2001).

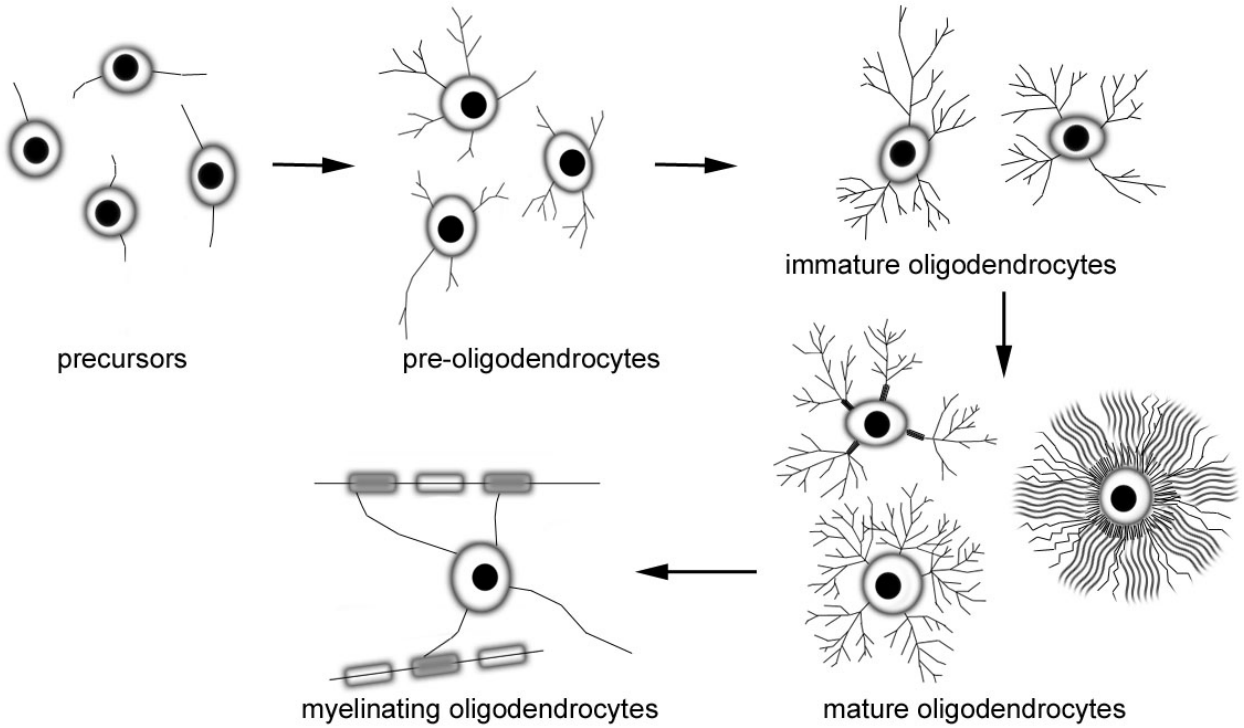

Figure 1.1 Oligodendrocytes differentiate in morphology

Table 1.1 Typical gene expression in each oligodendrocyte differentiation stage

Development stages	Typical gene expression
precursors	A2B5, GD3, NG2, PDGFRa, DM-20
pre-oligodendrocytes	A2B5, GD3, NG2, O4, PDGFRa, DM-20
immature oligodendrocytes	O4, GalC, CNP, DM-20, JN
mature oligodendrocytes	O4, GalC, CNP, MBP, PLP, MAG, JN
myelinating oligodendrocytes	O4, GalC, CNP, MBP, PLP, MAG, MOG, JN

To acquire maturation, more genes are programmed to be expressed, many of which are oligodendrocyte specific molecules, such as CNP, MBP, JN and PLP (**Table 1.1**). At the same time, the genes or proteins detected in precursors or

pre-oligodendrocytes mostly disappeared.

1.2.2 Molecules and mechanisms controlling oligodendrocyte development

A proper development program of oligodendrocytes from precursors until myelinating mature cells may require successful fate specification, proliferation, differentiation and myelination.

a. Morphological development of oligodendrocytes

First of all, dynamic arrangements of the cytoskeleton are required to confer cell migration, morphological differentiation and cytoplasmic spreading during myelination. For example, Fyn tyrosine kinase activity is important for the morphological differentiation (Osterhout et al., 1999). Studies also found matrix metalloproteinase, such as MMP-9, helps oligodendrocytes to extend their processes (Uhm et al., 1998; Oh et al., 1999). A recent report showed that Sec8 is a molecular important for oligodendrocyte morphological differentiation (Anitei et al., 2006). Via regulation of myosin phosphorylation and actomyosin assembly, Rho kinase functions in coordinating the movement of glial membrane to enwrap the axon in the onset of myelination (Melendez-Vasquez et al., 2004). Other cytoskeleton-associated oligodendroglial proteins are crucially involved in process outgrowth, gene expression, and/or myelin–axon interaction, such as CNP, JN, and the kelch-related actin-binding protein mayven (Jiang et al., 2005; Lee et al., 2005; Zhang et al., 2005).

b. Extracellular signals affecting oligodendrocyte differentiation

During CNS development, oligodendrocytes and other cell types shared the same

precursor cells, which are multipotent neuroepithelial cells (Chandran et al., 1998). Several molecules are found to be crucial to lead these cells into the program towards oligodendrocyte fates. For example, studies have shown that sonic hedgehog protein is both necessary and sufficient to induce oligodendrocyte fate specification (Trousse et al., 1995; Poncet et al., 1996; Pringle et al., 1996). Neuregulin/GGF at high levels was revealed as an inhibitor of lineage commitment of oligodendrocyte precursors (Canoll et al., 1996).

Cell cycle exit is a prerequisite for oligodendrocyte differentiation. Thus after adopting an oligodendrocyte lineage fate, these precursor cells either enter differentiation or keep proliferating. PDGF and basic fibroblast growth factor (bFGF) are two of the factors that play roles against differentiation but favoring proliferation of oligodendrocyte precursors (McKinnon et al., 1990; Barres and Raff, 1994). On the basis of such properties, these two growth factors are usually used for *in vitro* cell culture to induce a continuously proliferative population of oligodendrocyte precursor cells (Bogler et al., 1990). In addition, other growth factors such as insulin-like growth factor-1, neuregulin as well as neurotrophins such as brain derived neurotrophic factor and neurotrophin-3 are also shown to be mitogenic to promote proliferation (Lu et al., 2002; Casaccia-Bonnefil and Liu, 2003). Conversely, diverse factors promote oligodendrocyte differentiation, ranging from transforming growth factor-β (McKinnon et al., 1993), β-adrenergic receptor agonists (Ghiani et al., 1999) and thyroid hormone (Barres et al., 1994; Ahlgren et al., 1997). On controlling the proliferation/differentiation axis of oligodendrocyte precursors, the importance of a

couple of other elements, including chemokines (Robinson et al., 1998), cytokines (Benveniste and Merrill, 1986) are also known. In addition, differentiation of oligodendrocytes is greatly affected by the signaling molecules from axons. For example, the maturation of oligodendrocytes was promoted by the interaction of its surface Notch receptors with F3/contactin, which is expressed by axons (Hu et al., 2003). LINGO-1 is another oligodendroglial protein that receives signals from axons and negatively regulates oligodendrocyte differentiation and maturation (Mi et al., 2005; Zhao et al., 2007).

c. Intrinsic mechanisms regulating oligodendrocyte differentiation

Besides the external cues, oligodendrocytes have a built-in mechanism (also called the internal clock) which helps the cells exit from dividing and proceed to differentiation at a proper time (Barres et al., 1994; Barres and Raff, 1994). External molecules mostly function via modulating this internal clock to control proper oligodendrocyte differentiation.

The internal clock comprises of two aspects, one is a timing component which measures the elapsed time or dividing times; the other is effector component working to stop cell division and initiate differentiation (Raff et al., 2001). An early study by Temple and Raff (1986) showed that the maximum dividing times for an oligodendrocyte precursor cell is approximately eight, after which its daughter cells simultaneously cease proliferating and differentiate into oligodendrocytes (Temple and Raff, 1986). A recent report showed p57kip2 represents one of the molecules acting as a part of the timing components (Dugas et al., 2007). p57kip2 belongs to

Cip/Kip protein family, which are cyclin-dependent kinase inhibitor proteins that inhibit cyclinE-cdk2 complex formation (Cunningham and Roussel, 2001). This complex formation relates to G1-S phase checkpoint regulation and cell cycle arrest (Ghiani and Gallo, 2001). Dugas et al. (2007) found *in vitro*, that the levels of p57kip2 in oligodendrocyte precursors increased over time when the cells proliferate. The higher levels of p57kip2 inhibited precursors' proliferation and finally rendered them responsive to external differentiation cues (Dugas et al., 2007).

Many studies and evidences are reported on the effector component of the internal clock. Transcription factors including homeodomain family, bHLH proteins, and high-mobility-group (HMG) family proteins are demonstrated to play important roles at various stages of oligodendrocyte differentiation and myelination (Qi et al., 2001; Lu et al., 2002; Zhou and Anderson, 2002; Stolt et al., 2003 and 2004; Sohn et al., 2006).

Homeodomain transcription factors comprise of several subgroups including paired-type, Nk-type and POU domain proteins (Wegner, 2000). Nkx2.2 and Nkx6.2 belong to Nk-subtype are essentially involved in oligodendrocyte differentiation and myelination. In Nkx6.2 null mice, proteins in paranodal junction such as Nf 155 and contactin/F3 are abnormally expressed and myelinated axons are severely disorganized (Southwood et al., 2004). The number of MBP and PLP expressing oligodendrocytes dramatically decreased and myelination is delayed in Nkx2.2 knock-out mice (Qi et al., 2001). Also, POU domain proteins Oct-6 is important for myelination onset as its deficiency caused the delay of the later (Bermingham et al.,

1996; Ghazvini et al., 2002).

bHLH proteins are important regulators of development in various cell types. In oligodendrocytes, Olig1 and Olig2 are two closely related factors that start to express in precursor stage. Olig2 is necessary for specification of oligodendrocytes while Olig1 may be involved in repairing demyelination in patients with MS (Zhou et al., 2001; Lu et al., 2002; Zhou and Anderson, 2002; Arnett et al., 2004).

Sox proteins contain a HMG domain where they can bind DNA to modulate gene transcription. Sox10 for example is expressed in both oligodendrocytes and Schwann cells (Kuhlbrodt et al., 1998). In Sox10-deficient mice, progenitors of oligodendrocyte develop, but the terminal differentiation of the cell is disrupted (Stolt et al., 2002). Study also showed Sox10 regulate the transcription of adhesion molecular connexin32 and connexin47, which are important for myelin formation and maintenance (Schlierf et al., 2006). In other studies, Sox8 and Sox9 are identified as crucial determinants affecting oligodendrocyte fate specification (Stolt et al., 2003 and 2005).

Though great progresses have been made, there are still many largely undeciphered areas in oligodendrocyte development and the underlying mechanisms. In particular, there seems to be a deficiency in knowledge on how the morphological differentiation is coupled to controlled gene expression and cell cycle regulation.

1.3 Myelination

1.3.1 Myelination and myelin

Myelination is one of the most pivotal natural inventions in nervous system during evolution. The first ensheathed axon may have come into being around 400 million years ago (Baumann and Pham-Dinh, 2001). These sheaths are made up of lipid-abundant insulating myelin. Myelin sheaths around axons comprise of many discontinuous segments called internodes, in between which there are periodic interruptions ---nodes of Ranvier, where axolemma (surface of axon) are bare. These nodes are about 0.5 μm in width and are areas where axons are exposed. High lipid content of myelin sheaths, low water content as well as unique segmental structures enable these myelinated areas of axons to be insulated so that action potentials can "jump" from one unmyelinated node to the next rather than transmitting through entire axons. This kind of transmission is called saltatory conduction, which largely improved the efficiency and velocity of information transmission in the nervous system. Myelin sheaths confer three major advantages to the vertebrate nervous system: high-velocity conduction, fidelity of signal transduction across long distances and economical space-saving. Upon the invention of myelination, organisms are enabled to bear long axons. Also based on this feature, vertebrates can evolve and distinguish themselves from invertebrates (Kandel, 2001; Baumann and Pham-dinh, 2001).

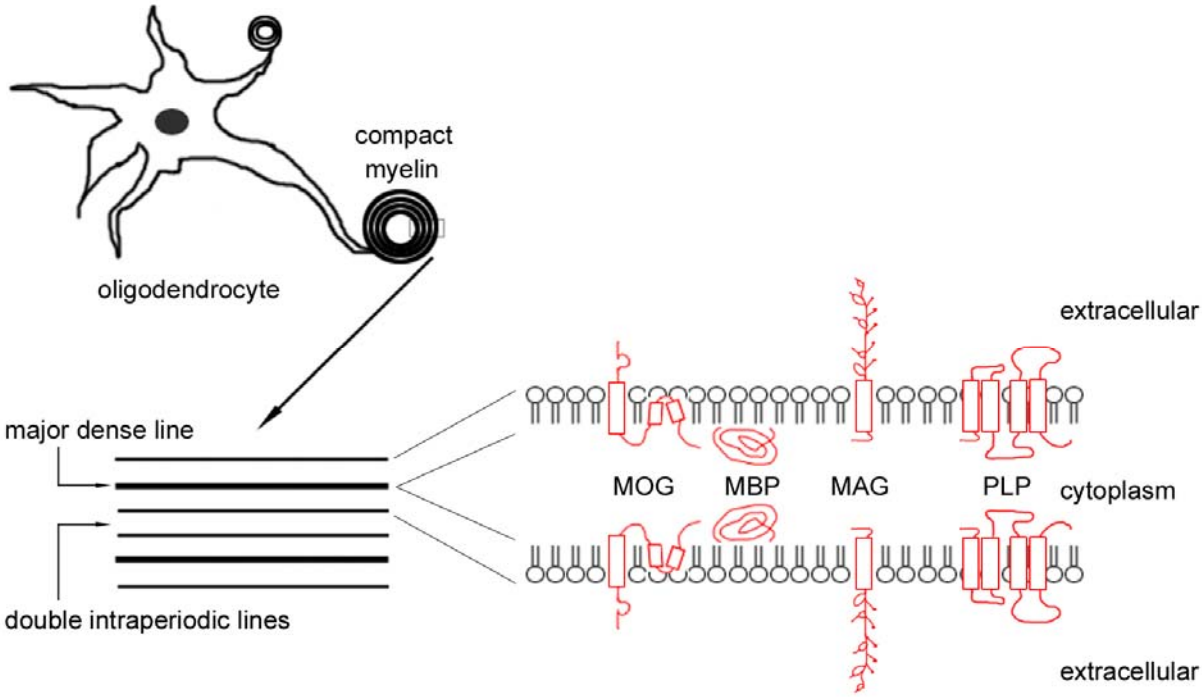

Figure 1.2 Periodic structure of myelin sheath

1.3.2 The polarized myelin sheath in morphology

Myelin sheaths are radially polarized structures. The transactional structure of myelin sheath has been well studied by others (as reviewed in Morell et al., 1994). These results demonstrated a periodic structure of myelin sheath, with concentric electron-dense and light layers. The electron-dense lines called major dense lines are formed by closely opposed cytoplasm of expanding myelinating processes of oligodendrocytes. The intraperiodic lines represent two fused outer leaflets, in between which are extracellular spaces (**Fig. 1.2**). Another reflection of the radial polarization of myelin sheath is the differential expression of myelin components. Myelin associated glycoprotein (MAG), for example, is expressed in adaxonal membrane (sheath adjacent to axon), but MBP is in compact myelin whereas myelin-oligodendrocyte glycoprotein (MOG) in abaxonal (outside layer of the sheath)

membrane (Salzer 1995; Buss and Schwab, 2003).

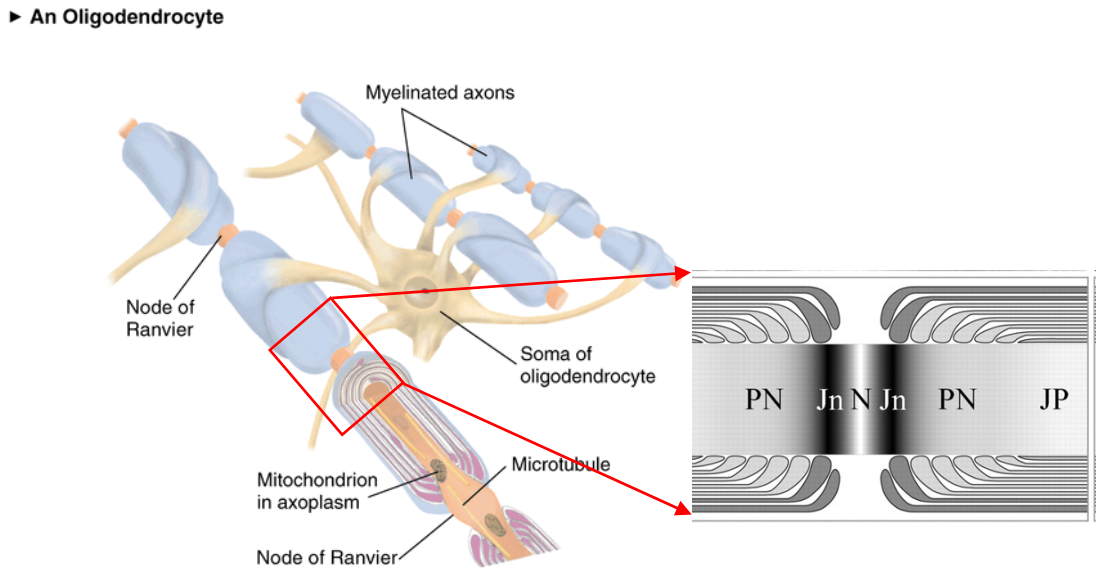

Figure 1.3 Axons myelinated by oligodendrocytes in the CNS
Adapted from Zhang et al., 2005.

Longitudinally, in between two nodes of Ranvier, each segment of myelin sheaths or internode measures 150-200 μm in length. A myelinated axon internode is also polarized that it could be divided into three distinct domains: juxtaparanodal region (JP), paranodal region (PN), juxtanodal region (JN) (**Fig. 1.3** and Zhang et al., 2005). Longitudinal polarization of myelinated axons is featured by several other characteristics. For example, the ion channels, adhesion molecules and other associated cytoskeletal elements that express uniformly on axonal surface of unmyelinated or demyelinated axons appear to be asymmetrically distributed on myelinated axons. Additionally, in different regions such as paranodes in comparison to juxtanodes, the velocity of axonal transport, level of neurofilament phosphorylation

or accumulation of membranous organelles vary (Salzer, 2003; Edgar et al., 2004).

In these distinct regions of the myelin, active interactions happen in between axons and oligodendrocytes in CNS (or Schwann cells in PNS). These interactions between neurons and oligodendrocytes on one hand affect proper differentiation and myelination of oligodendrocytes, and regulate the domain organization of axon on the other. Axons regulate oligodendrocyte survival, gene expression and the thickness of myelin sheath (Smith et al., 1982; Friedrich and Mugnaini 1983; Chakraborty et al., 1999; Lopresti et al., 2001; Michailov et al., 2004). Reciprocally, myelinating oligodendrocytes and Schwann cells regulate axon caliber, axon domain organization and clustering of ion channels and cell adhesion molecules (Sanchez et al., 1996; Arroyo and Scherer, 2000; Peles and Salzer, 2000; Rasband and Trimmer, 2001; Girault and Peles, 2002; Boiko and Winckler, 2006).

As mentioned in the previous section, myelin sheaths are generated by oligodendrocytes in CNS and Schwann cells in PNS. But the two kinds of myelination are different from each other in several important features. For example, one typical oligodendrocyte can envelop an average of 15 axonal internodes of different axons. But Schwann cells envelop just one internode (see below) of only one axon. Additionally, the most extremely outside boundary of Schwann cells, but not of oligodendrocytes, harbors a basal lamina structure (Bunge et al., 1986). In basal lamina, type IV collagen, laminin and heparin sulphate proteoglycan are demonstrated to play pivotal roles in completing the ensheathing process of Schwann cells (Bunge, 1987). Meanwhile, Schwann cells bear interlinked finger-like microvilli which project

closely to nodal axolemma. In the CNS, however, perinodal glial processes take the place of microvilli to form contacts with nodes (Bjartmar et al., 1994; Butt et al., 1999).

1.3.3 The chemical composition of myelin sheath

Myelin is a poorly hydrated structure, which only contains 40% water in contrast to gray matter of the brain (80%). Myelin is also peculiar in its high lipids abundance that 70% dry weight of myelin attributed to lipid contents while only 30% is protein (Morell et al., 1994). Lipids found in myelin also existed in other membrane structures, but a discerning characteristic of oligodendrocytes and myelin lipids is that they are rich in glycosphingolipids, especially galactocerebrosides. Of all, GalCs are the most typical and enriched lipids responsible for ~20% dry weight of myelin (Morell et al., 1994). In addition, many oligodendrocyte/myelin proteins are also covalently modified that they also possess hydrophobic properties (Agrawal et al., 1982). All these features including structure, thickness, low water content and wealth in lipids together endowed the myelin sheaths with the insulating capability.

The proteins in myelin have been extensively investigated and some of the well-established ones are specifically expressed in myelin. For example, MBP (Kies et al., 1965), PLP and its isoform DM-20 (Folch and Lees, 1951) are most abundant components, comprising 80% of the total proteins. There are also CNP (Sprinkle, 1989) and JN (Zhang et al., 2005), which are more recently identified as myelin specific proteins. Several glycoproteins are present in myelin, among which are MAG

and MOG (Quarles, 1997). These proteins together participated in almost every aspect of the cellular activities of myelin/oligodendrocyte, encompassing cellular transportation, structural maintenance and differentiation, even affecting neuronal survival and axon/myelin interaction (Baumann and Pham-Dinh, 2001).

2. Histone deacetylase (HDAC)

2.1 Histone deacetylation: an important modification of histones

Chromatin can be classified into euchromatin and heterochromatin. Heterochromatin represents a tightly packed form of hereditary materials, and its major characteristic is that transcription of genes is limited. Chromatins comprise of nucleosomes, each of which consists of ~146 bp of DNA wrapping around a histone octamer. One histone octamer is a complex made up of two molecules of the four core histone proteins, H2A, H2B, H3 and H4 (Kornberg, 1977). The amino acid terminals protruding from the nucleasomes, that is the N-terminal tail domains of those core histone proteins are prone to many different post-translational modifications including acetylation, methylation, ubiquitination, glycosylation, ADP ribosylation, carbonylation, sumoylation, biotinylation and phosphorylation (Strahl and Allis, 2000).

The first piece of investigation linking enhanced histone acetylation with active genes dated back to the work by Vincent Allfrey (Allfrey et al., 1964). Accumulated evidences in the past 40 years supported this notion that histones in heterochromatin are usually poorly acetylated and their acetylation is positively correlated with gene

transcription activity (Grewal and Elgin, 2002; Clayton et al., 2006). This correlation can be illustrated by highly acetylated histone H4 in chromatin near the active chicken globin gene (Hebbes et al., 1992), the human platelet-derived growth factor gene (Clayton et al., 1993), and the Drosophila male X chromosome (Bone et al., 1994). By contrast, for example, histone H4 usually is observed to be hypoacetylated at H4 lysine 5, 8, and 16 positions in human and yeast heterochromatin, in which gene transcription is largely repressed (Braunstein et al., 1993; Jeppesen and Turner, 1993).

The acetylation reaction happens by adding in an acetyl group to ε–amino group of specific lysines in N-terminal histone tails. Certain lysine sites of acetylation are particularly important in histone that these site-specific histone acetylation and deacetylation is involved in various essential processes including nucleasome assembly, chromatin folding, heterochromatin silencing, gene transcription and expression (reviewed in Shahbazian and Grunstein, 2007). One of the examples is the acetylation and deacetylation of histone H4 lysine 16. Its acetylation is preferentially found in the transcriptionally hyperactive X chromosome of Drosophila male larvae (Turner et al., 1992; Bone et al., 1994). In addition, chromatin compaction and folding was determined by acetylation at histone H4 lysine 16, which also prevents the spreading of heterochromatin components (Shogren-Knaak et al., 2006).

The mechanism by which the histone acetylation influences transcription regulation is still under debate. Some early studies proposed that conformational changes of chromatin and nucleasome would be the direct results of histone acetylation. The positive charge of the histone tails will be neutralized by the

acetylation so that the affinity between those tails and negatively charged DNA will be attenuated. Such an electrostatic release will result in increased accessibility of nucleasomal DNA to transcriptional regulators (Kuo and Allis, 1998). Recently, several groups of researchers seem to support a completely different function of histone acetylation (reviewed in Zeng and Zhou, 2002; Yang, 2004). Findings showed that acetylated lysine residues on histone tails can form binding sites for bromodomains, which are 110 amino acid long domains found in many chromatin associated proteins. This suggests that acetylation will introduce more binding opportunities for related proteins to nucleasome. The two kinds of models are different. In the conformation-modifying model, if multiple or all the lysine residues of a single histone tail are highly acetylated, the net effect would be much stronger than that of a single lysine. Whereas if the bromodomain-binding model is correct only adjacent amino acids of acetylated lysine determine binding specificity, increased number of acetylated lysine residues or even the hyperacetylation of the whole histone tail will not yield further increase to the binding properties and recruitment of transcription factors. It is possible that both these two models apply under different physiological circumstances. Meanwhile, other influential determinants should also be taken into consideration to estimate the mechanisms how acetylation influences gene activity, such as other covalent modifications of lysine and/or arginine residues on histone tails, including histone methylation and phosphorylation. The overall status of histones was a compromise between all those forces presented above. Such a status provides signals for recruitment of specific chromatin-associated proteins, which in

turn alter chromatin states and affect transcriptional regulation (Fuchs et al., 2006). But it may be important to note that the acetylation of histones is not a stably persisting modification, but rather as suggested by recent investigations undergoes rapid turnover upon the action of two counteractive but cooperative partners: histone acetyltransferases (HATs) and HDACs (Clayton et al., 2006).

2.2 Histone deacetylase family proteins

In yeast, a series of HDACs have been well investigated. For example, reduced potassium dependency protein 3 (RPD3) and RPD1 (also known as SIN3, SD11, and UME4) are two of the earliest yeast HDAC members (Vidal et al., 1991; Vidal and Gaber, 1991). The recessive mutations of these two proteins are found to augment the transcription activity of a subset of yeast genes with various unrelated functions. After that, Rundlett et al. (1996) identified Hda1 from transcriptional complexes they isolated. Histone deacetylase 1 protein (HDA1) possesses high sequence similarity to Rpd3 and affects histone H3 and H4 acetylation to control gene transcription in yeast. They also established that Hda1 and Rpd3 represented members of two distinct yeast histone deacetylase complexes (Rundlett et al., 1996).

The correlation between histone deacetylation and repressed gene transcription is equally established in mammals. Taunton et al. identified the first mammalian HDAC -- HDAC1 with high similarity to Rpd3 in yeast (60% identity at the protein level, Taunton et al., 1996). The past decades have witnessed tens of new members being enlisted into the HDAC family. On the basis of functional and structural properties, all

HDACs are classified into four subgroups or subfamilies----class I, II, III HDACs and HD-2 like proteins. But HD-2 like proteins present uniquely in plants and will not be discussed in this thesis (Lusser et al., 1997; Chen and Tian, 2007). In mammals, class I, II and II HDACs are enzymes respectively homologous to yeast RPD3, HDA1 and silent information regulator protein 2 (SIR2, Gray and Ekstrom, 2001). It is noteworthy that a common characteristic for almost all HDACs is that their enzymatic activity can be inhibited by one or more inhibitors.

2.2.1 Class I HDACs

As mentioned above, HDAC1, as the first mammalian member identified, possesses high homology to yeast RPD3 (Taunton et al., 1996). After that, several new members similar to RPD3 were successively reported by different groups and they are named HDAC2, -3, -8 and -11 (Yang et al., 1997; Zeng et al., 1998; Hu et al., 2000; Gao et al., 2002;). In addition to the structural similarity, class I HDACs are predominantly nuclear proteins expressed in most tissues and cell lines. All these five homologues of yeast RPD3 seem akin to each other on the basis of their functions. For example, all these five members are found to form protein complex with corepressors to inhibit gene-specific transcription. Two core complexes they formed are Sin3 and Mi-2/Nurd complex (reviewed in Knoepfler and Eisenman, 1999). Many other repressor complexes were also reported to contain one or several members of these four, such as TGIF/Smads (Wotton et al., 1999), glucocorticoid receptor (Ito et al., 2000), Groucho (Choi et al., 1999), Hus1/Rad9 (Cai et al., 2000), Retinoblastoma protein (Brehm et al., 1998), N-CoR (Li et al., 2000) and DNA methyltransferase 1

(Robertson et al., 2000). Class I HDACs also interact with a variety of other important proteins, such as Snail (Peinado et al., 2004), β–catenin (Billin et al., 2000), HOXB7 (Chariot et al., 1999), MBP-1 (Ghosh et al., 1999) and p65 (Ashburner et al., 2001).

Class I HDACs are crucial and versatile regulators of cell growth, differentiation or apoptosis in both physiological and pathological conditions. For example, the abnormal downregulation of HDAC3 and other class I HDAC members were found in human colon cancer cell lines (Wilson et al., 2006). Corepressor complexes containing HDAC1 and other class I HDACs play important roles in adipogenesis (Wiper-Bergeron et al., 2003; Lagace and Nachtigal, 2004). More recently, HDAC1 and HDAC2 are found to regulate cardiac morphogenesis, growth and contractility (Montgomery et al., 2007).

2.2.2 Class II HDACs

As homologues to yeast HDA1, class II HDACs comprise of a total 7 members, which are further subdivided into two subclasses, IIa (HDAC4, -5, -7, -9 and HDAC9 splice variant MITR) and IIb (HDAC6 and HDAC10) (reviewed in Verdin et al., 2003). A ~420 amino acids C-terminal catalytic domain is shared by all class II HDACs. However, their N-terminal domains seem to not have similarity with other proteins. One exception is MITR, the HDAC9 splice variant, which only has N-terminal domain but not C-terminal deacetylase domain. In analogy to Class I HDACs, these class II members incorporate into different corepressor complex to regulate gene transcription and expression. In addition to MEF2 family proteins as their major binding partners, class II HDACs also form complexes with E1A

C-terminal binding protein (CtBP, Chinnadurai, 2002), 14-3-3 proteins (Wang et al., 2000), calmodulin (CaM, Youn et al., 2000), transcriptional co-repressors SMRT and N-CoR (Huynh and Bardwell, 1998), heterochromatin protein HP1a and SUMO (Kirsh et al., 2002; Zhang et al., 2002). Distinct from Class I HDACs, the activity of class II HDACs is also modulated by their tissue-specific distribution and translocation in between nucleus and cytoplasm with the help of14-3-3 proteins (Wang et al., 2000).

Among others, the biological functions of Class IIa HDACs include their participation in the transcription inhibition of myogenesis (McKinsey et al., 2001) and regulation of thymocytes negative selection and maturation (Verdin et al., 2004). Recently, HDAC7 is also suggested to be an influential monitor of vascular integrity (Chang et al., 2006). Class IIb HDACs are distinct from traditional histone deacetylases which are usually localized in the nucleus to modify histone tails. By contrast, both HDAC6 and HDAC10 are mostly detected in the cytoplasm. Till now, limited information is available about exact function of HDAC10, though it is found to function in pre-mRNA processing and development of hepatocellular carcinoma after infection (Park et al., 2007; Shimazu et al., 2007). With regard to HDAC6, it may function in regulating protein ubiquitination through forming multi-protein complex with cytoplasmic partners, such as HDAC6/p97/VCP complex (Seigneurin-Berny et al., 2001). It is worth noting that HDAC6 is reported to be a cytoskeleton modifying deacetylase which removes the acetyl group from lysine-40 of α-tubulin, thus depolymerizing and destabilizing microtubules (Hubbert et al., 2002).

In addition, it is implicated in regulating aggresome formation and interaction with SIRT2.

2.2.3 Class III HDACs---SIR2 family of proteins

Class III HDACs are also well known as silent information regulator 2 (SIR2) proteins in yeast or Sirtuins in mammals. They are specially classified as a subfamily because they need a cofactor nicotinamide adenine dinucleotide (NAD) to be active as HDACs. SIR2 proteins control transcription silencing at ribosomal DNA, HM mating type loci and telomeres (Shore et al., 1984; Schnell and Rine, 1986; Smith and Boeke, 1997; Imai et al., 2000). It suppresses the generation of toxic extrachromosomal DNA circles, and mediates the lifespan extension by CR (Sinclair and Guarente, 1997; Lin et al., 2002). In mammals, SIR2 is represented by seven homologs (collectively named Sirtuins) and related to various important functions such as cell cycle regulation, cell differentiation, CR and aging in rodents and in cultured human cells (see below for detailed introduction).

2.2.3.1 SIR2 in lower animals and mammalian Sirtuins

Yeast Sir2 is initially found to be required for silencing of repeated sequences in yeast, including mating type loci, telomeres and rDNA (Shore et al., 1984; Schnell and Rine, 1986). These gene-silencing functions allowed sir2 in yeast as an aging-related molecular promoting lifespan extension (Sinclair and Guarente, 1997; Lin et al., 2002). Similar effects had been revealed for its ortholog (molecules across species but shared ancestry during evolution) in *C. elegans* (Tissenbaum and Guarente, 2001). The silencing results in compacted, closed and inaccessible chromatin structure.

The lysine residues of the amino-terminal tails of histone H3 and H4 were found to be particularly required for the silencing (Thompson et al., 1994). Coincidently, these amino-terminal lysines are usually subjected to acetylation modification and are preferably deacetylated in silencing status (Braunstein et al., 1996). Another study indicated that overexpressed Sir2 resulted in global deacetylation of yeast histones (Braunstein et al., 1993). All these early results seemed to implicate Sir2 as a histone acetylation modifier. However, the role of the gene product as a histone deacetylase was not established until the finding by Imai et al., (2000). The authors successfully demonstrated that yeast and mouse SIR2 proteins are NAD-dependent histone deacetylases, which deacetylate lysines 9 and 14 of H3 and specifically lysine 16 of H4. This conclusion was further supported by their discovery that two mutations of SIR2 attenuated the deacetylase activity of this protein (Imai et al., 2000).

SIR2 is highly conserved across species ranging from archaea to humans (Brachmann et al., 1995). In mammals, these families of proteins, with a conserved Sirtuin core domain as reported by Frye (Frye, 1999 and 2000), are represented by SIRT1-7, also interchangeably named Sirtuin 1-7. In the past several years, extensive studies have focused on investigating the functions of these seven members. As a consequence, they are found to be expressed widely and have essential functions. In addition to histones, Sirtuins possess a dozen of other substrates. For example, SIRT1's substrates include p53, Ku70, nuclear factor-B (NF-κB), Forkhead box class O (FOXO) and hypermethylated in cancer 1 (HIC1) (Luo et al., 2001; Vaziri et al., 2001; Brunet et al., 2004; Cohen et al., 2004; Motta et al., 2004; Yeung et al., 2004).

For SIRT2, α-tubulin was identified as another substrate in addition to histone tails (North et al., 2003). Recently, FOXO1 and FOXO3a were also shown to be deacetylated by SIRT2 (Jing et al., 2007; Wang et al., 2007a). There are also a couple of substrates found for other Sirtuin members. Through regulating acetylation/deacetylation of these substrates, Sirtuins are known as crucial regulators of a diversity of cellular functions, ranging from cell cycle regulation, cell differentiation and survival, cell metabolism and calorie restriction (CR) related anti-aging (reviewed in Haigis and Guarente, 2006; li-Youcef et al., 2007). Meanwhile, they (especially SIRT1 and 2) are also of great pathophisological importance in the mechanistic understanding as well as clinical treatment of several diseases, such as AD, ALS and type II diabetes (Kim et al., 2007; Milne et al., 2007; Outeiro et al., 2007).

2.2.3.2 The biochemistry of SIR2 and Sirtuins

Though classified as Class III HDACs, both SIR2 and Sirtuins possess a distinctive NAD-dependent histone deacetylases activity. Frye for the first time showed that Sir2 proteins from bacteria, yeast, and mammals could transfer an ADP-ribose group from NAD to a protein carrier (Frye, 1999). Later, yeast SIR2 protein was revealed as indeed an ADP- ribosyltransferase *in vitro*, and its activity was essential for the silencing function *in vivo* (Tanny et al., 1999). In the report by Imai et al., SIR2 was found to be a histone deacetylase, they also indicated that the amino-terminal tails of histone H3 or H4 peptides could accept ADP-ribose from NAD, but only if the peptides were acetylated (Imai et al., 2000). Another piece of

finding by the authors showed that the relative molecular weight of the product was actually smaller than that of the substrate, indicating that the major modification catalyzed by Sir2 was deacetylation but not ADP-ribosylation. In the absence of NAD, SIR2 exhibited no deacetylase activity, which could not be compensated by addition of NADH, NADP or NADPH. Studies by other groups confirmed the conculsion that SIR2 is a histone deacetylase depending on NAD as a cofactor to be effective (Landry et al., 2000; Smith et al., 2000).

SIR2 and Sirtuins catalyze a reaction in which NAD and an acetylated substrate are converted into a deacetylated protein, nicotinamide, and a novel metabolite O-acetyl ADP-ribose (Tanner et al., 2000). In this regard, some literatures also called this family NAD-dependent deacetylase (NDAC) in comparison to HDAC. The metabolite O-acetyl ADP-ribose is proposed to bear certain unique cellular function linked to the gene-silencing effect of SIR2 and Sirtuins (Tanner et al., 2000; Borra et al., 2002), which may also be an essential factor in physiology (Grubisha et al., 2006)

2.3.3.3 Biological functions of Sirtuins

SIRT1

SIRT1 is the Sirtuin member that received the most extensive investigations. It localizes in nucleus and interacts with diverse partners. It is found to regulate CR and aging, cell survival, cell differentiation and metabolism (Anastasiou and Krek, 2006).

Firstly, SIRT1 is a positive master controlling cell growth and survival. Luo et al. and Vaziri et al. reported that SIRT1 interacts with and deacetylates p53 both *in vivo* and *in vitro* (Luo et al., 2001; Vaziri et al., 2001). The biological consequence after

p53 deacetylation is the repression of p53-dependent transcription and apoptosis. Confirmative evidence came from another study, where a SIRT1 knockout mouse was shown to have hyperacetylated p53 (Cheng et al., 2003). SIRT1 also interacts with promyelocytic leukemia protein 4 (PML4), which constitutes nuclear bodies as one of the distinct substructures of nucleus implicated in the control of cell growth, gene regulation and apoptosis (Seeler and Dejean, 1999; Langley et al., 2002). Overexpression of PML4 induces the arrest of cell growth, which could be rescued by overexpression of SIRT1 (Langley et al., 2002). Together with the report that SIRT1 deacetylates NF-κB to affect cell survival (Yeung et al., 2004), SIRT1 obviously plays a crucial role in cell growth and survival.

Secondly, SIRT1 is broadly involved in lifespan extension induced by calorie restriction (CR). CR refers to a dietary regime, low in calories without undernutrition. CR extends life spans in many organisms ranging from rotifers, spiders, worms, and fish to rodents and primates (Weindruch, 1996). Physiology of mammalian CR involves increased insulin sensitivity and corresponding reductions in blood glucose and insulin levels. In response to glucose, insulin is secreted by pancreatic β-cells to maintain glucose homeostasis. In this aspect, SIRT1 was a crucial connector of glucose metabolism to CR and aging. SIRT1 positively regulates glucose-stimulated insulin secretion in pancreatic β-cells (Moynihan et al., 2005).

Also, SIRT1 promotes the survival of pancreatic β-cells under stress (Kitamura et al., 2005). In the liver, SIRT1 deacetylates and activates PGC-1α, which promotes gluconeogenesis following fasting (Rodgers et al., 2005). PGC-1α, upon activation by

SIRT1, also promotes mitochondrial function in the skeletal muscle and the brown adipose tissue, leading to enhanced energy expenditure, increased exercise performance, and protection from diet-induced insulin resistance and hepatosteatosis (Baur et al., 2006; Lagouge et al., 2006). All these effects in mitochondria are associated with longevity extension.

In addition, SIRT1 has also been shown to deacetylate cytoplasmic Acetyl-CoA synthetase 1 (AceCS1), which is an enzyme that controls acetyl-CoA levels in the cytoplasm for fatty acid synthesis (Hallows et al., 2006). Since impaired acetate metabolism is usually a typical feature in diabetes and aging, this piece of finding also implicates a potential role of SIRT1 in pathophysiology of these diseases. Finally, SIRT1 is demonstrated to be a central player in modifying diseases of CNS (see below).

SIRT2

A point also of broad interest is that SIRT2 was found to possess several different substrates in addition to histone and play roles in cell cycle regulation, cell differentiation and aging. To date, SIRT2 is the only Sirtuin that is localized mainly in cytoplasm (North et al., 2003). Sirtuin-2 or SIRT2 is the second family member of Sirtuins, which was firstly identified by Frye as a protein with activity to transfer radioactivity from $^{[32P]}$NAD to other proteins (Frye, 1999). After that two other studies found that SIRT2 was an enzyme deacetylating α-tubulin and controlling mitotic exit of cell cycles (Dryden et al., 2003; North et al., 2003). Recent progresses also illustrated a possible linkage of SIRT2 to neurodegenerative diseases. In a mode of

PD, inhibition of SIRT2 activity rescues cellular toxicity mediated through α-synuclein (Outeiro et al., 2007). In another piece of study on Wallerian degeneration mice, SIRT2 upon activation by resveratrol (a nontoxic molecular activator of Sirtuins found in Asian medicinal herbs and red wines, see Zhuang et al., 2003) abolished the resistance of the animal to axonal degeneration (Suzuki and Koike, 2007).

As addressed in previous sections, the proper differentiation of oligodendrocytes requires precisely regulated cell cycle exit from proliferative stage on one hand and complex morphological arborizations that involve microtubule network reorganization on the other hand. SIRT2 is involved in regulating both cytoskeletal elements and cell cycle proteins. SIRT2 regulates mitotic cell cycle exit (Dryden et al., 2003) and its overexpression delays cell proliferation (North and Verdin, 2007); SIRT2 is also a regulator of tubulin acetylation/deacetylation (North et al., 2003). Importantly, in tissues other than brain, by regulating the acetylation/deacetylation of FOXO1, SIRT2 was an essential controller of adipocyte differentiation (Jing et al., 2007). Moreover, two independent groups reported that SIRT2 was expressed in oligodendrocytes and myelin sheath (Vanrobaeys et al., 2005; Southwood et al, 2007). All these investigations raise the possibility that SIRT2 might be a functional player in oligodendrocyte differentiation. A proteomic study further strengthened the possibility. Hiratsuka et al. found that the expression level of SIRT2 in gliomas biopsy was downregulated (Hiratsuka et al., 2003). Because gliomas may happen due to uncontrolled differentiation or growth of glial cells, this piece of evidence might

implicate a regulative role of SIRT2. All together, evidences seem to implicate an undeciphered important role of SIRT2 in oligodendrocyte differentiation or growth.

Other Sirtuins

SIRT3 is a mitochondrial Sirtuin deacetylase (Onyango et al., 2002). One recent study also showed its expression in nucleus, which translocates to mitochondria upon cellular stress (Scher et al., 2007). SIRT3 is linked to adaptive thermogenesis and apoptosis regulation (Shi et al., 2005; Allison and Milner, 2007).

SIRT4, also as a mitochondrial Sirtuin, seems not to possess deacetylase activity but instead functions as an ADP-ribosyltransferase (Ahuja et al., 2007). SIRT4 downregulates glutamate dehydrogenase (GDH) in pancreatic β-cells and counteracts the effects of calorie restriction, which seems to be opposite to that of SIRT1 (Haigis et al., 2006).

Knowledge on SIRT5, the third mitochondrial Sirtuin, is still limited to date. It is known to bear NDAC activity and may influence the localization of SIRT3 when the two Sirtuins are coexpressed (Schuetz et al., 2007; Nakamura et al., 2008).

SIRT6 is a broadly expressed but predominantly nuclear-localized ADP-ribosyltransferase (Liszt et al., 2005). Mostoslavsky et al. established SIRT6 knockout mouse and demonstrated that this enzyme is a controller of genomic DNA stability and repair (Mostoslavsky et al., 2006). In addition, the phenotype of the SIRT6 knockout mice mimics multiple pathologies found in elderly humans. This study also suggested an *in vitro* deacetylase activity of SIRT6 using histones and DNA polymerase β (polβ) as its substrates (Mostoslavsky et al., 2006). Further

understandings of the exact roles and functional partners of SIRT6 are still required.

SIRT7 is a nuclear protein that correlates with cell growth. It is expressed with vast abundance in highly proliferative tissues but low in nonproliferating tissues (Ford et al., 2006). It is yet unknown whether SIRT7 possesses enzyme activities like other Sirtuins, but study has suggested that it interacts with RNA polymerase I (Pol I) as well as with histones and promotes Pol I transcription (Ford et al., 2006).

The summary of HDACs is shown in **Table 1.2**.

Table 1.2 Summary of histone deacetylases

Families	Members		Functions
Class I HDACs	HDAC1, -2, -3, -8, -11	homologue to yeast RPD3	1) form protein complex with corepressors to inhibit gene transcription 2) are crucial and versatile regulators of cell growth, differentiation or apoptosis in both physiological and pathological conditions
Class II HDACs	IIa: HDAC4, -5, -7, -9 and MITR	homologue to yeast HDA1	form protein complex with corepressors to inhibit gene expression and transcription
	IIb: HDAC6 and HDAC10		localize in cytoplasm; HDAC6 is α-tubulin deacetylase and HDAC10 functions in pre-mRNA processing
Class III HDACs (SIR2)	SIR2 in yeast Sirtuins (SIRTs) in mammals: SIRT1-7	1) homologue to yeast SIR2 2) NAD-dependent HDACs	extends animal lifespan via silencing genes SIRT1: (nuclear) deacetylates p53, FOXO3a, PGC-1α, AceCS1 and NF-κB, regulates CR, aging, cell survival, differentiation and metabolism SIRT2: (cytoplasmic) α-tubulin deacetylase SIRT3: (nuclear/mitochondrial) functions in adaptive thermogenesis and apoptosis regulation SIRT4: (mitochondrial) is not a deacetylase but a ADP-ribosyltransferase, downregulates GDH in pancreatic β-cells, counteracting the effects of CR SIRT5: (mitochondrial) affects localization of SIRT3 when the two were coexpressed SIRT6: (nuclear) controls genomic DNA stability and repair SIRT7: (nuclear) correlates with cell growth; interacts with RNA polymerase I (Pol I) as well as with histones and promotes Pol I transcription

2.3 Involvement of HDACs and Sirtuins in nervous system functions

As extensively presented above, histone deacetylation is an important regulatory mechanism of the transcription activity of chromatins. On the basis of modifying histone acetylation, HDACs participate crucially in controlling gene transcription and expression. HDACs are also pivotal regulators of cell cycles. In a variety of different cell models, the inhibition of HDACs' activity resulted in cell cycle arrest (Davis et al., 2000; Finzer et al., 2001; Ryu et al., 2006; Yamashita et al., 2003), which would be embedded with a therapeutic hope to control the growth of and induce the apoptosis of cancer cells (Kim et al., 2006).

HDACs control both cell cycle and gene transcription. This raises a possibility that HDACs play pivotal roles in cell differentiation. In the nervous system, such a possibility was supported by many elegant studies. For example, HDACs participate in the formation of transcriptional complexes to regulate neuronal or glial differentiation (Ballas et al., 2001; Ballas et al., 2005). Studies have also shown that HDACs played roles in regulating neural/glial fate specification in development. For example, inhibition of class I and class II HDACs was discovered to induce adult neural progenitors to differentiate toward neurons as opposed to a glia fate (Hsieh et al., 2004). In other investigations, delayed oligodendrocyte lineage progression and thus prolonged differentiation process was observed in presence of attenuated activities of class I and II HDACs (Marin-Husstege et al., 2002; Shen et al., 2005). These and many other evidences together implicated that HDACs might act essentially in oligodendrocyte differentiation.

Sirtuins have also been illustrated as crucial players in a variety of physiological functions or diseases in the nervous system. This could be firstly evidenced by the finding that a protective role against neuronal death and dysfunction lies in resveratrol. Treatment with resveratrol can prevent mutant polyglutamine−specific neuronal death (Parker et al., 2005). The studies in animal or cell models implicated resveratrol as an effective modulator for pathomechanisms of debilitating neurological disorders, such as strokes, ischemia, Huntington's disease (HD) or even AD (Anekonda, 2006). Other investigations on Sirtuins-modulating drugs or compounds in nervous system diseases also yield dramatic evidence supporting the essential roles Sirtuins have been playing (Mattson and Cheng, 2006).

Sirtuins also function in nervous system through regulating CR. As discussed in above sections, SIRT1 plays essential regulative roles in the effects of CR. CR improves neuronal health, and some studies suggested that the global beneficial effects of CR to the lifespan were crucially mediated via improving nervous system function. CR protects against neurodegenerative pathology in mouse models for AD (Zhu et al., 1999; Patel et al., 2005) and PD (Duan and Mattson, 1999). Accordingly, a recent study showed the preventive effects of CR on β-amyloid accumulation in AD could be mediated by SIRT1 (Qin et al., 2006). SIRT1 is found to be upregulated in mouse models for AD, ALS and in primary neurons challenged with neurotoxic insults and promote neuronal survival in cell models. Direct injection of SIRT1 into the hippocampus of disease model or application of SIRT1 activators conferred significant protection against neurodegeneration or neuronal damage (Kim et al., 2007;

Shindler et al., 2007). Moreover, SIRT1 seemed to have a protective role against the delayed Wallerian degeneration and in the peripheral nervous system of C57BL/Wlds mouse (Araki et al., 2004; Wang et al., 2005). Because mitochondrial dysfunction is commonly observed in many neurodegenerative diseases, SIRT1 is even suggested to be a central target for pharmaceutical modulation to combat these diseases since SIRT1/PGC-1 interaction has an essential role in regulating mitochondria metabolism (Rasouri et al., 2007).

Other members of Sirtuins were also involved in nervous system functions or diseases. For example, pathomechanisms of AD may involve the activities of SIRT2, SIRT3 (Anekonda and Reddy, 2006), in addition to SIRT1. The expression of SIRT2 was downregulated in gliomas (a cancer of glial cells) biopsy (Hiratsuka et al., 2003). SIRT5 polymorphisms are possibly associated with schizophrenia (Chowdari et al., 2007).

3. Protein mutations and cellular aggregates

3.1 Abnormal aggregation of proteins in CNS diseases

Abnormal accumulation and aggregation of filamentous proteins is considered as one of the important characteristics shared by various neurodegenerative diseases or disorders, such as AD, PD, HD, prion diseases and some kinds of dementias (Taylor et al., 2002; Selkoe, 2003). During the past decade, a variety of etiologically distinct diseases have been linked together by the likelihood that they are resulted from the progressive misfolding of specific proteins into aggregates that injure and kill cells.

Several physicochemical features are typically observed for almost all these protein aggregates: fibrillar morphologies, predominantly beta-sheet secondary structures, birefringence upon staining with the dye Congo red, insolubility in common solvents and detergents, and protease-resistance (Braun, 2005).

As the cell types to myelinate axons, Schwann cells in PNS and oligodendrocytes in CNS were also found to possess similar intracellular aggregations in diseases. For example, aggregation-prone mutations of a series of Schwann cell proteins lead to inherited motor and sensory neuropathies (HMSN, Berger et al., 2006). Protein aggregation in oligodendrocyte existed in diseases ranging from frontotemporal dementias with Parkinsonism linked to chromosome 17 (FTDP-17), corticobasal degeneration (CBD) and progressive supranuclear palsy (PSP) (Chin and Goldman, 1996; Goedert et al., 1998; Komori, 1999; Berry et al., 2001).

3.2 Specific protein mutations and aggregates

Studies have illustrated mutations of proteins as an important factor inducing cellular protein aggregation. Typical examples are β-Amyloid in extracellular plaques in AD and Parkin and α-synuclein in Lewy bodies in PD (Taylor et al., 2002); mutations of huntingtin are related to protein aggregation and cytotoxicity in HD (Bates, 2003); the mutated forms of photopigment rhodopsin and progranulin were respectively responsible for autosomal dominant retinitis pigmentosa (RP) and tau-negative frontotemporal dementia linked to chromosome 17 (FTDP-17) (Dryja et al., 1990; Baker et al., 2006).

Among proteins expressed in Schwann cells or oligodendrocytes, PMP22 and PLP are two aggregation-prone examples with disease-associated mutations. In the primary cultured neurons from mouse carring PMP22 mutations, aggregates were observed, which also presented when the mutated PMP22 was overexpressed in cultured cells (Ryan et al., 2002). The mutations in coding region of PLP gene are found to be responsible for Pelizaeus-Merzbacher disease. The overexpression of these mutated PLP proteins caused prominent aggregate formations in primary oligodendrocytes (Southwood et al., 2002).

3.3 Aggregates in their two appearances

On the basis on the distinctive morphologies and cellular localization, aggregates can be classified into two types: inclusion bodies (IBs) and punctate aggregates (PAs) (Gosavi et al., 2002; Lee and Lee, 2002). Inclusion bodies represent the type of aggregation localized juxtanuclearly which usually was highly fibrillar, whereas prefibrillar punctate aggregates dispersed more widely and peripherally in the cells and may denote the early stage form of inclusion bodies. This kind of inclusion bodies mimics in morphology, but are different from those “inclusion bodies” in neurodegenerative diseases. However, the abbreviation IBs here is used to describe a type of cellular aggregates in cells upon overexpression of mutant proteins or under stress. They are actually different from those “inclusion bodies” observed *in vivo* in patients and animal models.

3.4 Aggresomes

Aggresome was firstly designated and characterized in cells overexpressing a mutant form (ΔF508) of cystic fibrosis transmembrane conductance regulator (CFTR) (Johnston et al., 1998). Aggregates of CFTRΔF508 were found to be ubiquitinated, localized in the microtubule organization center (MTOC) of the cells and formed in a dynein-dependent manner. Inhibition of proteasome activity in cells overexpressing wide type CFTR also led to accumulation (Johnston et al., 1998; Johnston et al., 2002). Aggresome formation was proposed to be a general cellular mechanism against overproduced misfolded proteins exceeding the capacity of degradation machinery. Later, another research group reported that cellular aggresomes indistinguishable from those observed in CFTR-overexpressing cells were also produced by transfecting cells with GFP-250 (GFP-250 designates a protein chimera composed of an entire GFP protein fused at its C terminus to a fragment of p115 protein; Garcia-Mata et al., 1999). In contrast to the former type, the aggresomes in this study were not ubiquitinated and independent of proteasome inhibition. These studies established that aggresome formation represents a general cellular response to misfolded proteins.

Aggresomes share both morphological and biochemical similarities with inclusion bodies that characterize common neurodegenerative diseases, suggesting a close relationship between aggresome formation and neurodegeneration diseases mechanisms (McNaught et al., 2002). For example, the overexpression of α-synuclein and its interacting partner synphilin-1 caused typical aggresome formation in cultured cell lines, which mimicked both morphological and molecular characteristics of Lewy

bodies (Tanaka et al., 2004). In Lewy bodies in PD or 'dementia with Lewy bodies' (DLB), aggresome-related protein α-tubulin and pericentrin were distributed much similarly to that in aggresomes (McNaught et al., 2002). HDAC6, which is an essential factor for aggresome formation, was also found to be concentrated in the Lewy bodies of PD (Kawaguchi et al., 2003). All these evidences suggested that the understanding of aggresome formations may provide clues to decipher mysteries of neurodegenerative diseases.

3.5 The mechanisms behind protein aggregation

Although the relationship between mutations of proteins and their aggregation seems undoubted, the mechanism by which the aggregates are formed remains uncertain.

Studies suggested several causes of aggregate formation, one of which is the perturbation of protein degradation system in the cell. Ubiquitin-proteasome system (UPS) is the degradation machine of the cell. Johnston et al., (1999) reported that the inhibition of proteasome activity by ALLN resulted in aggresome formation. Studies of mutated parkin and other proteins also confirmed the result (Junn et al., 2002; Bardag-Gorce et al., 2004; Fratta et al., 2005). The resulted protein aggregations further exacerbate the disruption of UPS (Bence et al., 2001). Moreover, the mutations or overexpression of the protein may modify the structures or normal interactions of the protein. Studies suggested that overproduced proteins are overwhelming in both amounts and synthesis rate which would exceed the capacity of normal folding

machinery and degradation system in the cell. For example, Golgi apparatus is reported as fragmented in an aggregate-containing cell model overexpressing α-synuclein (Gosavi et al., 2002), suggesting the interruption of folding machinery.

Investigations also provided insights into the processes how aggregates are formed and the crucial molecules involved. For example, they are thought to form in a way depending on the microtubule network (Bauer and Richter-Landsberg, 2006). Active transport involving HDAC6 and dynein/dynactin is also reportedly important mediators for assembly of aggresomes (Johnston et al., 2002; Kawaguchi et al., 2003).

3.6 Consequences of protein aggregation

In some cases, protein aggregation represents a necessary and active regulatory step in normal cell functions, such as that in dendritic cell maturation (Lelouard et al., 2002 and 2004). But most aggregation formed because of protein mutations acts as an essential factor causing cell death or cellular toxicity in diseases. For example, the aggregation status of huntingtin protein determines neuronal loss in HD (Bates, 2003). Fibrillar α-synuclein aggregation into Lewy bodies is associated with nigrostriatral degeneration in PD (Lee and Trojanowski, 2006). One study suggested that, in protein misfolding diseases, the aggregates in host cells bearing them are inherently toxic (Bucciantini et al., 2002). They found that *in vitro* generated proteinaceous aggregates formed by various non-disease-associated proteins sharing specific domains are equally toxic and suggested the avoidance of protein aggregation is crucial for the preservation of biological functions in diseases. In a study on familial-associated

mutations of parkin, researchers suggested that the aggregation of parkin sequestered the enzyme from its native substrates, which results in accumulation of its substrates and cellular toxicity (Sriram et al., 2005).

Some other studies suggested an interesting interpretation that aggregate formation could be a cytoprotective mechanism by which the mutated or misfolded proteins could be sequestered so that the cytotoxicity was mostly eliminated. For example, aggresomes formed by overexpression of α-synuclein and synphilin-1 are found as protective forces against cell apoptosis (Tanaka et al., 2004). Aggresomes formed in pancreatic cancer cells are also considered as cytoprotective (Nawrocki et al., 2006). However, to date, no consensus has been reached with regards to whether aggregation contributes to cell death or plays protective roles.

4. The objectives of the current study

Though SIRT2 was reported to exist in oligodendrocytes (Vanrobaeys et al., 2005; Southwood et al., 2007), its exact distribution in these cells as well as in the whole CNS is still mostly unexplored. Equally limited understanding is available about its functional roles and its action mechanisms. SIRT2 is involved in stability of microtubule network (North et al., 2003), which is also important for aggregate formation (Iwata et al., 2005; Bauer and Richter-Landsberg, 2006). Also, SIRT2 is reported to interact with HDAC6 (North et al., 2003), a master regulator of aggregate formation process (Kawaguchi et al., 2003; Iwata et al., 2005).

Furthermore, if SIRT2 plays important roles in oligodendrocyte, the abnormality

of SIRT2 expression, activity or structure would be possibly correlated to the malfunction of the cellular system of oligodendrocyte or even CNS as a whole. It is more interesting since single nucleotide polymorphisms (SNPs) or variants/mutants of either rat or human SIRT2 are well documented (**Table 2.3**). The report that SIRT2 was downregulated in diseases (such as gliomas, Hiratsuka et al., 2003) as well as that it is a functional player in cellular cytotoxicity (Outeiro et al., 2007) strengthened the possibility. However, with respect of the exact roles of SIRT2 in diseases and the underlying mechanisms, very little information is reported.

The current research will be focused on the ensuing topics:

1. Mapping SIRT2 expression in CNS;

2. Investigating the functional roles of SIRT2 in the rat CNS and elucidating the molecular mechanisms underlying its effects.

3. Illustrating, if and how, the SNPs and variants/mutants of SIRT2 would change the the structural or functional properties of SIRT2, thus affecting its functions.

CHAPTER 2
MATERIALS AND METHODS

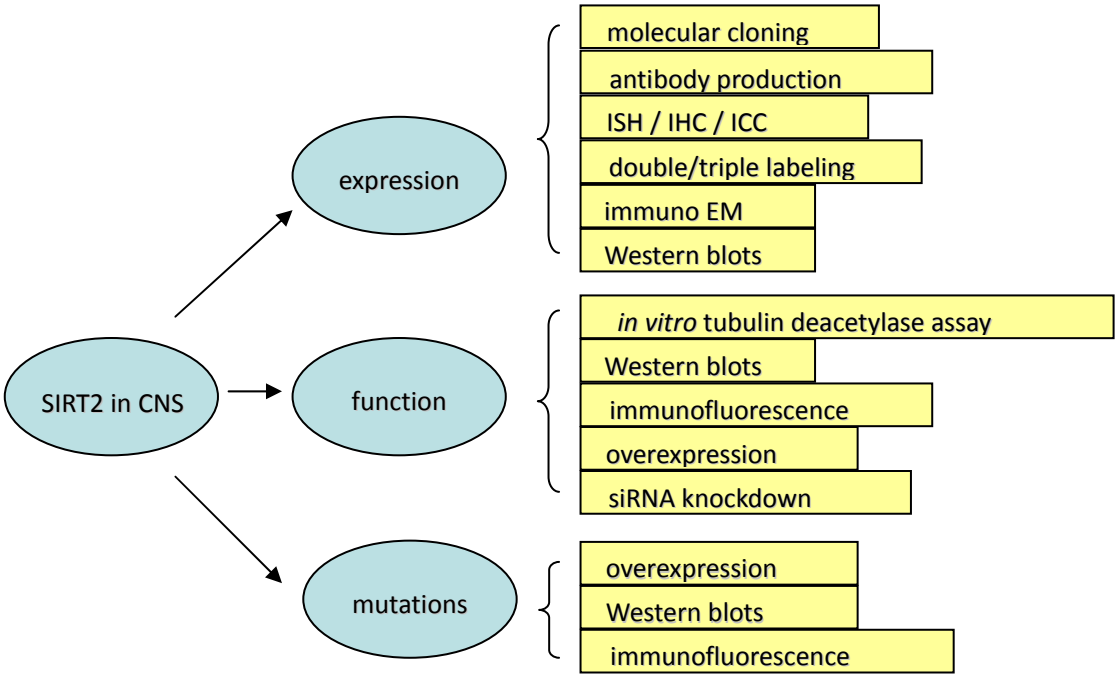

Figure 2.1 Flow chart of the methodology used in this study

The methodology used in the current study is summarized in **Figure 2.1**.

1. Chemicals

Bovine serum albumin (BSA), 4',6-diamidino-2-phenylindole (DAPI), thyroxine (T4), triiodothyronine (T3), nicotinamide (NAM), nicotinamide adenine dinucleotide (NAD), 1,4-Dithiothreitol (DTT), formaldehyde, 4-(2-Hydroxyethyl)-piperazine-1-ethanesulfonic acid (HEPES), glycine, Tris base, Tween 20, Triton X-100, putrascine, NP-40, deoxycholate, gentamicin, platelet-derived growth factor (PDGF), nocodazole and taxol were all purchased from Sigma (St. Louis, MO). Basic fibroblast growth factor (bFGF), fetal bovine serum (FBS), insulin-transferrin-selenite (ITS solution), glutamine, sodium pyruvate and low melting point agarose were all purchased from Invitrogen (Carlsbad, CA). All HPLC grade reagents (e.g. methanol and ethanol) were from Merck KGaA (Darmstadt, Germany).

2. Experimental animals

All animal uses in this study were approved by the Institutional Animal Care and Use Committee at the National University of Singapore. For antibody generation, two New Zealand White rabbits were injected with antigen every two weeks (described below). Ten days after the sixth injection, blood was withdrawn from the rabbits under anesthesia (ketamine 35 mg and xylazine 5 mg/kg body weight). Euthanasia was then administered by intracardiac injection of Nembutal (100 mg/kg). For histology, adult Wistar rats were anesthetized and euthanized with Nembutal (100 mg/kg of body weight), and subsequently perfused with saline and 3% paraformaldehyde (or 4% for immunoelectron microscopy). Brain sections of the CNS were then prepared on a cryostat (for light microscopy) or vibratome (for immunoelectron microscopy). For Western blots or primary cell culture the animals were anesthetized and euthanized with Nembutal (100 mg/kg of body weight), and their CNS or cerebra were dissected for extracting total protein or preparing primary OLPs.

3. Cloning and *in vitro* expression of rat SIRT2

This was described previously (Zhang et al., 2005). Briefly, cDNA clones from a rat brain cDNA library (Invitrogen) were sequenced and analyzed by Blast (Altschul et al., 1997). Digoxigenin-labeled cRNA probes were synthesized by *in vitro* transcription against 274 unannotated cDNA sequences. I*n situ* hybridization histochemistry (ISH) on CNS histological sections was then performed and rSIRT2 was chosen because of the predominant expression of its mRNA in neuroglial cells.

Table 2.1 Primers used for cloning and *in vitro* expression

The incorporated sites for restriction digestion as well as the codons subjected to mutagenesis are presented in capital cases.

	Name	Sequence (5'-3')	Digestion site	Remarks
1	pETrSirt2_ORF_f	GGTACC atgcagtcagacttctcaaa	KpnI	Clone nt625-1053 of
	pETrSirt2_ORF_r	GAGCTC ctagtgttcctctttctctt	SacI	rSirt2 ORF
2	pXJ-rSirt2_f	CCCGGGc atggacttcctacggaatt	SmaI	Clone rSirt2 ORF
	pXJ-rSirt2_r	GGTACC ctagtgttcctctttctctt	KpnI	
3	pEGFP-rSirt2_f	cgGAATTCt atggacttcctacggaatt	EcoRI	Clone rSirt2 ORF
	pEFGP-rSirt2_r	ggGGTACC ctagtgttcctctttctctt	KpnI	
4	rSirt2-S53CΔΔ_f	tgggagctggaatctccacaTGCatccctgact		Mutagenesis
	rSirt2-S53CΔΔ_r	tgtggagattccagctcccaccaaacagat		
5	rSirt2-N69A_f	catccactggcctctatgcaGCCttggagaaata		Mutagenesis
	rSirt2-N69A_r	tgcatagaggccagtggatggggagcggaa		
6	rSirt2-A80S_f	accaccttccatacccagagTCCatctttgaga		Mutagenesis
	rSirt2-A80S_r	ctctgggtatggaaggtggtatttctccaa		
7	rSirt2-K107Δ_f	agctctatcctgggcagttcccgaccatct		Mutagenesis
	rSirt2-K107Δ_r	gaactgcccaggatagagctccttagcaag		
8	rSirt2-N131A_f	tgctgcgctgctacacgcagGCTattgacactc		Mutagenesis
	rSirt2-N131A_r	ttccccgacg acgacgcgacgatgtgcgtc		
9	rSirt2-D133A_f	gctgctacacgcagaatattGCCactctggaacg		Mutagenesis
	rSirt2-D133A_r	aatattctgcgtgtagcagcgcagcagcag		
10	rSirt2-H150Y_f	cccaggacctggtggaggccTACggcaccttct		Mutagenesis
	rSirt2-H150Y_r	ggcctccaccaggtcctggggctccagccc		
11	rSirt2-P182L_f	agatcttctcagaagcaactCTCaagtgtgaga		Mutagenesis
	rSirt2-P182L_r	agttgcttctgagaagatcttctctttcat		
12	rSirt2-P182K_f	agatcttctcagaagcaactAAGaagtgtgaga		Mutagenesis
	rSirt2-P182K_r	agttgcttctgagaagatcttctctttcat		
13	rSirt2-K302Δ_f	ctgacctcctgggatggaaggagctggaagacc		Mutagenesis
	rSirt2-K302Δ_r	cttccatcccaggaggtcagcgagagccag		
14	hSirt2_ORF_f	cgGGATCC atggcagagccagacccc	BamHI	Clone hSirt2 ORF
	hSirt2_ORF_r	ccgCTCGAG tcactggggtttctccc	XhoI	
15	hSirt2_A117S_f	accatcttccctacccagagTCCatctttgaga		Mutagenesis
	hSirt2_A117S_r	ctctgggtagggaagatggtacttctctaggtt		
16	hSirt2_R126C_f	aggacaaggggctactcctgTGCtgctacacgc		Mutagenesis
	hSirt2_R126C_r	caggagtagccccttgtccttcagcaggcgcat		
17	hSirt2_N168A_f	tcctgcgctgctacacgcagGCCatatataccc		Mutagenesis
	hSirt2_N168A_r	ctgcgtgtagcagcgcaggagtagccccttgtc		
18	hSirt2_A198T_f	acacatcacactgcgtcagcACCagctgccggc		Mutagenesis
	hSirt2_A198T_r	gctgacgcagtgtgatgtgtagaaggtgccgtg		
19	hSirt2_P219L_f	agatcttctctgaggtgacgCTCaagtgtgaag		Mutagenesis
	hSirt2_P219L_r	cgtcacctcagagaagatcttctctttcatcca		
20	hSirt2-K339Δ_f	ctgagctccttggatggaaggagctggagg		Mutagenesis
	hSirt2-K339Δ_r	cttccatccaaggagctcagcaagggccag		

The ORF of rat rSirt2 was cloned from aforementioned cDNA library by Polymerase Chain Reaction (PCR) technique. The nucleotides 625-1053 of rSirt2 ORF, encoding the c terminus fragment of rSIRT2 (rSIRT2c), was amplified by PCR (1st pair in **Table 2.1**) and subcloned into pET41a (Novagen) for *in vitro* expression of GST tagged recombinant protein. The GST-rSIRT2c fusion protein was GST-affinity purified and used to immunize adult New Zealand white rabbits (n=2) for the generation of anti-rSIRT2 polyclonal antibody (pAb). For expression in mammalian cells, ORF sequence of rat Sirt2 was amplified by PCR and cloned in between SmaI and KpnI sites of pXJ40-FLAG (Manser et al., 1997) or EcoRI and KpnI sites of pEGFP-C1 (Clonetech), creating FLAG-rSIRT2 and EGFP-rSIRT2 overexpressing vectors (primers used are the 2nd and 3rd pairs in **Table 2.1**). Human Sirt2 was amplified by standard PCR, for which primers used are the 14th pair in **Table 2.1** and templates used are plasmids extracted from IMAGE clones 2820929 and 6093541. The generated fragment was inserted in between BamHI and XhoI sites of HA tagged pXJ40 vector, creating HA-hSIRT2 overexpressing plasmids. All human Sirt2 gene and it mutants are tagged with HA, whereas those rat Sirt2 and its mutants are FLAG tagged.

4. Mutagenesis and construction of sirt2 variants/polymorphisms

All mutants of rat or human Sirt2 were generated by GeneTailor™ Site-Directed Mutagenesis Kit (Invitrogen) as instructed by manufacturer. Briefly, wild-type plasmids were firstly methylated by a DNA methylase provided in the kit. A cycle

PCR was then performed with pairs of primers (as listed in **Table 2.1**), the forward one of which was designed to carry the target mutations. These PCRs in this study were conducted with Platinum™ *Taq* DNA polymerase (Invitrogen). Through these PCRs, linear double-stranded DNA products would be generated carrying either deletions or mutations at the desired points. Subsequently transformation of these products into DH5α^{TM}-T1^{R} competent cells was performed. These competent cells can circularize the linear mutated PCR products, but at the same time digest to clear out methylated original wild-type plasmids because of the presence of M*cr*BC endonuclease in the cells. Therefore, the colonies that subsequently arise would only be those carrying mutated forms of genes.

All residues subjected to point mutation in the present study are conserved between human and rat Sirt2 except A198T (shown in **Table 2.2** and **Fig. 3.16**), which only presents in human Sirt2. Capital case "SIRT2" usually designates the protein while lowercase "Sirt2" represents the DNA. Thus rSirt2N131A, for example, is the abbreviation for pXJ-FLAG-ratSirt2N131A plasmid, whereas hSIRT2N168A designates HA-humanSIRT2N168A protein. Other abbreviations of mutations are: rSirt2R/N: rSirt2 with double mutations at R126C and N131A; rSirt2N/H: rSirt2 with double mutations at N131A and H150Y; rSirt2N/K: rSirt2 with double mutations at N131A and K302Δ; rSirt2R/N/K: sirt2 with triple mutations at R126C, N131A and K302Δ; rSirt2S53CΔΔ: point mutation S53C together with deletions of A54 and G55.

Table 2.2 Point mutations of human and rat Sirt2 in the current study

Single- or multiple-point mutated forms of human and rat Sirt2 gene are generated by GeneTailor mutagenesis kit and used for transfecting cells in the current study. Several of those mutants are documented in SNP or gene/protein databases in NCBI or exist in MGC cDNA clones.

human Sirt2	rat Sirt2	multiple-point mutation	documentation
-	S53CΔΔ	S53C+A54Δ+G55Δ	EAW56836
-	N69A		-
A117S	A80S		Gn1/dbSNP/rs 2241703
-	K107Δ		EAW56834
R163C	R126C		-
N168A	N131A		-
-	D133A		-
-	H150Y		-
A198T	-		Gn1/dbSNP/rs 34321258
P219L	P182L		CAD43717
-	P182K		-
K339Δ	K302Δ		MGC: 105900
-	R/N	R126C+N131A	
-	R/N/K	R126C+N131A+K302Δ	
-	N/K	N131A+K302Δ	
-	N/H	N131A+H150Y	

All together, a total of 15 rSirt2 mutants consisting of rSirt2S53CΔΔ, rN69A, rA80S, rK107Δ, rR126C, rN131A, rR/N, rR/N/K, rN/K, rD133A, rH150Y, rN/H, rP182L, rP182K or rK302Δ were derived from mutations of codons for 12 conserved amino acid residues of rSIRT2. Of the mutants highlighted in bold, in particular, the human corresponding point to **rA80S** (or hA117S) has been reported as a single nucleotide polymorphism of human Sirt2 (Gn1/dbSNP/rs 2241703); the human counterparts for **rS53CΔΔ** (NCBI accession: EAW56836), **rK107Δ** (EAW56834) and **rP182L** (CAD43717) are also found in human Sirt2 DNA/protein sequences in NCBI databases. **rK302Δ** is present in a rat Sirt2 cDNA clone (MGC: 105900). **hA198T** is also documented as a SNP but not conserved between rat and human (Gn1/dbSNP/rs

34321258).

5. siRNA knockdown

Table 2.3 siRNAs used in the current knockdown experiments

siRNA	name	Sequence (5'-3')	Position in gene	Knockdown efficiency
1	siSirt2a	ggagcgucugcuggacgag dTdT	518-540	+++++
2	siSirt2b	gggagcaugccaacauaga dTdT	1390-1412	+++
3	siSirt2c	ggcucugccuccaacaaag dTdT	1927-1949	+
4	siHDAC6	gggaugacagcuucccggaag dTdT	284-306	+++
5	siJN	auuuaagacaugccagcagu dTdT	3235-3257	+++

As shown in **Table 2.3**, siRNA duplexes against nucleotides 518-540, 1390-1412 and 1927-1949 of rat SIRT2 (NM_001008368), nucleotides 284-306 of human HDAC6 (BC013737) and nucleotides 3235-3257 of rat Juxtanodin (NM_001008311) were commercially synthesized (1stBase, Singapore). Expression plasmids were transfected into the primary OLPs and immortalized cell lines using either electroporation by MP-100 Microporator (Digital Bio Technology, Kyonggi, South Korea), or Lipofectamine 2000 (Invitrogen, Carlsbad, CA); siRNAs were transfected using RNAiMax (Invitrogen). Nocodazole and taxol (Sigma) was added into the culture medium at indicated concentrations 12 h before the cells were fixed or lysed.

6. Antibodies

For purification of the rabbit anti-rSIRT2 polyclonal antibody, the GST-rSIRT2c$^{209-351}$ recombinant protein was resolved by SDS-PAGE, transferred to polyvinylidene difluoride membranes (PVDF, PerkinElmer) and used for affinity purification of anti-rSIRT2 antibody. In detail, with the help of ponceau S staining, the

membrane slices containing the recombinant protein bands could be visualized and excised. These slices were then minced into small pieces and incubated for overnight at 4^0C with the antiserum from aforementioned rabbits after 6 times immunization (diluted with equal volume of ice cold PBS). The immunoglobulin bound to these slices was eluted down by three times wash with Glycine-HCl (pH 2.5-3.0).

All other antibodies used in this thesis are commercially available. Anti-acetylated α-tubulin 6-11B-1 (ICC 1:1000, IB 1:2000), anti-α-tubulin B-5-1-2 (ICC 1:1000, IB 1:2000), anti-FLAG M2 (ICC 1:1000, IB 1:5000), anti-β-actin (IB 1:5000), anti-pan sodium channel (NavP, 1:200), anti-β-COP (ICC 1:500, IB 1:1000), and anti-neurofilament 200 (ICC 1:1000) were all purchased from Sigma. Anti-actin C4 (IB 1:2000), anti-MBP (ICC 1:200), anti-GFAP (ICC 1:200), and anti-A2B5 (ICC 1:200) were obtained from Millipore (Billerica, MA). Other primary antibodies included anti-CNP (ICC 1:200, IB 1:400, US biological, Swampscott, MA), anti-GD3 (ICC 1:200, AbCam), anti-OX42 (ICC 1:50, Harlan Sera-lab, Leicestershire, UK) anti-EGFP (ICC 1:500, IB 1:1000, Invitrogen), anti-ubiquitin (ICC 1:300, IB 1:1000, Santa Cruz biotechnology, Santa Cruz, CA), anti-histone 3 and anti-potassium channel Kv1.2 (1:300, Upstate Biotech, Lake Placid, NY). Secondary antibodies consist goat anti-rabbit and/or mouse IgG conjugated to alkaline phosphatase (AP, Millipore) or biotin (Vector Labs, Burlingame, CA), and Alexa fluro 488 or 568 conjugated goat anti-rabbit or mouse IgG or IgM antibodies (Invitrogen).

7. Cell culture

Cell lines used in the experiments included OLN-93, 293T and HeLa (generous gifts from A/P Xiao Zhicheng's laboratory, Singapore General Hospital), SHEP (purchased from The American Type Culture Collection, USA) and B104 (kindly provided by Dr. Franca Cambi, University of Kentucky, USA). All these cells were routinely cultured in Dulbecco's modified Eagle's medium (DMEM, Sigma) supplemented with 10% FBS.

Isolation and culture of primary oligodendrocyte precursor cells (OLP) followed previous protocols (McCarthy and de, 1980; Armstrong, 1998). Cerebra of 1-2 day old Wistar rats were dissected and minced, and the dissociated cell suspension was cultured for 9-10 days in DMEM plus 10% FBS, 1 mM sodium pyruvate and 25 μg/ml gentamicin before immature OLPs (purity > 90%) were isolated by shaking and selective detachment. The OLPs were then maintained proliferating for 3-5 days in DMEM plus sodium pyruvate (1 mM), gentamicin (25 μg/ml), insulin (5 μg/ml), transferrin (50 μg/ml), selenium (30 nM), glutamine (2 mM), thyroxine (T4, 0.4 μg/ml), triiodothyronine (T3, 0.3 μg/ml), FBS (2%), platelet-derived growth factor (PDGF, 10 ng/ml, Sigma) and basic fibroblast growth factor (bFGF, 10 ng/ml, Invitrogen). One to six days before transfection or fixation for immunocytochemistry, the mitogens were withdrawn from the medium to allow the cells to differentiate on poly-D-lysine (PDL, 10μg/ml) coated Thermanox pre-treated cover slips (NUNC, Nalge Nunc International, Rochester, NY) in the culture plates.

All cell culture plastic wares were purchased from NUNC or Falcon (Becton

Dickinson, San Jose, CA).

8. Transfection of cells

Two kinds of transfection methods were used in the experiments.

Method 1: All the cell lines or OLPs were grown on coverslips until ~50% confluence. They were then transfected by overexpressing plasmids with Effectene transfection reagent (Qiagen) or with Lipofectamine 2000 (Invitrogen), or by siRNA with Lipofecamine RNAiMax (Invitrogen). The transfection method with Effectene was slightly modified that, in comparison to manufacturer's instruction, we added 0.16μg plasmid instead of 0.2μg into each well of 24-well plate, and the buffer volumes for each well were also proportionally decreased. The transfection with the other two kits was carried out according to the manufacturers' instructions.

Method 2: In the studies to test rat and human SIRT2 detergent-solubility and aggregation-prone properties, OLN-93 cells or 293T cells were transfected by using MP-100 Microporator (Digital Bio Technology, Kyonggi, South Korea). For OLN-93 transfection, cells were kept in DMEM supplemented with 10% FBS until ~80% confluence and detached from flasks by trypsin. Cells were washed twice with Ca^{2+}-free PBS and cell densities were calculated with hemacytometer. For one single shoot with the 10μl golden tip, 3×10^5 cells were used, which were resuspended in buffer R and combined with 0.5μg plasmids. Three crucial parameters for the electroporation were pulse voltage, width and pulse numbers, which were set as1400V, 20ms and 2 times for OLN-93 cells; the transfection procedures for 293T is mostly

same as for OLN-93 cells except the parameters being set as1300V, 30ms and 3 times.

After transfection, cells were harvested and lysed for western blotting by M-PER® Mammalian Protein Extraction Reagent (Pierce, Rockford, IL), or fixed with 3% paraformaldehyde for immunocytochemistry.

9. Western blotting

Samples from animal tissues or cell lysates were generated using T-PER® or M-PER® Protein Extraction Reagents (Pierce) supplemented with cocktail protease inhibitor (Pierce), following instructions from the manufacturers. These samples were resolved by 10% or 12% SDS-PAGE and transferred to PVDF membranes. After blocking by PBS-T-NGS-milk [PBS, 0.1% Tween 20, 2% normal goat serum and 5% non-fat blocking milk (BioRad, Hercules, CA)] for 1hr at RT, membranes were probed with designated primary antibodies at RT overnight. The membrane was then washed and incubated with alkaline phosphate-conjugated secondary antibody. Immunodetection was performed using CDP-Star chemiluminescent reagent (Roche, Basel, Switzerland) and X-ray films (Kodak, New Haven, CT).

10. Immunoprecipitation and *in vitro* tubulin deacetylase assay

For immunoprecipitation of GFP-rSIRT2 or its mutants, 2-mg transfected OLN-93 lysate was firstly pre-cleared with 30 μl protein A-agarose (Amersham Pharmacia) at 4°C for 3h, followed by incubating with 6 μg anti-EGFP (Invitrogen) for 8h at 4°C and finally 50 μl protein A-agarose for 4h at 4°C. For *in vitro* α-tubulin

deacetylase assay, refer to North et al. (2003). Briefly, we resuspended the immunoprecipitate harvested as described above in 150 µl deacetylase buffer (50 mM Tris-HCl pH9.0, 4 mM MgCl2, and 0.2 mM DTT) and divided it into three portions of 50 µl each, to which 40 µg OLN-93 cell lysate was added together with either NAD or NAM (as described in Result chapter). Reactions were terminated by adding SDS-PAGE sample buffer.

11. Solubility tests of SIRT2 mutants

To isolate soluble and insoluble fractions of rSirt2 or hSirt2 transfected cells, please refer to a previous study (Garcia-Mata et al., 1999). Briefly, OLN-93 or 293T cells were transfected with Microporator and seeded onto wells of 6-well plates. Transfected cells were harvested by trypsinization at various time points (for solubility kinetics analyses), or at 36/48 hours after transfection (for other analyses), washed and resuspended with PBS. After centrifugation, the cell pellets were lysed in one of the following three lysis buffers of increasing detergent strength for 30 min on ice. These buffers are: PBS with 2% Triton X-100, IPB (10 mM Tris-HCl, pH 7.5, 5 mM EDTA, 1% NP-40, 0.5% deoxycholate, and 150 mM NaCl), and RIPA buffer [50 mM Tris-HCl, pH 8, 1% NP-40, 0.5% deoxycholate, 0.1% sodium dodecyl sulfate (SDS) and 150 mM NaCl], all supplemented with protease inhibitor cocktail (Pierce). The lysates were then passed 10 times through 27-gauge needles, and centrifuged at 13,000×g for 15 min at 4°C to separate the soluble supernatants from the insoluble pellets. Pellets were then resuspended in PBS with 1% SDS (equal volume to the

supernatants) and sonicated to dissolve. Equal volumes that represent equal percentages of each pellet and supernatant were used for further Western blots analysis.

12. *In situ* hybridization histochemistry

This is done as previously described (Liang et al., 2000; Zhang et al., 2005). Briefly, *in vitro* transcribed digoxigenin-labeled cRNA probe was generated using the same rSirt2 cDNA fragment (as template) as for developing antibody (nucleotides 625-1053 of the open reading frame). Free-floating histological brain sections representing different regions were rinsed sequentially in PBS, 0.75% glycine, 0.3% Triton X-100, 1 μg/ml proteinase K and 0.25% acetic anhydride in 0.1 M triethanolamine. Following that, sections were washed in saline sodium citrate (SSC) and at 60°C in a hybridization buffer omitted probes. The hybridization of sections with the probe generated (0.6 μg/ml) was carried on for overnight at 62°C. The hybridization buffer consisted of 2× SSC, 2% blocking reagent (Boehringer Mannheim, Germany), 50% deionized formamide, and 0.1% N-lauroylsarcosine.

After the hybridization step, sections were sequentially treated in (all containing 0.1% N-lauroylsarcosine except ribonuclease A) these solutions: 1) 2× SSC plus 50% deionized formamide at 60°C; 2) ribonuclease A buffer (0.01 M Tris-HCl buffer, pH 8.0, plus 1 mM ethylenediaminetetraacetic acid and 0.5 M NaCl) at RT; 3) ribonuclease A(0.02 mg/ml in ribonuclease A buffer) at 37°C; 4) 2× SSC at 60°C; 5) 0.2× SSC at RT once and then at 60°C once. Finally, the hybridization signals were

detected by AP conjugated anti-digoxigenin antibody and the NBT (nitro-blue tetrazolium)-BCIP (5-bromo-4-chloro-3´-indolylphosphate) reaction. Rinsed sections in 0.1 M Tris-HCl buffered saline (TBS, pH 7.5) were incubated in 1% blocking reagent in TBS, and then in alkaline phosphatase-conjugated sheep anti-digoxigenin antibody. After three washes in TBS plus 0.1% Tween 20, AP activity was visualized by NBT-BCIP reaction. All the reagents and enzymes for RNA *in vitro* transcription and hybridization were purchased from Roche.

13. Immunofluorescent double/triple labeling

For immunofluorescent double/triple labeling, histological sections of the rat CNS or fixed cells were washed with PBS and pre-incubated with PBS-T-NGS [0.1M PBS, 0.3% triton X-100 and 6% NGS] to block non-specific binding sites. Primary antibodies were then added for overnight incubation at RT. Secondary antibodies conjugated with either Alexa fluor 488 or 568 were used for detecting the primary antibodies. After washing with PBS, fixed cells were routinely stained for 15 minutes with 200ng/ml DAPI solution before being mounted and analyzed, whereas histological sections were mounted directly.

14. Immunohistochemistry (IHC) and transmission electron microscopy (TEM)

For immunoperoxidase (avidin-biotin-peroxidase method) and immunoelectron microscopy, refer to protocols described previously (Ling et al., 1992; Liang et al., 2000). Briefly for IHC, free-floating sections were washed with PBS for 4 times at RT,

followed by PBS-T-NGS blocking for 1hr at RT. The sections were then incubated with primary antibodies dissolved in PBS-T-NGS at RT for overnight. After 4 times wash with PBS, they are incubated with biotinylated secondary antibodies at RT for 75 minutes with shaking. Again after 4 times wash with PBS, avidin-biotin complex (1:100 avidin and biotin in 0.1M phosphate buffer with 0.15% triton X-100 and 3% NGS) was used to incubate the sections for 75 minutes at RT. Then sections were washed with 0.05M tris buffer (TB) pH 7.4-7.6 for 4 times, followed by washing with 0.05% ammonium nickel sulphate [$(NH_4Ni(SO4)_2$] in 0.05M TB for 3-5 minutes. The sections were lastly incubated with 0.05 % DAB dissolved in 0.05M TB plus 0.01% H2O2 and 0.05% [$(NH_4Ni(SO4)_2$], this step is color reaction step. The reaction was stopped when clear signals can be observed (usually ranged from 3-120 minutes), by removing the color reaction solution and refilling the wells with 0.05M TB.

For immuno EM, the immunohistochemical signals were harvested by same procedures as IHC. The tissue sections with IHC signals are cut into small pieces (1-4 mm^2) and post fixed in 1% OsO4, pH 7.4 for 1 hour at RT (perform in fume hood). After that, these small section pieces were dehydrated through an ascending ethanol series at room temperature:

25% Ethanol - 5 minutes
50% Ethanol - 10 minutes
75% Ethanol - 10 minutes
95% Ethanol - 10 minutes
100% Ethanol - 10 minutes
100% Acetone - 10 minutes (2 changes)

Next, small sections are infiltrated sequentially with:

a. 100% acetone : resin (1 : 1) for 30 minutes at room temperature (optional).
b. 100% acetone : resin (1 : 6) for overnight at room temperature.

c. 1st change of fresh resin --- 20 minutes at room temperature then transfer to 40^0C for 30 minutes.
d. 2nd change of fresh resin --- 1 hour at 45^0C.
e. 3rd change of fresh resin --- 1 hour at 50^0C.

The tissues were then embed in fresh resin and polymerise at 60^0C for 24 hours. After which the sections could be sliced into ~100nm thickness pieces for observation under TEM.

15. Data analyses

All data were verified by at least two repeats of the experiments. Statistical significance between experimental and control groups were calculated by Student's *t-test*. Immunofluorescent microscopic results were analyzed using a laser scanning confocal microscope (Olympus Fluoview FV1000, Olympus). Western films were scanned by GS-710 Calibrated Imaging Densitometer (BioRad), and the band density was calculated by multiplying the mean OD (after subtracting background) with the band area (mm2) using Quantity-One (v3.1, BioRad). Relative expression abundance of rat SIRT2 during developmental stages was calculated by dividing the ODs of SIRT2 or CNP bands by corresponding β-actin bands of the same stage.

For complexity analyses, SIRT2 or CNP-positive OLPs were classified as simple if they only had 1-3 primary processes, as intermediate if they had over 3 straight radial primary branches with small secondary processes, as complex if many tertiary and further branches emerged, and as highly complex if the distal processes became wooly or fused to form lamellipodia around the cell bodies (see examples in Results; Marin-Husstege et al., 2002).

The solubility of SIRT2 mutants was calculated by dividing the percentage of bands densities in soluble portion with the sum of the soluble and insoluble portions together. Aggregate-positive cell percentage represents the percentage of cells showing cytoplasmic aggregates relative to total transfected cells from at lease five random fields (>200 transfected cells) under 20× objective of the microscope.

CHAPTER 3
RESULTS

1. The generation of rabbit polyclonal anti-SIRT2 antibody

1.1 Expression of recombinant GST-SIRT2c protein

The rat Sirt2 mRNA contained an open reading frame encoding a 351-amino-acid protein. The C terminus of rat SIRT2 (amino acid 209-351, SIRT2c) bears a high antigenicity score. Therefore a polyclonal antibody against this part of rat SIRT2 protein was generated. PCR was first performed using the No.1 pair of primers (**Table 2.1**), the product of which was then inserted in between KpnI and SacI sites of the pET 41a vector. High level of GST-SIRT2c expression could be observed after the generated plasmids were transformed into BL21 (DE3) host cells and induced to express recombinant protein by addition of 0.5mM IPTG (**Fig. 3.1 A**). This recombinant protein was used to immunize rabbit and generate polyclonal rabbit anti-SIRT2 antibody (refer to Material and methods for details).

1.2 Specificity tests of the antibody

The specificity of this recombinant protein was firstly tested by Western blot analyses. Recombinant GST-SIRT2c (~44kDa) could be successfully detected by this affinity-purified GST-adsorbed anti-SRIT2 antibody; similarly a commercial GST antibody did detect a band at the same position (**Fig. 3.1 B**, lanes 1 and 2). On other blots, the antibody detected a doublet band around 37 kDa in adult rat brain protein samples (**Fig. 3.1 B**, lane 4), whereas preimmune serum could not reveal immunoreactivity at this position (**Fig. 3.1 B**, lane 3).

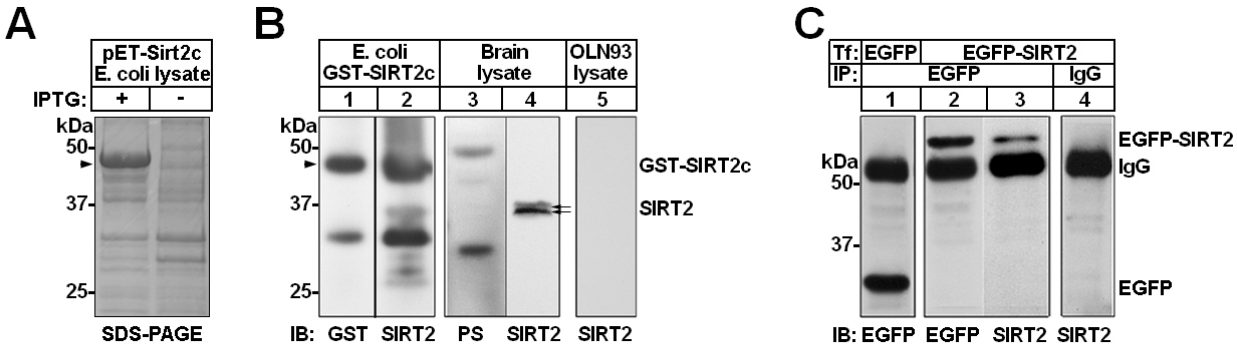

Figure 3.1 Molecular features of rat SIRT2 protein

(A) pET-Sirt2c (625-1053) plasmid was transformed into BL21 (DE3) host bacteria and recombinant GST-SIRT2c protein was induced to express. Arrowhead points to an abundantly expressed protein band, which was proposed to be GST-SIRT2.
(B) Western blots, showing specificity tests of rabbit polyclonal anti-SIRT2 antibody. Labels above and below blots indicate the protein sample origins and antibodies used for immunoblotting detection (IB), respectively. GST-SIRT2c, recombinant GST-SIRT2c (209-351) protein expressed in E. coli; PS, pre-immunization serum (rabbit serum before the first time immunization); Double arrows indicate the SIRT2 doublet band detected by rabbit anti-SIRT2. Arrowhead points to the position of GST-SIRT2c.
(C) OLN-93 cells were transiently transfected (Tf) with either pEGFP-C1 vector (lane 1) or pEGFP-Sirt2 (lanes 2-4). Forty-eight hours after transfection, lysates of the cells were subjected to immunoprecipitation (IP) using anti-EGFP or irrelevant IgG, followed by immunoblotting (IB) with antibodies indicated below.

To further determine the specificity of the antibody, we inserted Sirt2 open reading frame into pEGFP-C1 mammalian expression vector. OLN-93 (a rat oligodendrocyte cell line, Richter-Landsberg and Heinrich, 1996) cells transfected with the pEGFP-SIRT2 were lysed, immunoprecipitated using anti-EGFP antibody, and then subjected to immunoblots. The band for the recombinant EGFP-SIRT2 emerged at around 66 kDa, as detected by either the anti-SIRT2 or an anti-EGFP antibody (**Fig. 3.1 C**, lanes 2 and 3). In the lysate of OLN-93 transfected with empty pEGFP vector, EGFP was precipitated and migrated to around 29 kDa (**Fig. 3.1 C**,

lane 1). By contrast, irrelevant IgG (anti-FLAG M2, Sigma) cannot precipitate the recombinant protein (**Fig. 3.1 C**, lane 4). Together, the antibody proved adequately specific for further experiments.

2. SIRT2 was expressed predominantly in rat CNS

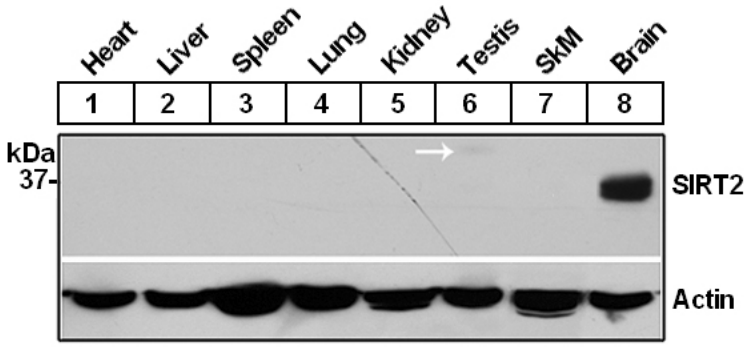

Figure 3.2 Distribution of rat SIRT2 protein in different tissues
In this multi-tissue Western blot, samples from 8 different tissues were probed with rabbit polyclonal anti-SIRT2 antibody or anti-pan-actin antibody. Only in rat brain but not in other seven tissues, could significant SIRT2 signal be detected, although there seemed a very faint band (around 41 kDa, white arrow) in testis lysate. The pan-actin signals in the lower panel work as the loading control. (SkM, skeleton muscle).

To test the overall distribution of SIRT2 protein, we harvested protein samples from 7 different rat tissues and identified the expression of SIRT2 by Western blots. On the blots probed with this anti-SIRT2 antibody, the 37 kDa SIRT2 doublet band was detected in brain protein sample, but not in that of the heart, liver, spleen, lung, kidney, testis, or skeletal muscle, although a weak 41 kDa band, which we presumed to be a SIRT2 splicing variant, was seen in testis protein lysates (**Fig. 3.2**).

3. Postnatal SIRT2 expression level co-fluctuates with that of CNP

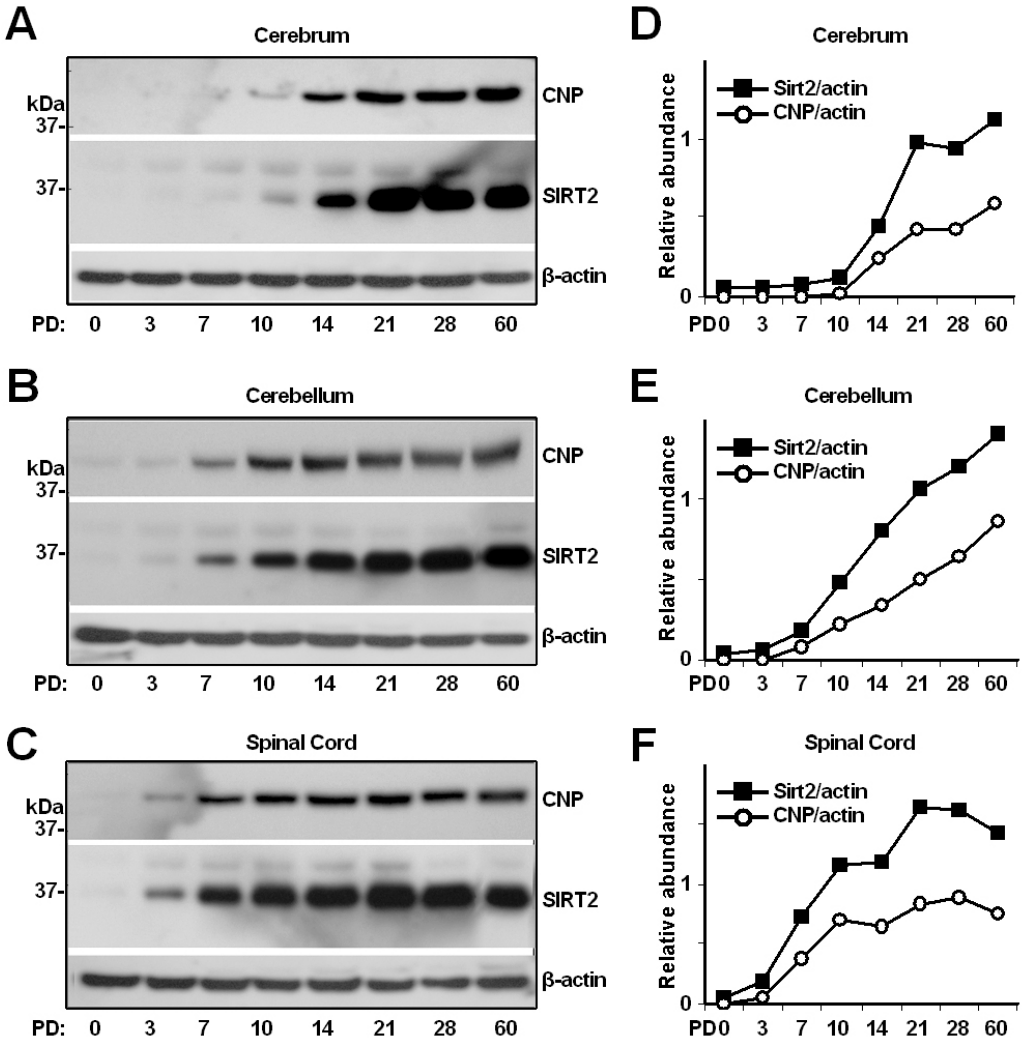

Figure 3.3 Developmental expression of SIRT2 protein in rat CNS
(A-F) Western blot analyses comparing the expression profiles of SIRT2 and CNP in postnatal 0, 3, 7, 10, 14, 21, 28, 60 rat cerebrum, spinal cord and cerebellum, respectively. Each lane was loaded with 20 μg of soluble tissue lysate. Signals for β-actin served as loading controls. Quantitative analyses of expression levels of SIRT2 and CNP relative to β-actin in the different CNS regions are shown on the right (panels G, H and I). PD, postnatal day.

To investigate the developmental expression of SIRT2, protein samples of the cerebra, cerebella and cervical spinal cords of rats aged 0, 3, 7, 10, 14, 21, 28, and 60

postnatal days were subjected to western blots. In the cerebrum, the 37 kDa SIRT2 was expressed marginally at PD7, clearly visible at PD10, increased sharply at PD14, and approximated adult level at PD21 (**Fig. 3.3 A**). In both cervical spinal cord and cerebellum, the signal appeared at PD3, but higher abundance and earlier approximation to adult level (PD10) was detected in spinal cord (**Fig. 3.3 B and C**). In comparison, immunoblotting signals for the 42 kDa CNP emerged at approximately the same time as SIRT2 in all the three CNS regions, and co-fluctuated with those of SIRT2 along the various postnatal ages (**Fig. 3.3 D-F**). Interestingly, the 41 kDa minor band of SIRT2 showed up earlier than the 37 kDa band, and then decreased to very low levels in all three regions of PD60 CNS.

4. SIRT2 as a protein of oligodendroglia and myelin

4.1 *In situ* hybridization histochemistry (ISH)

The digoxigenin-labeled cRNA probe for ISH was generated against the same fragment as for antibody development, which is the nt625-1053 part of Sirt2 ORF. As shown in **Figure 3.4**, Sirt2 mRNA-positive signals were seen not only in the gray matter but also in the white matter throughout most CNS regions. Positive cell bodies in the gray matter were typically dispersed, round-shaped and of relatively small sizes, whereas those in the white matter were more variable in morphology (**Fig. 3.4 A-D**). The strength of hybridization signals was highest in corpus callosum and hippocampal formation, followed by thalamic nuclei, the cerebral and cerebellar cortices, caudate puteman and spinal cord. In the neocortex, the Sirt2 mRNA-positive cells distributed

more intensely in layer IV and V (**Fig.3.4 G**). In the cerebellum, staining sometimes appeared in proximal processes in addition to cell bodies, suggesting a possibility of local translation (**Fig. 3.4 E**).

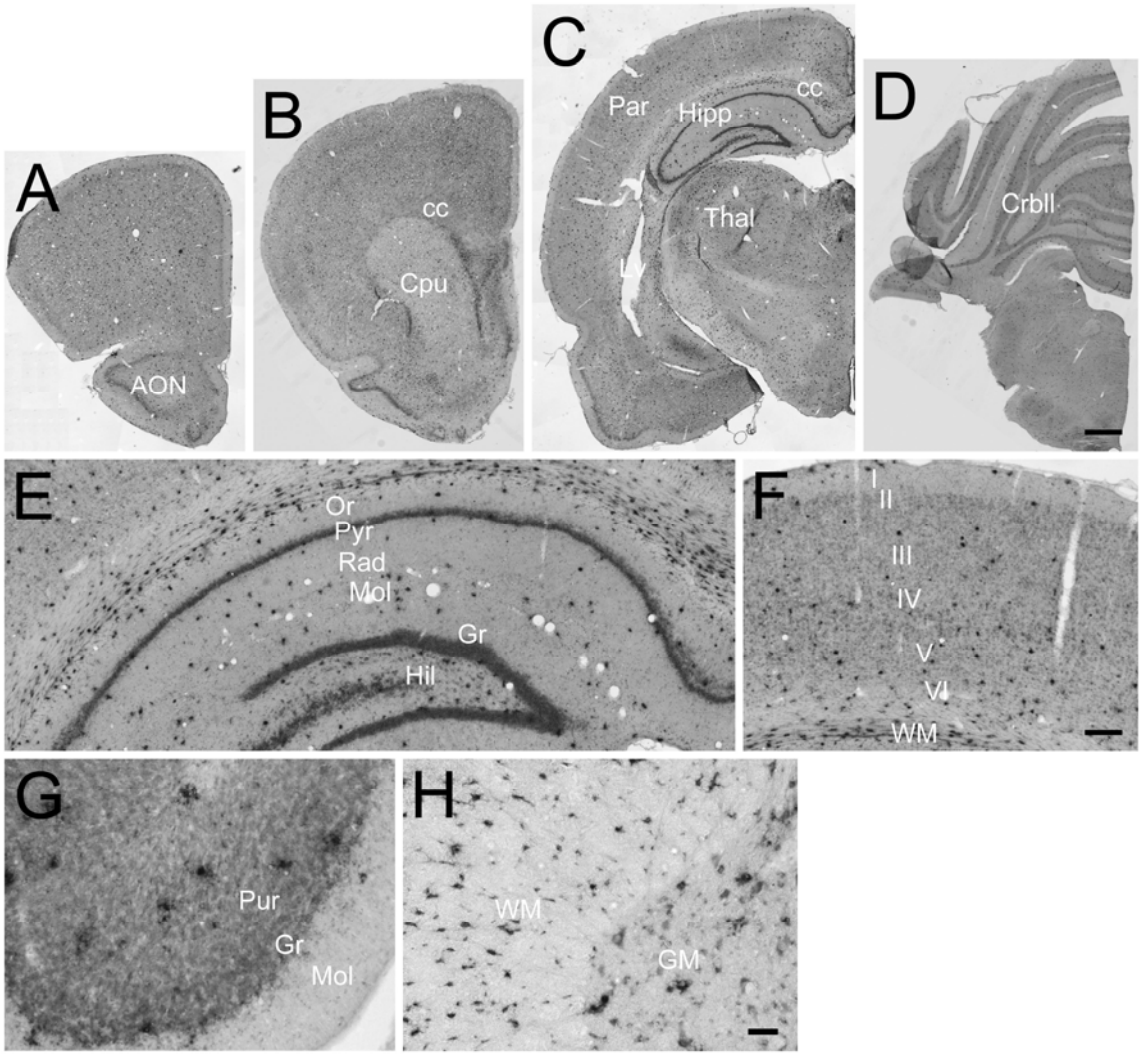

Figure 3.4 Distribution of Sirt2 mRNA in rat CNS

In situ hybridization histochemical photomicrographs showing expression of Sirt2 mRNA in representative CNS regions, including forebrain (A-C), cerebellum (D, G), hippocampal formation (E), parietal cortex (F) and spinal cord (H). Abbreviations: AON, anterior olfactory nucleus; Cpu, caudate puteman; cc, corpus callosum; I–VI, layers of cerebral cortex; GM, gray matter; Gr, granule cell layer of dentate gyrus (E) or cerebellar cortex (G); Hil, hilar region of hippocampal formation; Hipp, hippocampus; LV, lateral ventricle; Mol, stratum lacunosum-moleculare of hippocampal CA1 (E) or molecular cell layer of cerebellar cortex (G); Or, stratum orien; Par, parietal cortex; Pyr, stratum pyramidale; Rad, stratum radiatum; Thal, thalamus; WM, white matter. Scale bars: 800 μm in A-D; 200 μm in E and F; 20 μm in G and H.

4.2 Immunohistochemistry (IHC)

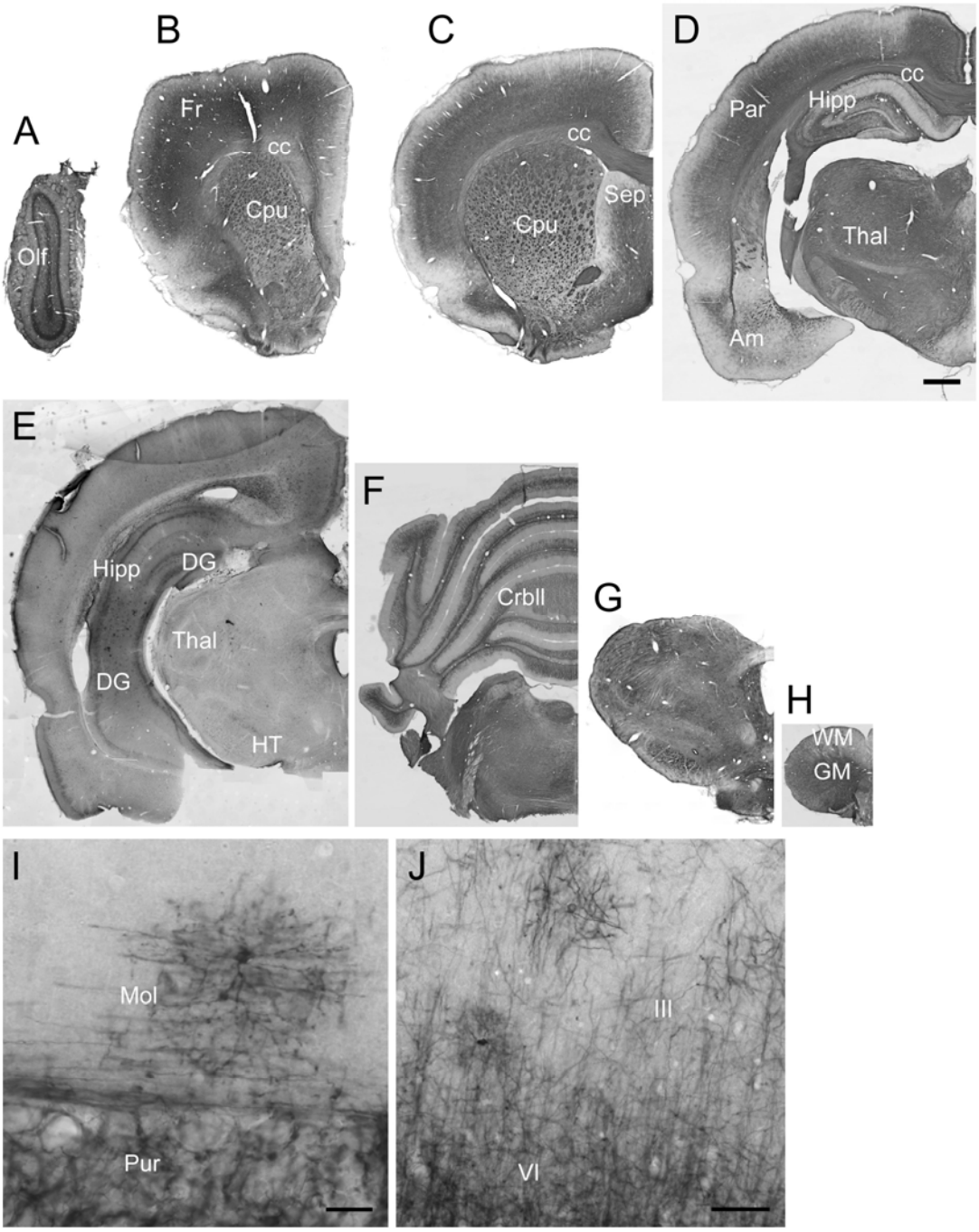

Figure 3.5 Distribution of SIRT2 protein in rat CNS

Immunohistochemical photomicrographs showing expression of SIRT2 protein in representative CNS regions, including olfactory bulb (A), forebrain (B-E), cerebellum (F, I), parietal cortex (J) and spinal cord (G, H). Abbreviations: Am, amygdala; cc, corpus callosum; Cpu, caudate putamen; III and VI, layers of cerebral cortex; DG, dentate gyrus; Fr, frontal cortex; GM, gray matter; Hipp, hippocampus; HT, hypothalamus; Mol, molecular cell layer of cerebellar cortex; Olf, olfactory bulb; Par, parietal cortex; Thal, thalamus; WM, white matter; Crbll, cerebellum and . Scale bars, 800 μm in A-H, 20 μm in I and J.

IHC with the anti-SIRT2 antibody revealed distribution of SIRT2 protein in various regions of the brain (**Fig. 3.5 A-H**). The expression was most abundantly detected in corpus collusum, cerebral and cerebellar cortex, followed by caudate puteman, hippocampus and spinal cord. In the cerebral cortex, the histochemical signals of of SIRT2 are very low in superficial layer I and II, but become stronger in layer V and VI and subcoritcal white matter (**Fig. 3.5 J**). In the cerebellar cortex, SIRT2 immunoreactivity was abundant in the granule and Purkinje cell layers. The molecular layer, however, was mostly devoid of SIRT2 signals with the exception of a few scattered cells and related processes near the Purkinje cell layer (**Fig. 3.5 I**). These scattered cells with processes are also occasionally observed in other regions of the CNS, such as cerebral cortex (**Fig. 3.5 J**).

4.3 Immunofluorescent double labeling

Double immunofluorescent study established that SIRT2 expression in the CNS was primarily confined to oligodendrocytes. Colocalization between SIRT2 and CNP, a well-characterized oligodendrocyte marker in the CNS, was seen in all CNS regions examined (**Fig. 3.6 A-D**). **Figure 3.6A** shows the cerebellar cortex where SIRT2 immunoreactive signals overlapped those of CNP in the oligodendroglial processes, along myelinated axons in the Purkinje cell and granule cell layers, and in the subcortical white matter. The CNP-positive perikarya of oligodendrocytes, however, were frequently devoid of detectable SIRT2 (insets in **Fig. 3.6 A and K**). Similar colocalization of SIRT2 and CNP in oligodendroglial processes/along myelinated

axons, and absence of SIRT2 in the oligodendrocytic cell bodies were found in, among others, the caudate nucleus and in the gray and white matters of cervical spinal cord (**Fig. 3.6 B-D**). Double labeling against SIRT2 and MBP, another group of marker proteins for oligodendroglia and myelin sheath, confirmed the above findings. Figure 3.5I and J illustrate such examples of SIRT2 colocalization with MBP in oligodendroglial processes and along myelinated axons in the cerebral cortex and the hippocampal formation, respectively. SIRT2 was not detected in astrocytes marked by glial fibrillary acidic protein (GFAP), in microglia marked by OX42, nor in neurons marked by neurofilament 200 (NF200) (**Fig. 3.6 E-H**). It is noteworthy that in certain areas such as cerebral and cerebellum cortex, the positivity of SIRT2 usually formed a cluster and seemed to present only in bundles surrounding a cell but never in the cell body or perikerya (**Fig. 3.6 K, L**).

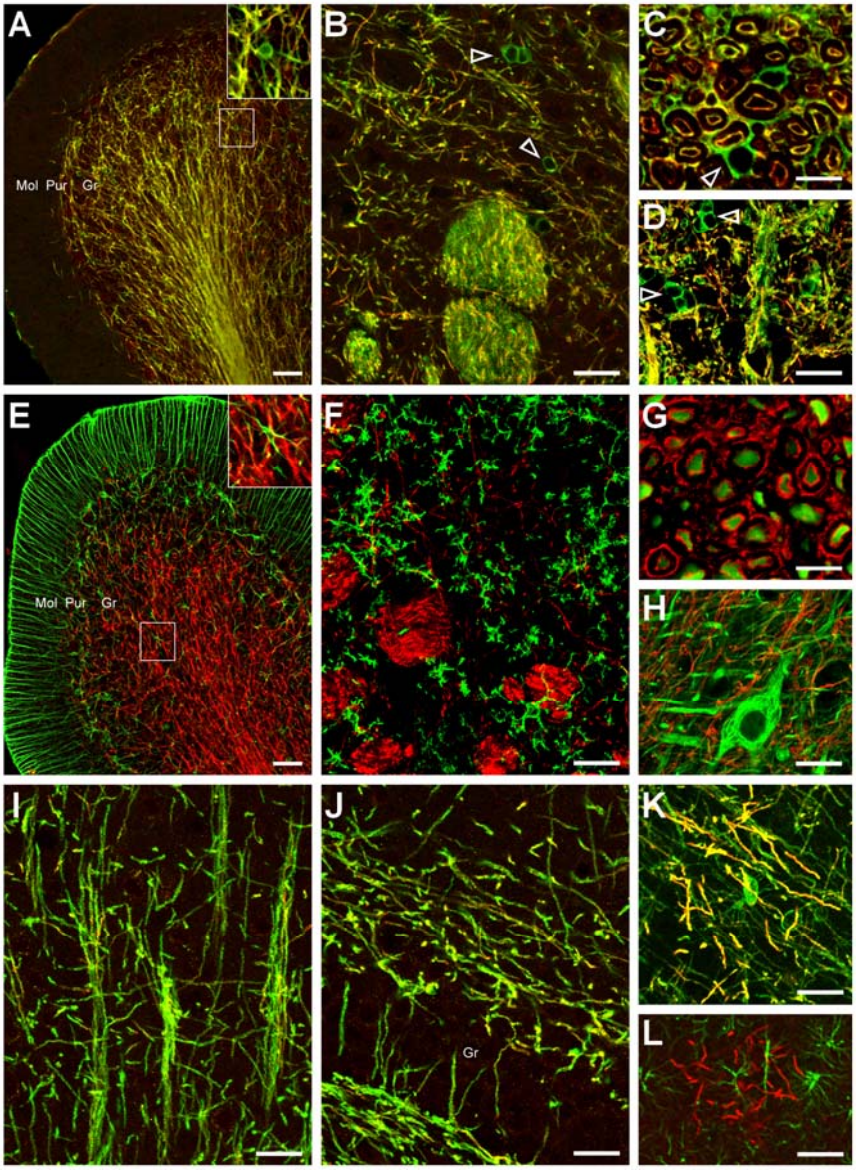

Figure 3.6 SIRT2 is predominantly an oligodendroglial protein

A–H, Double-immunofluorescent labeling of SIRT2 (red in all panels) plus CNP (A–D and K), GFAP (E and L), OX42 (F), neurofilament (G,H), or MBP (I, J) in the rat cerebellar cortex (A, E), caudate-putamen (B, F), cerebral cortex (layers III and IV in I; layers II and III in K and L), dentate gyrus (J), cross (C, G) or longitudinal sections (D, H) of cervical spinal white (C, G) or gray (D, H) matter. The inset in A or E is the observation of the marked area at a higher magnification. In A–D, note that, although it overlapped CNP (green) in most oligodendrocytic processes, SIRT2 (red) was undetected or only faintly positive in most oligodendroglial cell bodies that showed strong CNP staining (open arrowheads). Gr, Granule cell layer of cerebellar cortex (A, E) or the dentate gyrus (J); Mol, Molecular layer of cerebellar cortex; Pur, Purkinje cell layer of cerebellar cortex. Scale bars: B, D, F, H–J, 20 μm; A, E, 50 μm; C, G, 10 μm.

5. SIRT2 was localized to juxtanodal area in the myelin sheath

Under high magnification, in certain axon bundles near the pia surface of cross-sectioned cervical spinal white matter, SIRT2 positive profiles, similar to those of CNP labeling, were observed in concentric double rings around the NF200-positive neuronal axons. The inner rings often seemed in contact with the centrally positioned axons, but not with the outer rings. Careful comparison with SIRT2 immunoelectron microscopic data (see below) suggested that the concentric rings most possibly corresponded to the cytoplasm-containing innermost and outermost layers of myelin sheaths, respectively (**Fig. 3.6 C and G**).

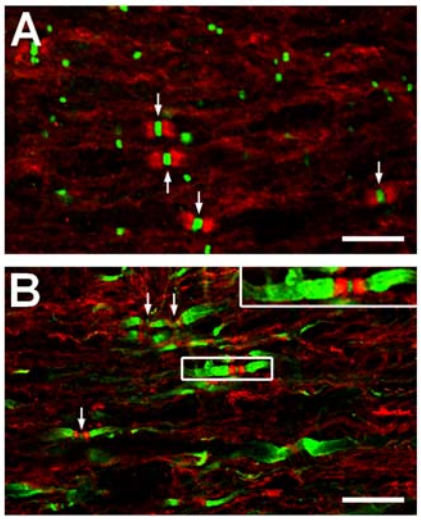

Figure 3.7 SIRT2 localized in the juxtanodal region adjacent to nodes of Ranvier
On longitudinal sections of cervical spinal white matter, double-immunofluorescence labeling (A) of SIRT2 (red) together with pan-sodium channel (NavP, green), or triple labeling (B) of SIRT2 (red) together with NavP (green) and potassium channel Kv1.2 (green) showing SIRT2 distribution in the juxtanodal and paranodal domains of myelin sheath. The arrows point to examples of the NavP clusters at the nodes of Ranvier. The inset in L shows an example from the marked area at a higher magnification. Note the SIRT2-positive bands flanking the node of Ranvier and in between the strongly Kv1.2-positive juxtaparanodes. Scale bar: 10 μm.

In most other axon bundles of cervical spinal cord, SIRT2 signals could be seen

around the NF200-positive axons but mostly did not directly contact or overlap the latter, indicating their localization mainly in the outermost layer of myelin sheath.

To more clearly understand the localization of SIRT2 in the myelin sheath, we performed a triple labeling experiment on longitudinal sections of cervical spinal white matter. As revealed, SIRT2 was frequently found enriched in the juxtanodal and paranodal region in between the sodium channel-clustered node of Ranvier and the potassium channel Kv1.2-enriched juxtaparanodal domain (**Fig. 3.7 A, B**).

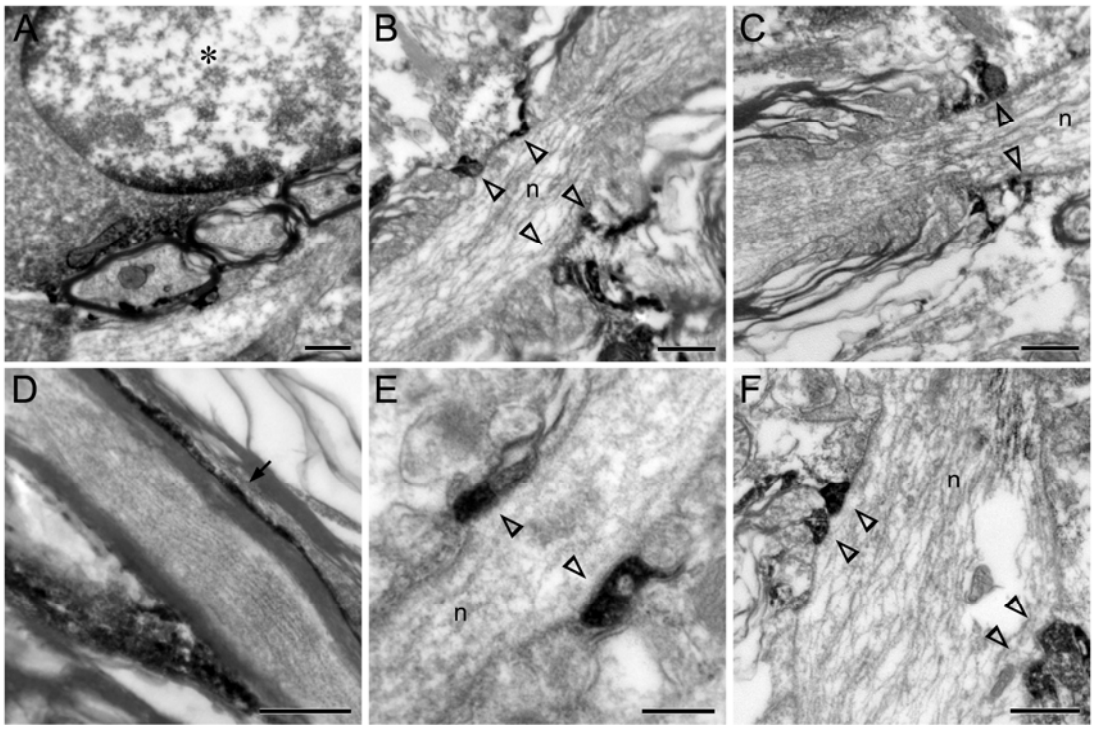

Figure 3.8 SIRT2 localization in oligodendrocytes and myelin sheaths under electron microscope

(A) Immunoelectron micrograph of cervical spinal cord showing occasional SIRT2 immunoreactivity in the perikaryal cytoplasm and in marginal heterochromatin clumps of nucleus of oligodendrocyte (denoted by an asterisk).

(B-F) Immunoelectron micrographs of cervical spinal cord (B, C, F) or corpus callosum (D, E) showing SIRT2 immunoreactivity in the cytoplasm-containing outer layer of myelin sheaths (arrow in D) or the juxtanodal loops of myelin sheaths (open arrowheads in B, C, E, F) on the sides of the nodes of Ranvier (marked by "n" in the middle of the axons). Scale bars, 0.5 μm (panels A-D, F) and 0.2 μm (panel E).

Under the electron microscope, SIRT2 immunoreactivity was mainly found in the cytoplasm-containing non-compact portions of myelin sheath such as the abaxonal (outer) layer of myelin sheath (**Fig. 3.8 A-D**), the juxtanodal terminal loops (**Fig. 3.8 B, C, E and F**), and in processes of oligodendroglia. Electron-dense immunoreactive products were also occasionally found in the perikaryal cytoplasm and in the marginal heterochromatin areas of oligodendrocytic nucleus (**Fig. 3.8 A**). No SIRT2 signal was detected in the compact laminae of myelin sheath, and no association of the signals with cytoplasmic organelles could be unequivocally established.

6. SIRT2 NAD-dependently deacetylates α-tubulin

As presented in the "introduction" chapter, SIRT2 is an NAD-dependent histone deacetylase. In addition to histones, it can also deacetylate α-tubulin (North et al., 2003). We sought to identify the candidate SIRT2 substrates in oligodendrocytes as the protein is predominantly localized in cytoplasm (**Fig. 3.6** and North et al, 2003). Western blot analysis showed no endogenous SIRT2 expression in OLN-93 rat oligodendroglia cell line (**Fig. 3.1 B**, lane 5). We then incubated the lysate supernatant of pXJ-Sirt2 transfected OLN-93 cells (mainly cytoplasmic proteins) with NAD for 30 min at room temperature, and subjected them to Western blots probed with an anti-acetylated-lysine antibody (AKL5C1, Matsuyama et al., 2002) or a mouse monoclonal antibody specific to lysine 40-acetylated α-tubulin (6-11B-1, Piperno et al., 1987). The former antibody revealed a predominant positive band at 52 kDa. This signal was presumed to be acetylated α-tubulin since 1) anti-acetylated α-tubulin

detected a single band at exactly the same position, 2) in comparison with normal OLN-93 cell lysate (also treated with NAD for 30 min), the lysate with overexpressed FLAG-SIRT2 showed significantly decreased levels of both the acetylated-lysine (48% reduction compared to control) and acetylated α-tubulin (57% reduction compared to control) immunoreactivities (**Fig. 3.9 B**). Levels of total α-tubulin were not affected by FLAG-SIRT2 overexpression (**Fig. 3.9 B**). The anti-acetylated lysine antibody also stained two other bands in OLN-93 immunoblots, but in comparison with acetylated a-tubulin these signals were much weaker, and seemingly not much influenced by overexpression of FLAG-SIRT2 (**Fig. 3.9 B**). Since SIRT2 is also reported to deacetylate histones (North et al., 2003; Vaquero et al., 2006), we next tested if the acetylation levels of histones in the transfected cells were altered. In addition to the supernatant portion mentioned above, the pellet of the cell lysate in which most nuclear proteins presented was subjected to Western blots. As shown in **Figure 3.9 C**, almost all the recombinant FLAG-SIRT2 was expressed in the supernatant portion. In presence of FLAG-SIRT2 rather than FLAG-SIRT2N131A, α-tubulin was obviously deacetylated in the cytoplasm.

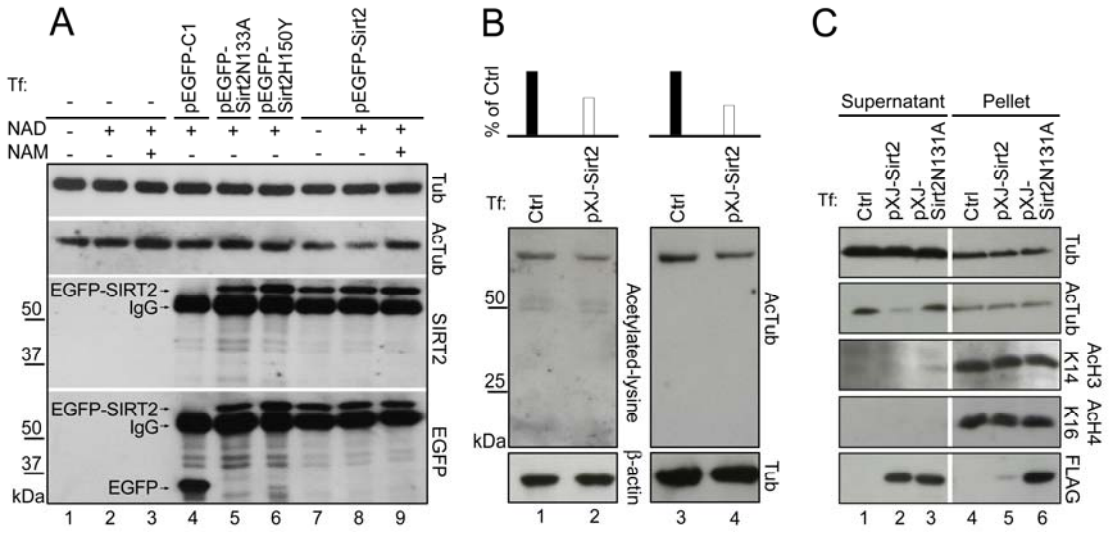

Figure 3.9 SIRT2 is an NAD-dependent histone deacetylase with as α-tubulin its preferable substrate

(A) OLN-93 cells were transiently transfected as indicated, lysed and immunoprecipitated with anti-EGFP. The immunoprecipitates were then added to OLN-93 cell lysate (as the source for acetylated α-tubulin) together with various combinations of NAD (1 mM) or NAM (5 mM), and incubated for two hours at room temperature. Samples after that were subjected to Western blots analyses (5 μg each lane).

(B and C) OLN-93 cells were transiently transfected with indicated plasmids, lysed and centrifuged, the supernatant (B, C) and pellet (C) of which were subjected to Western blots. Crtl: normal OLN-93 cell lysate. The bar chart on the top of panel B represents the densitometric analysis of the bands densities in lanes1-4. The bands densities of acetylated-lysine in lane 2 and acTub in lane 4 (white bars) were calculated as percentages of the control groups in lane 1 and lane 3 (black bars), respectively.

Conversely, the acetylation levels of the histone H3 (acetylated at lysine 14) and histone H4 (acetylated at lysine 16) (North et al., 2003; Vaquero et al., 2006) were not changed (**Fig. 3.9 C**). These results suggested that the main substrate for SIRT2 is α-tubulin in the cytoplasm of OLN-93 cells.

To further determine the α-tubulin deacetylase activity of rat SIRT2, point-mutated or wildtype forms of SIRT2 with EGFP tag were overexpressed in

OLN-93 cells, immunoprecipitated by EGFP antibody and used as enzymes to treat untransfected normal OLN-93 cell lysate as a substrate. Western blots were finally employed to semi-quantitatively assess the tubulin deacetylase activity of the immunoprecipitates. The results showed that, in the presence of NAD (1mM), the addition of immunoprecipitated EGFP-SIRT2, rather than EGFP, caused a significant decrease of acetylated α-tubulin in the cell lysate (**Fig. 3.9 A**, lane 8). The EGFP-SIRT2 did not influence the level of total α-tubulin, and its tubulin deacetylase activity was abolished when NAD was removed or sufficient nicotinamide (NAM, 5mM) added into the system (**Fig. 3.9 A**, lanes 7 and 9). Point-mutated SIRT2s, in which aspartic acid-133 of SIRT2 was replaced by alanine (SIRT2D133A) or histidine-150 by tyrosine (SIRT2H150Y) (Finnin et al., 2001), showed significantly diminished deacetylase activity (**Fig. 3.9 A**, lanes 5 and 6). SIRT2N131A (replacement of asparagine-131 by alanine) exhibited similar reduction of deacetylase activity (data not shown). These results indicated that SIRT2 could deacetylate α-tubulin in an NAD-dependent manner.

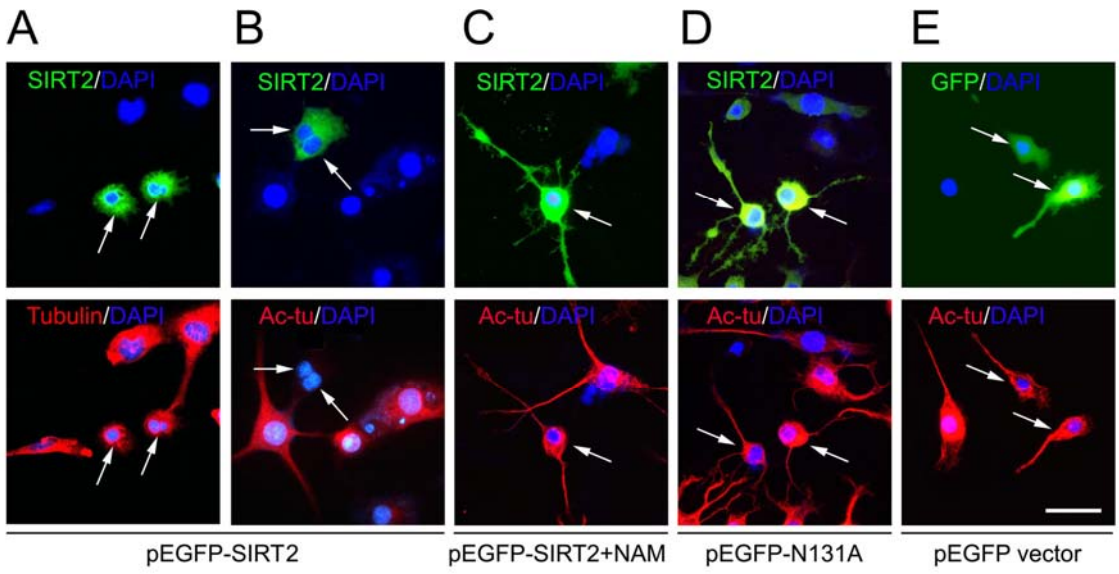

Figure 3.10 Overexpressed SIRT2 deacetylates α-tubulin in OLN-93 cells
OLN-93 cells were transfected with plasmids as indicated under each panel column after being cultured on coverslips for 24 hours in presence of 1mM NAD. Forty-eight hours after transfection, cells were fixed and immunofluorescent staining was performed using antibodies indicated in the top of each panel. The results shows that overexpressed EGFP-SIRT2 attenuated the acetylated level of α-tubulin, but the effects of which could be inhibited by 1mM NAM. Scale bar: 20μm

We further tested the deacetylase activity of overexpressed SIRT2 *in vivo* in OLN-93 cell lines. EGFP-SIRT2 or its point-mutated forms were transfected into cells and observation was done 48 hours after that. As shown, overexpressed SIRT2 specifically abolished the staining of acetylated form of rather than normal α-tubulin (**Fig. 3.10 A, B**). Additionally, in accordance with *in vitro* data presented above, the deacetylase activity of overexpressed SIRT2 can be inhibited by presence of NAM or when specific point mutation was introduced into the protein (**Fig. 3.10 C, D**).

7. Association among SIRT2 expression, tubulin acetylation levels and oligodendrocyte maturation in culture

We next investigated the relations between SIRT2 expression, tubulin acetylation and development of oligodendroglia in OLP cells extracted from postnatal day 1-2 rat cerebra. After 3-4 days' differentiation, a quarter of the primary OLPs exhibited complex morphology with tertiary processes. Roughly 20% of them started to express SIRT2. Surprisingly, abundance of endogenous SIRT2 expression was positively correlated with the acetylation levels of α-tubulin in the same cells. Subcellular distribution of acetylated α-tubulin and SIRT2 also mostly overlapped. More importantly, the process arbors of SIRT2-positive and EL-acTub (elevated acetylation, refer to "materials and methods" for morphological scoring criteria) primary OLPs were clearly more complex in morphology than those of the surrounding SIRT2-negative and BL-acTub (basic level acetylation) cells, and the increase of SIRT2 expression and acTub levels was accompanied by the differentiation progression of those OLP cells' arborization (**Fig. 3.11 J,L**). Similar correlation between CNP expression and OLP cells' arborization differentiation was detected (**Fig. 3.11 K**). It was also noteworthy that primary and secondary processes of the SIRT-positive/CNP-positive/EL-acTub OLP cells were often tortuous along the way and enlarged at the distal end from where many finer processes originated. In contrast, processes of the SIRT2-negative/ CNP-negative/BL-acTub OLPs often radiated out straight from the cell bodies, and gave rise to relatively fewer further branches. Levels of total α-tubulin, however, were not closely correlated with SIRT2 expression (**Fig.**

3.11 C,F,I).

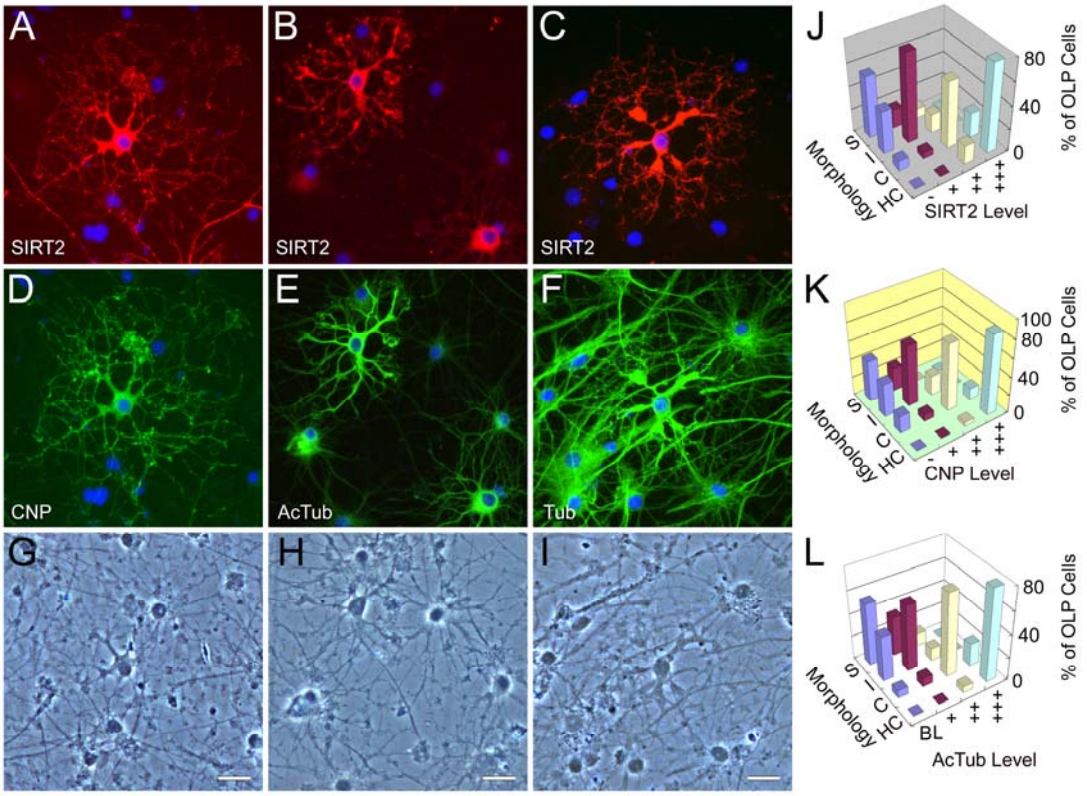

Figure 3.11 Cofluctuation between the morphological complexity of primary OLPs , the acetylation levels of α-tubulin and expression of SIRT2 and CNP

(A-C, E-G and I-K) Double-immunofluorescent photomicrographs showing close correlation of SIRT2 expression (A-C) with CNP (D) and levels of α-tubulin acetylation (E) in cultured OLPs. Levels of total α-tubulin (F) were, however, not closely associated with SIRT2 expression (C). Morphologies of the immuno-negative cells could also be appreciated in the respective lower panels of phase-contrast photomicrographs (G-I). Note the increased α-tubulin acetylation and emergence/increases of SIRT2 and CNP immunoreactivities in the pre-maturity-stage oligodendrocytes, as compared with the earlier-stage cells that showed no SIRT2 or CNP signals, and low levels of α-tubulin acetylation. Abbreviations: Tub, α-tubulin; AcTub, acetylated α-tubulin. Scale bars, 20 μm.

(J, K and L) Three-D bar charts representing the differentiation progression of cellular arborization was accompanied by the emergence/increase of cellular expression levels of SIRT2, CNP and elevated levels of acetylated -tubulin. “S”, “I”, “C” and “HC” are abbreviations for “Simple”, “Intermediate” “Complex” and “Highly Complex” hierarchies of cellular arborization. ”BL” “-”, “+”, “++” and “+++” are used to designate the levels of expression. Please refer to Material and Methods for detailed criteria. “% of OLP cells” on the z-axis represents that, in each of the four expression level hierarchies, the percentage of cells in each complexity category relative to the total.

Further double immunofluorescent stainings and statistical analysis proved that the concurrent SIRT2 and CNP emergence, α-tubulin acetylation increase and typical morphological changes of cultured primary OLPs marked the entry of oligodendrocyte differentiation into the pre-maturity stage (Barry et al., 1996; Armstrong, 1998; Baumann and Pham-Dinh, 2001; Woodruff et al., 2001). All cells positive for SIRT2 became immunoreactive for the oligodendroglial functional protein CNP as well, whereas those lacking SIRT2 remained negative for CNP. The two enzymes showed overall co-variation in levels, and colocalization at subcellular domains (**Fig. 3.11 A,E,I**).

The raised α-tubulin acetylation levels in spite of the appearance of SIRT2 tubulin deacetylase activities in the pre-maturity-stage oligodendrocytes seemed paradoxical. We hypothesized that the heightened α-tubulin acetylation (possibly due to activities of certain acetyltransferases) and CNP activity promoted OLP differentiation. The concurrent SIRT2 increase functioned as a counterbalance to prevent uncontrolled tubulin acetylation, to offset over-differentiation, and to avoid premature myelination in the CNS. To test this hypothesis, the following overexpression and siRNA knockdown experiments were carried out.

8. SIRT2 overexpression lowered α-tubulin acetylation levels and inhibited OLP differentiation

Two days after Sirt2 transfection, primary OLP cells (in their third or fourth day of differentiation) showed retarded morphological differentiation (**Fig. 3.12 A, B, F, G**)

and marked decreases in α-tubulin acetylation levels (**Fig. 3.12 A**). Many of the transfected cells expressed considerable levels of intrinsic CNP, but failed to assume the typical morphology of the normally CNP-positive pre-maturity-stage oligodendrocytes (refer to **Fig 3.11 F**). Process arbors of these cells still appeared relatively immature, much like those of earlier-stage cells (**Fig. 3.12 A,C,F,G**). By contrast, morphologies of cells expressing EGFP only or FLAG-juxtanodin141 (FLAG-JN141, Zhang et al., 2005) appeared to be highly complicated, similar to untransfected neighboring cells (**Fig. 3.12 D,E,H**). Overall, at the end of the 3-4 days differentiation, the OLP cells untransfected or transfected with control plasmids exhibited mostly intermediate or complex morphology, whereas the majority of the OLPs transfected by Sirt2 were simple or intermediate in cell arbor complexity (see "materials and methods" for morphological scoring criteria). In comparison to the JN141 transfected controls, for example, the percentage of simple cells increased by three fold in the pXJ-Sirt2 transfected group, whereas those with complex morphology dropped from 53.6% to 34.9% (**Fig. 3.12 I**, average of 3 experiments, n>300 cells for all groups).

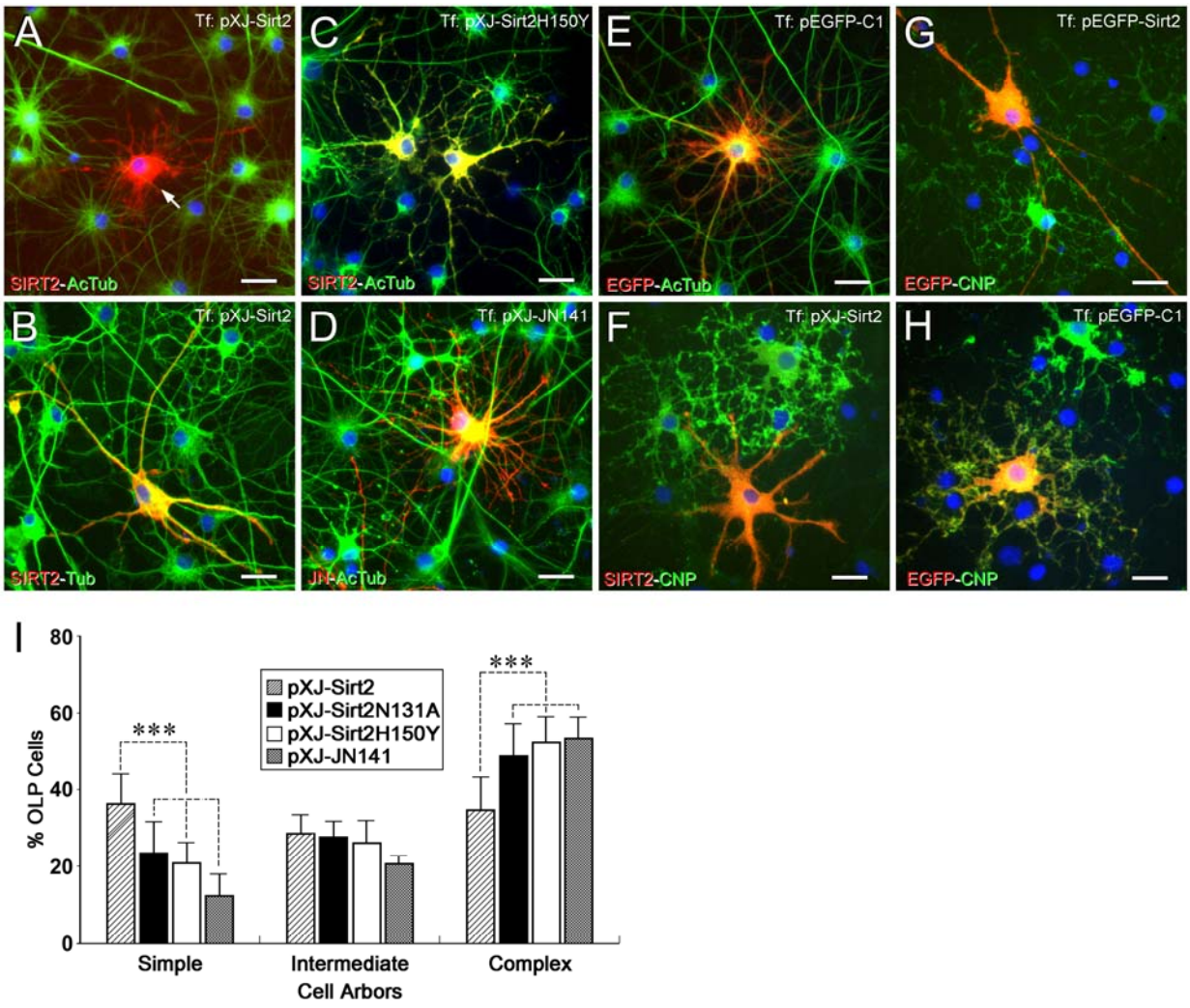

Figure 3.12 Overexpression of SIRT2 inhibits the morphological differentiation of primary OLPs

(A-H) Sirt2-transfected OLP cells showed decreased α-tubulin acetylation levels (arrow in A), and simpler morphology in comparison with neighboring untransfected cells (A, C, F and G), with cells transfected with SIRT2H150Y, the deacetylase partially inactive form of SIRT2 (B), and with pEGFP-C1 or JN141-transfected controls (E, H and D). Total α-tubulin levels in the Sirt2-transfected cells were not significantly affected (C). For the visualization of the much higher intensity of overexpressed SIRT2 signals in the transfected cells, normal endogenous SIRT2 signals in the neighboring cells, if any, were underexposed and therefore could not be optimally appreciated in some of the panels (A, B, C and G).

(I) Statistic analyses of morphological maturation of primary OLPs transfected with pXJ-Sirt2, pXJ-Sirt2N131A, pXJ-Sirt2H150Y and pXJ-JN141 plasmids. Data are from three independent experiments (n>300 transfected cells for each transfection group). ***, $p<0.001$ (Student's t-tests).

Plasmids/drugs for transfection/treatment of cultures are indicated on the upper right of the panels, and antibodies for immunofluorescence on the lower left. Refer to Fig.3.11 for abbreviations. Scale bars, 20 μm.

To test if the deacetylase activity of SIRT2 is essential for its inhibitory effect on OL arborization, SIRT2H150Y which has largely lost deacetylase activity (**Fig. 3.12 C**; Finnin et al., 2001) was used to transfect OLP cells. The results showed that the deacetylase activity loss of SIRT2H150Y almost completely abolished the inhibitory effect of wild-type SIRT2 on OL arbor complexity (**Fig. 3.12 C,I**). Transfection of another deacetylase-inactive mutant of SIRT2, SIRT2N131A, gave rise to similar results (**Fig. 3.12 I**).

To further determine the effects of SIRT2 overexpression, we co-transfected OLN-93 cells with both pEGFP-Sirt2 and pXJ-JN. Cells overexpressing FLAG-tagged JN alone showed marked increases in the process arbor complexity (**Fig. 3.13 B**; Zhang et al., 2005), of which, statistical analysis revealed 43.1% exhibited complex morphology while 25.6% were simple. In contrast, cells overexpressing both FLAG-JN and EGFP-SIRT2 proteins showed remarkably less-developed branches or only rounded-up cell bodies (13.1% and 50.0% of transfected cells fell into complex and simple group respectively; **Fig. 3.13 C, G**), much similar to cells overexpressing only SIRT2 (**Fig. 3.13 A, G**). The simultaneous overexpression of SIRT2N131A or EGFP together with JN did not significantly counteract the arborization-promoting effect of the latter (**Fig. 3.13 D, E and G**). Addition of 5 mM nicotinamide to the JN-SIRT2 co-transfected culture partly blocked the arborization-inhibiting effect of SIRT2 (**Fig. 3.13 F,G**).

Together, these results supported the notion that SIRT2 decelerated oligodendroglial maturation through its tubulin deacetylase activity.

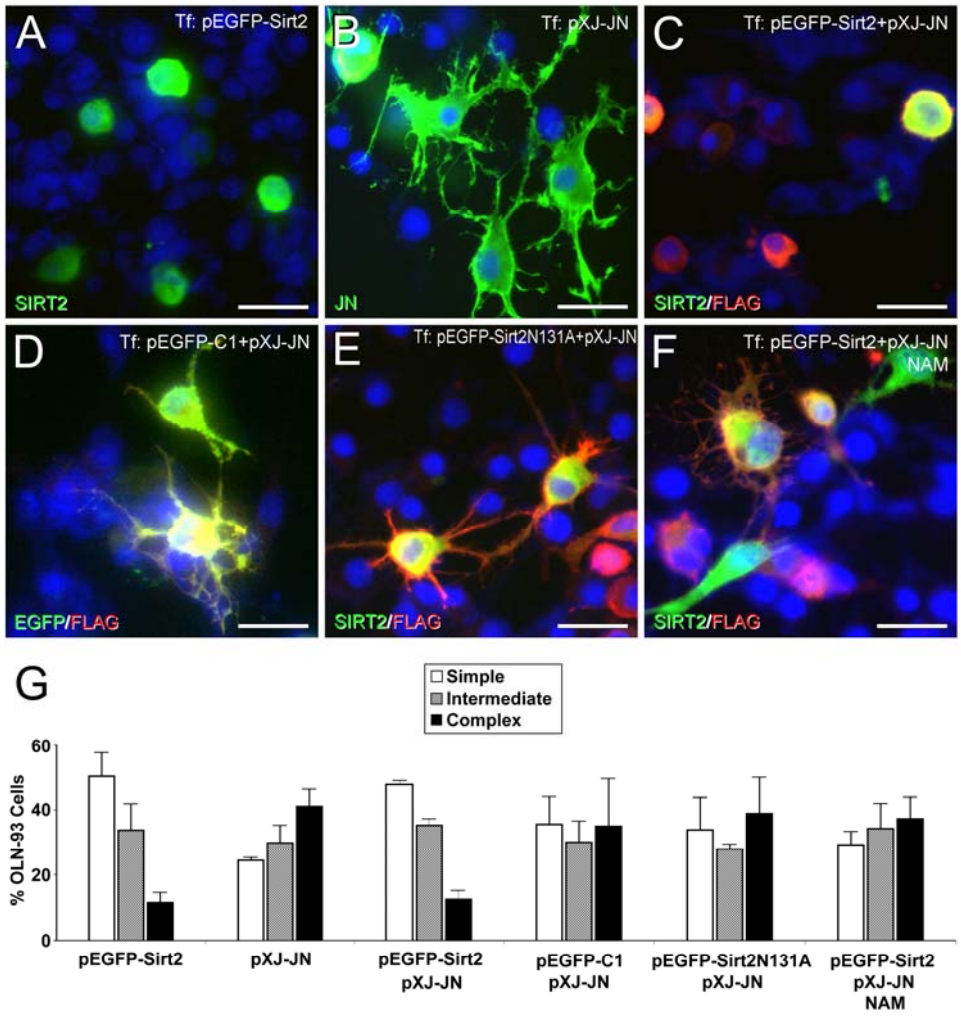

Figure 3.13 Overexpressed SIRT2 counteracts the promotive effects of JN on cell arborization in OLN-93 cells

(A-F) pEGFP-Sirt2 transfected OLN-93 cells showed much fewer cell processes (A), in comparison with cells transfected by pXJ-JN alone (B) or pXJ-JN plus pEGFP-C1 (D). When cotransfected with pXJ-JN, pEGFP-Sirt2 counter-regulated the arborization-promoting effect of the former (C), whereas the inhibitory effect of pEGFP-Sirt2N131A was much less obvious (E). Addition of nicotinamide (5 mM) to the culture medium partly abolished the arborization-inhibiting effect of SIRT2 (F). Cells in all groups except panel F were transfected and grown in presence of NAD.

(G) Statistic analyses showing the counteractive activity of overexpressed SIRT2 on cellular arborizations of OLN-93 cells promoted by JN overexpression. OLN-93 cells were transfected or treated as indicated in A-F. Data are from two independent experiments (n>300 transfected cells for each transfection group).

Plasmids/drugs for transfection/treatment of cultures are indicated on the upper right of the panels, and antibodies for immunofluorescence on the lower left.

Refer to Fig.3.11 for abbreviations. Scale bars, 20 μm.

In agreement with previous results (Marin-Husstege et al., 2002; Liu et al., 2003; Hsieh et al., 2004; Shen et al., 2005), addition of trichostatin A (TSA), an inhibitor of class-I/II HDACs, to the medium delayed differentiation of all primary OLPs in the culture, as evidenced by their much simpler process arbors. This repressive effect of the drug was obvious before the onset of endogenous oligodendroglial SIRT2 expression (data not shown).

9. Knockdown of endogenous SIRT2 by siRNA promotes α-tubulin acetylation and accelerates OLP differentiation

To verify the above SIRT2 effects from a different angle, we used siRNAs to interfere with intrinsic SIRT2 expression in cultured primary OLPs starting at 2-4 days into their differentiation. Transfections by siRNAs for JN or histone deacetylase 6 (HDAC6), both of which showed no detectable expression within the OLP differentiation time window under the present study (data not shown), served as controls.

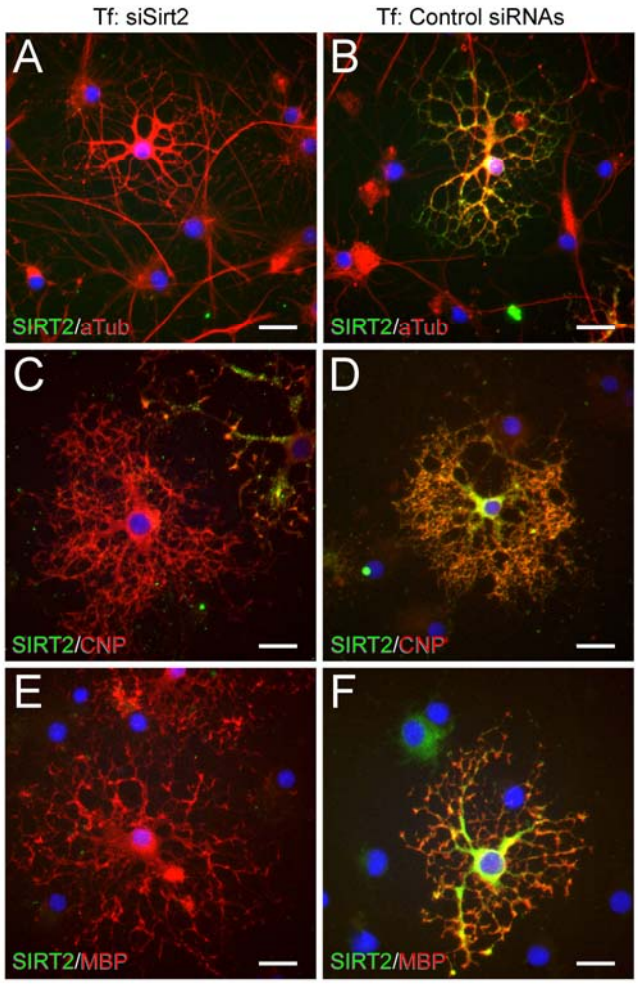

Figure 3.14 Knockdown of endogenous SIRT2 in primary OLPs in early stages of cell differentiation

(A-F) siRNA knockdown of endogenous SIRT2 for 3 days (days 2-5 into differentiation) did not significantly alter OLPs' morphological complexity or distribution of acetylated α-tubulin (A), CNP (C) and MBPs (E) as compared to cells transfected with JN or HDAC6 siRNAs (B, D, F). OLPs within 10 days into differentiation had no JN or HDAC6 immunoreactivity (data not shown). Thus the latter two siRNAs served here as negative controls.

Plasmids/siRNAs for transfection are indicated on the top of the columns, and antibodies for immunofluorescence on the lower left of individual panels.

Scale bars, 20 μm.

All three Sirt2 siRNA duplexes depleted or lowered SIRT2 immunoreactivity in a majority of the cultured OLPs. The knockdown effect of the siRNA targeting Sirt2 nucleotides 518-540 (NM_001008368) was nearly complete and lasted for at least eight days. When examined 3-4 days into the knockdown, OLPs showed no obvious

changes in the levels and distribution of CNP or MBPs, nor did the cells display marked alteration in their process arbors (**Fig. 3.14 A-F**). After 7-8 days of nullified/reduced Sirt2 expression by the siRNAs, however, significantly more OLPs in the experimental cultures adopted complex or highly complex morphologies, as compared with JN/HDAC6 siRNA-treated or with siRNA-omitted controls. Percentage of OLPs with simple morphologies, indicative of less differentiation, accordingly decreased in the experimental group (**Fig. 3.15 A**). Accompanying the morphologically enhanced differentiation in the experimental group were the decreased deacetylation of tubulin and increased expression of an immature form of MBP at around 50 kDa (Ursell et al., 1995). Immunoreactivities for CNP, total tubulin, or β-actin in the OLPs, as detected by Western blotting analyses, were not significantly altered by SIRT2 siRNAs (**Fig. 3.15 B**). JN or HDAC6 siRNAs transfection gave rise to no significant influence on differentiation or gene expression of OLPs at the present developmental stage.

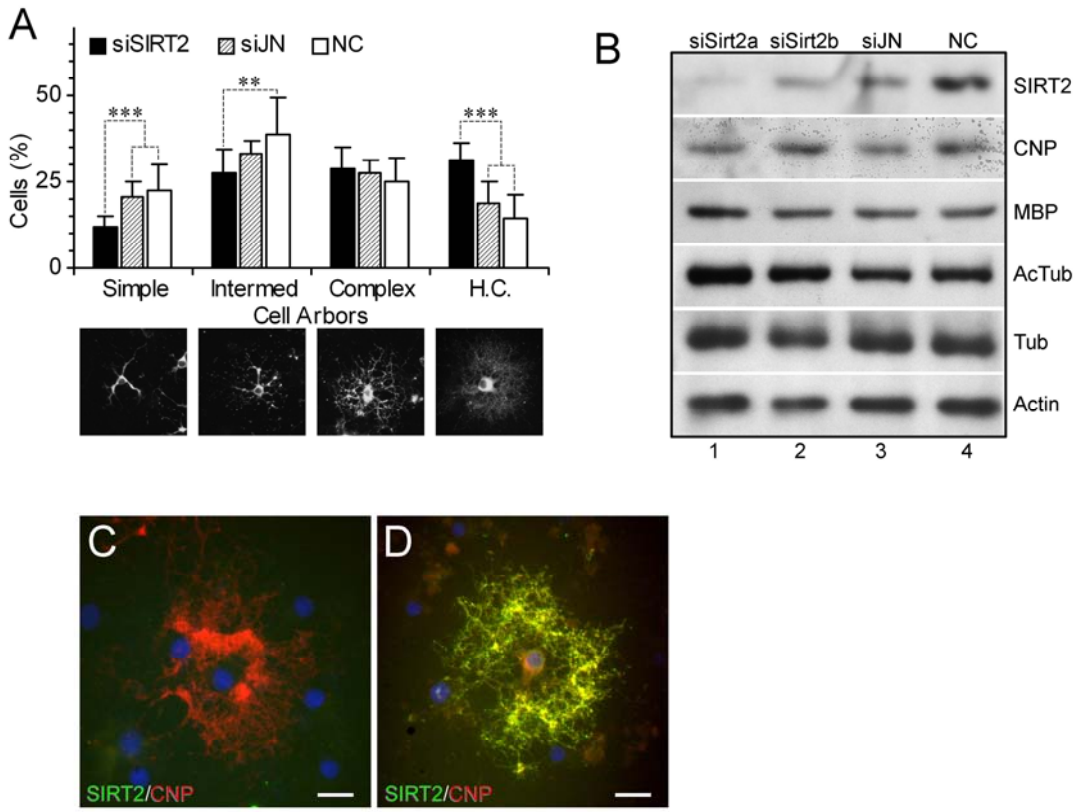

Figure 3.15 Prolonged knockdown of endogenous SIRT2 expression promotes differentiation of primary OLPs

(A and B) siRNA knockdown of endogenous SIRT2 for 6 or 8 days (days 2-8 or 2-10 into differentiation) promoted the differentiation of OLPs as evidenced by increased morphological complexity (A) and upregulation of acetylated α-tubulin and MBP expression (B) in comparison with untransfected or JN/HDAC6 siRNA-treated controls. No difference was observed in the expression of CNP, total α-tubulin and β-actin between the SIRT2 knockdown and the control groups (B). Example morphology and CNP expression in cell after 8-day SIRT2 knockdown and in untransfected control cell are shown in panels C and D. In panel A, grayscale pictures under the graph represent typical examples for the four morphological hierarchies (A). Abbreviations: HC, highly complex; NC, untransfected negative control; siJN, JN siRNA 3235-3257; siSIRT2a, Sirt2 siRNA 518-540; siSIRT2b, Sirt2 siRNA 1390-1412; ***, $p<0.001$; **, $p<0.01$ (Student's t-tests).

Plasmids/siRNAs for transfection are indicated on the top of the columns, and antibodies for immunofluorescence on the lower left of individual panels. Scale bars, 20 μm.

10. Overexpression of specific rSIRT2 mutants triggers aggregates formation in cultured cells

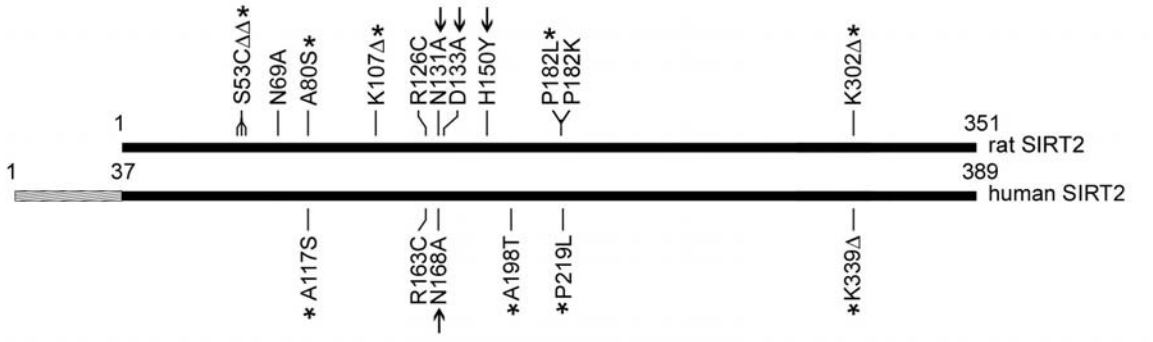

Figure 3.16 Schematic diagram showing the mutated residues of rSIRT2 and hSIRT2 in the current study

All the 15 rSIRT2 mutants were derived from various combinations of these 12 point mutations. Arrows indicate known deacetylase-defective point mutations; asterisks denote human Sirt2 SNP point (**rA80S/hA117S**, **hA198T**), or mutations found in human Sirt2 sequences in NCBI databases or a MGC rat clone (**rK302Δ/hK339Δ**).

Fifteen different mutants of rSirt2 and six of hSirt2 are included in the current study and the positions of these points are shown in **Figure 3.16**. There is a 37 reside N terminus domain that only presents in hSIRT2 but not in rSIRT2.

OLPs were transfected with rSirt2 mutants or control plasmids 48 hours after the start of differentiation, and fixed for immunofluorescent staining after another 48 hours in culture. Overexpression of rSIRT2R/N mutant resulted in the formation of aggregate structures in the cytoplasm of a majority of transfected primary OLPs (**Fig. 3.17 A,D**). By contrast, the transfection with wildtype rSirt2 or point-mutant rSirt2H150Y did not result in similar phenomenon (**Fig. 3.17 G,J**).

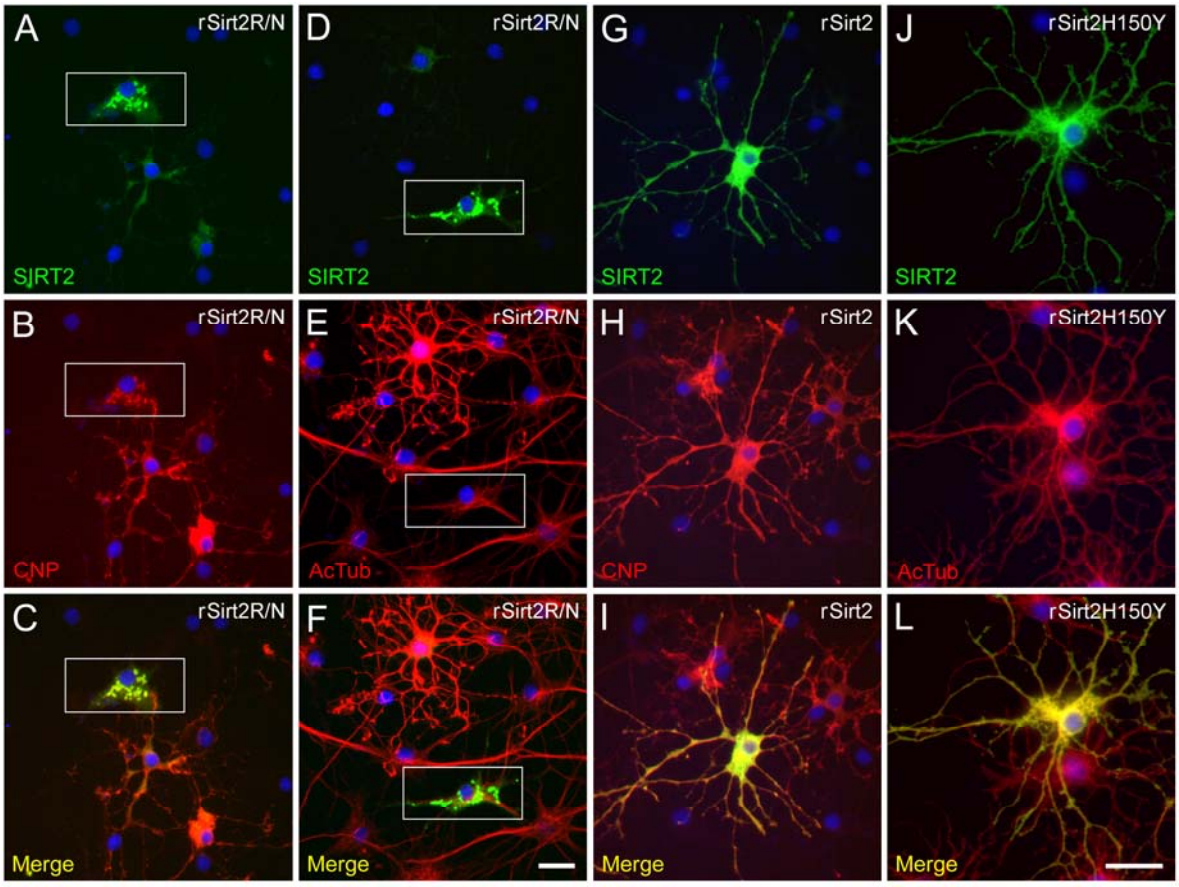

Figure 3.17 Overexpression of specific mutants of rSIRT2 induced cellular aggregates in primary OLPs

Primary OLP cells were differentiated for 2 days and transfected with rSirt2R/N (A, B, D, E), wildtype rSirt2 (G, H) or rSirt2H150Y (J, K). The cells were then subjected to immunofluorescent analyses after 48 hours in culture. Antibodies used for staining are indicated in the lower left part of each panel, and DAPI was used to visualize the nuclei. Scale bars in F and L: 20μm (the one in F is shared by A-F, and in H shared by G-L). **rSirt2K302Δ** single codon-deletion mutant and rSirt2R126C point mutant transfected OLPs also exhibited perikaryal aggregates, although in a relatively smaller percent of transfected cells. The clumps or granules of aggregation were found mostly in the perikarya and occasionally in the cell processes of OLPs (data not shown). By contrast, transfection of OLPs with wildtype rSirt2 or several other rSirt2 mutant constructs (rN131A, rH150Y, rN69A and rN/H) did not produce overt aggregate formation in the host OLPs (such as those in Fig. 3.12).

We next investigated such aggregation induced by overexpression of rSirt2 mutants in immortalized cell lines. OLN-93, 293T, HeLa, SHEP and B104 cells were transfected with wildtype rSirt2 or various rSirt2 mutants. As in the primary OLPs, overexpression of rSIRT2R/N, rK302Δ and rR126C caused prominent aggregate

formation in all cell lines tested (**Fig. 3.18** and data not shown), whereas wildtype rSirt2 did not give rise to observable aggregation (**Fig. 3.18 E**). This result indicated that aggregation by the rSirt2 mutants in transfected cells was not specific to any cell type or species, but a generalized property of the specific protein mutants. rSirt2N69A, rN131A and rH150Y transfection in OLN-93 cells produced occasional aggregates (in 2.9%, 7.0% and 2.9% of the respectively transfected cells), while rN/H gave rise to aggregates in about 15% of the overexpressors. The percentages of aggregate-positivity by other rSIRT2 mutants ranged from 3.5±1.4% (**S53CΔΔ**) to 99.2±1.0% (R/N/K) of transfected OLN-93 cells (**Fig. 3.22 B**). Transfection by **rSirt2A80S**, **rK107Δ**, **rP182L** and **rK302Δ**, in particular, resulted in aggregates in 6.0±1.2%, 9.5±1.9%, 16.1±3.3% and 64.9±5.0% of the transfected cells, respectively, whereas the number stood at 72.8±3.3% for rSirt2R126C and 85.4±4.5% for rSirt2R/N. The slight discrepancy between primary oligodendrocytes and immortalized cell lines in aggregates formation by overexpressed rSIRT2N131A, rH150Y, rN69A and rN/H might lie in the different properties, such as the error-correcting reserve, of the cells (see Discussion).

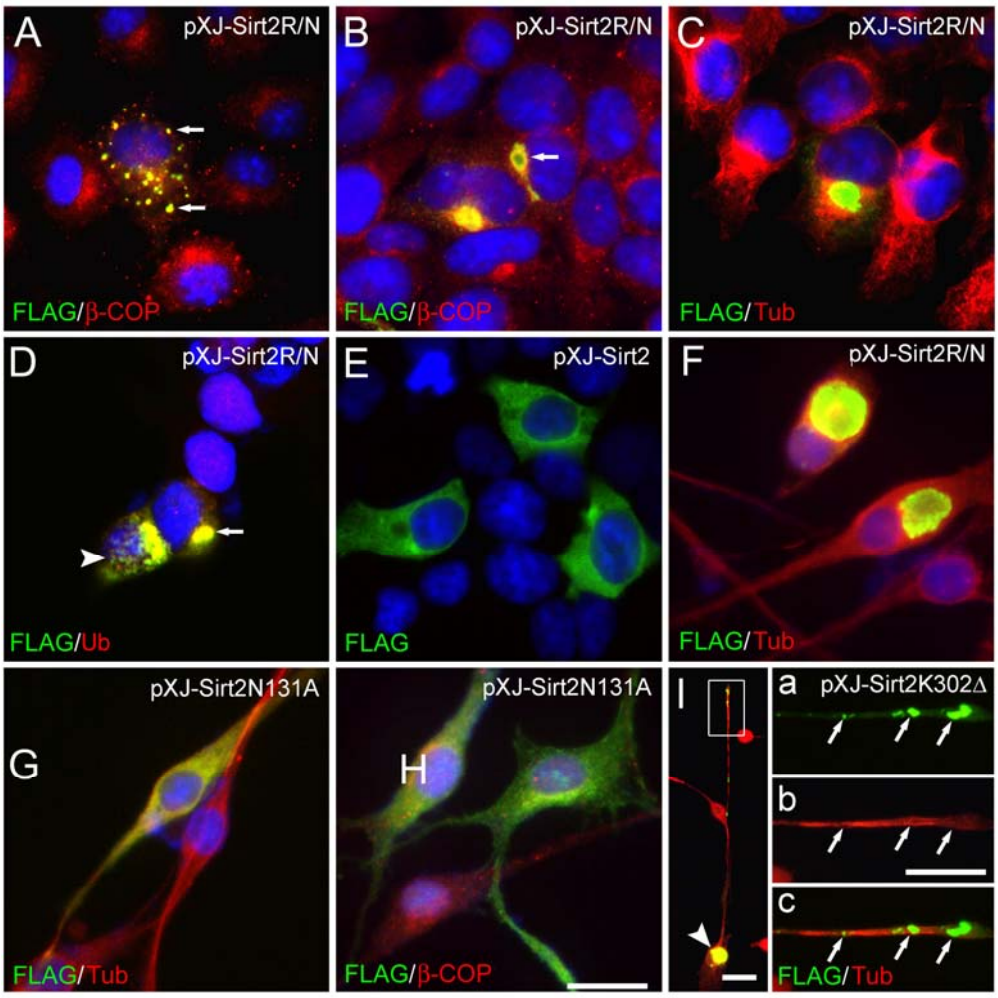

Figure 3.18 Cellular aggregates triggered in 293T and OLN-93 cells by overexpression of specific SIRT2 mutants

(A-I) Cellular aggregates were triggered by rSIRT2R/N or **rK302Δ** overexpression in OLN-93 (E, I) and 293T (A-D) cells, in comparison to overexpressors of wildtype rSIRT2 (H, 293T cell). The aggregates were found as either larger perinuclear inclusion bodies (B-E, and I) or smaller punctuate aggregates dispersed widely in the cytoplasm (A, D and I). Normal appearances of α-tubulin and β-COP staining were observed in most rSirtN131A transfected OLN-93 cells except very sporadic occasions (F, G). Antibodies or DAPI used for staining are indicated in the lower left part of each panel. Double immunofluorescent staining show overexpressed rSIRT2R/N localized in Golgi apparatus (A, B) and occasionally encaged by the latter (arrow in B). Arrows and arrowheads in panel D represent IBs and PAs respectively. Panels Ia-c are depictions at higher magnification of marked area in I. All scale bars (bar in panel H is shared by panels A-H and Ia-c, bar in I): 20μm.

According to the morphology and distribution, the aggregates appeared either as large juxtanuclear inclusion bodies (IB) (**Fig. 3.18 B-D, F and I**) or as smaller

punctate aggregates (PA) that were distributed more diffusely in both the cell body and cell processes (**Fig. 3.18 A, D, I**). Usually one individual transfected cell contain only one, though occasionally both, type of the aggregates (**Fig. 3.18 I**). These two types of accumulation resembled previously reported aggregates after mutated α-synuclein or GFP-250 overexpression (Garcia-Mata et al., 1999; Gosavi et al., 2002; Lee and Lee, 2002). Although distinct in morphologies and distributions, PAs and IBs share common characteristics in immunofluorescence for β-COP and ubiquitin. The differences between the two did not seemingly lie in their detergent-solubility, either (see below).

11. Mutated SIRT2 clumps deform Golgi apparatus and coaggregate with endogenous cellular molecules

Next, the subcellular distribution and molecular composition of the rSIRT2 mutant aggregates were assessed. As revealed by double immunofluorescence, the IBs by mutated rSIRT2 in transfected OLN-93 and 293T cells were clearly surrounded by immunoreactivity of the Golgi-apparatus marker β-COP (**Fig. 3.18 B**). Accompanying formation of the smaller PA particles in rSIRT2 mutant-transfected cells, β-COP-positive Golgi apparatus was usually fragmented, but its close relation with the aggregates seemed unchanged (**Fig. 3.18 A**). This proximity/overlap of β-COP with aggregated rSIRT2 mutants differed significantly from the normal distribution pattern of β-COP in the untransfected control cells (**Fig. 3.18 A, B**), and in the aggregate-free cells transfected with wildtype rSirt2 or rSirt2N131A (**Fig. 3.18 H**). On

Western blots, however, no β-COP was detected in the insoluble pellets of any mutated or wildtype rSirt2 transfected cell lysates (**Fig. 3.19**), in contrast to the insolubility of rSIRT2R/N or **rSIRT2K302Δ** (**Figs. 3.21, 3.22 and 3.23**). Together, these results suggest that the rSIRT2 mutants did not coaggregate with, but were nevertheless related to the Golgi apparatus. The formation of PAs may be accompanied by disintegration of Golgi apparatus, a phenomenon also seen in certain neurodegenerative diseases or cell models (Sakurai et al., 2000; Fujita et al., 2002; Gosavi et al., 2002).

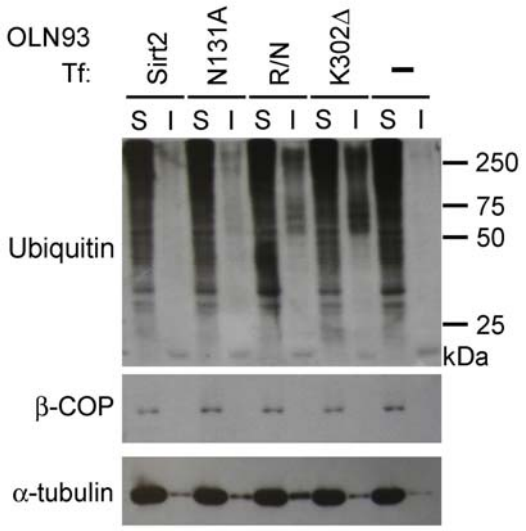

Figure 3.19 The aggregates induced by mutated rSIRT2 overexpression contain ubiquitinated proteins
The OLN-93 cells overexpressing different rSIRT2 mutants were lysed in RIPA buffer and divided into detergent-soluble (S) and –insoluble (I) fractions, probed with anti-ubiquitin and anti-β-COP. "-": transfection without plasmid.

The ubiquitin-proteasome system (UPS) has been reported to be involved in several cases of cellular aggregate formation (Bence et al., 2001; Bennett et al., 2005). To test if the aggregates in the rSIRT2 mutants-expressing cells are ubiquitinated, double immunofluorescent staining of ubiquitin and FLAG was first performed. In

both 293T and OLN-93 cells, mutated rSIRT2 largely overlapped with ubiquitin staining in either IB or PA aggregates (**Fig. 3.18 D** and data not shown). Though also detected in the cytoplasm of control cells, levels of ubiquitin were significantly higher in the aggregates (**Fig. 3.18 D**). Between the soluble and insoluble portions of the rSIRT2 mutants-overexpressing cell lysates, the transfection of rSirt2R/N and **rK302Δ,** but not wildtype rSirt2 or rSirt2N131A, resulted in significant increases of detergent-insoluble ubiquitin signals although most ubiquitin immunoreactivity was detected in the supernatants in all five transfection groups (**Fig. 3.19**). Combined with immunofluorescent colocalization of ubiquitin with both IBs and PAs (**Fig. 3.18 D**), these results suggested trapping of ubiquitinated proteins in the aggregates of specific rSIRT2 mutants. However, overexpressed rSIRT2 mutants themselves were most possibly not significantly ubiquitinated as judged by the absence of obvious polyubiquitinated ladder-like bands with ~7kD intervals (Ward et al., 1995; Garcia-Mata et al., 1999) at anywhere near the ~37 kD FLAG-rSIRT2 bands in either soluble or insoluble parts (**Fig. 3.19**). Instead, ubiquitinated intrinsic cellular proteins probably coaggregated with overexpressed rSIRT2 mutants.

In primary OLPs that often began to bear endogenous CNP expression at the end of the transfection experiments, rSIRT2 mutant aggregates often immunostained also positive for CNP (**Fig. 3.17 A-C**). The cytoplasmic space surrounding the aggregates, in contrast, unusually showed low levels of both rSIRT2 and CNP immunoreactivities. This result indicates coaggregation of CNP together with the overexpressed aggregation-prone low-solubility rSIRT2 mutants (**Fig. 3.17 A-C**).

The overall distribution of the microtubule network as revealed by immunostaining of α-tubulin or acetylated α-tubulin in the transfected cells, was not overtly affected by the formation of rSIRT2 mutants aggregates (**Figs. 3.17 D and 3.18 C, F, G, I**). Neither IB nor PA clumps colocalized with α-tubulin staining to any significant extent (**Figs. 3.17 D-F and 3.18 C, F, G, I**). Immunostaining of α-tubulin in the area of rSIRT2 mutants aggregates, on the contrary, was usually lower in comparison to that in other part of the cytoplasm or in cells without aggregates (**Fig. 3.18 C, F, G, I**). As compared to that in the wildtype Sirt2-transfected or the untransfected controls, solubility of α-tubulin was also not significantly affected by overexpression of aggregation-prone rSIRT2 mutants. The majority of α-tubulin was consistently detected in soluble portion of cell lysates on Western blots of all transfection groups. **Figure 3.18B** shows such examples with rSirt2, rSirt2N131A, rR/N and **rK302Δ** transfected cell lysates.

12. Cytoplasmic aggregates were not induced by the loss of rSIRT2 deacetylase activity

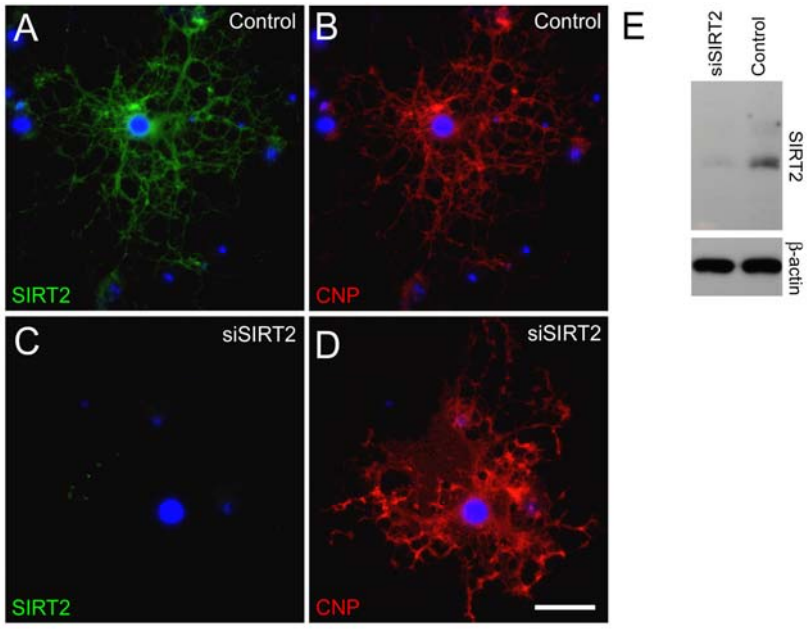

Figure 3.20 rSIRT2 mutant-induced aggregation is not resulted from loss of deacetylase activity

Primary OLP cells were differentiated for 6 days and transfected with siRNA against rSIRT2 (C, D, E); they were analyzed after 48 hours in culture. The knockdown effect of endogenous rSIRT2 was obvious as judged by either immunofluorescence (C) or Western blots (E) in comparison to untransfected controls (A, E). No aggregate formation was observed in these rSIRT2-deficient cells. Normal OLP cells in panels A and B were presented as controls. β-actin was used as loading control in Western blots (E). Antibodies or DAPI used for staining are indicated in the lower left part of each panel. Scale bars in all panels: 20μm.

rSIRT2 as an α-tubulin and histone deacetylase could be partially inactivated by specific point mutations (Finnin et al., 2001; North et al., 2003). These results were confirmed in our previous experiments (Li et al., 2007). We next investigated if the present mutation-induced aggregate formation is related to the deacetylase activity loss of rSIRT2 mutants in transfected cells. Though both rSIRT2H150Y and rD133A are both known to be partially deacetylase-defective, their propensity to cause

aggregate formation in transfected cells differed markedly. rSIRT2H150Y triggered none or only occasional aggregates formation, whereas rSIRT2D133A caused aggregates in over 60% of the transfected OLN-93 cells (**Fig. 3.22 B**). To further clarify the issue, we used three siRNA duplexes of rSIRT2 to transfect and knockdown endogenous rSIRT2 activity in primary OLPs. As shown by immunofluorescence and Western blots, the knockdown of rSIRT2 mRNA effectively diminished native rSIRT2 expression (**Fig. 3.20 C,E**), but produced no observable aggregates in the rSIRT2-depletd cells (**Fig. 3.20 D**). These results indicated that aggregate formation in the transfected cells was unlikely a result of deacetylase activity loss of the aggregation-prone rSIRT2 mutants.

13. Solubility decrease contributes to aggregate formation by rSIRT2 mutants

If not the biological enzyme activity loss, we next questioned whether mutation-induced modifications of the protein biophysical properties determined or related to aggregates formation. In fact, through quantitative analyses, an obvious trend of inverse correlation between solubility and aggregate formation propensity of rSIRT2 mutants was established (**Fig. 3.22 B**). Solubility in RIPA buffer, for example, was 80.5±2.9% for rSIRT2, 23.2±6.7% for rSIRT2N131A and 0.6±0.1% for rSIRT2R/N (Western blots were at least repeated twice for each sample), whereas aggregate formation by the three was in 0.5±1.1%, 7.0±2.3% and 85.4±4.5% of transfected OLN-93 cells, respectively. There also seemed a cumulative effect of selected point mutations on insolubility and aggregation-prone property.

Overexpressed rSIRT2N/H, for example, appeared to be less soluble than either rSIRT2N131A or rH150Y, and this rSIRT2 double-mutant gave way to higher percentage of aggregate-positive cells. All together, these results suggested that the decreases in solubility of the rSIRT2 mutants contributed to their aggregates formation.

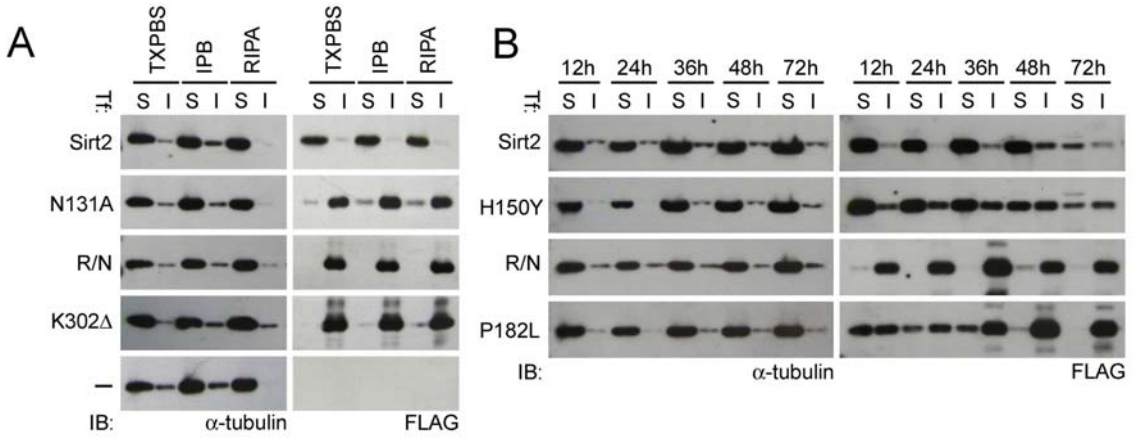

Figure 3.21 Decreased solubility may contribute to aggregate formation by SIRT2 mutants

(A) OLN-93 cells transfected with different plasmids as indicated were lysed 48h after transfection in three buffers with increasing detergent strength: PBS with 2% triton X-100 (TXPBS), IPB, RIPA, divided into detergent-soluble (S) and –insoluble (I) fractions and probed with anti-FLAG or anti-α-tubulin antibodies. "-": transfection without plasmid;

(B) Solubility kinetics of rSIRT2 mutants after overexpression. OLN-93 cells were transfected with three representative mutants as indicated. After 12, 24, 36, 48 or 72 hours, the cell lysates were divided into RIPA soluble and insoluble portion and subjected to Western blotting.

Next, we tested the solubility kinetics of selected SIRT2 mutants after overexpression in OLN-93 cells. OLN-93 cells were lysed 12, 24, 36, 48 or 72 hours after transfection, and subjected to Western blot analyses. From the early stages (e.g., 12 hours) after overexpression, all SIRT2 mutants tested (H150Y, R/N and **P182L)**

showed decreased solubility in comparison with that of wildtype SIRT2. SIRT2R/N, which formed aggregates in most transfected cells (**Fig. 3.22 B**), was almost completely insoluble throughout the course of the overexpression (**Fig. 3.21 B**). Gradual decreases of solubility were observed for both SIRT2 wildtype and two other mutants. The attenuations for the SIRT2H150Y and **P182L** mutants, however, seemed accelerated and more significant than for wildtype SIRT2 (**Fig. 3.21 B**).

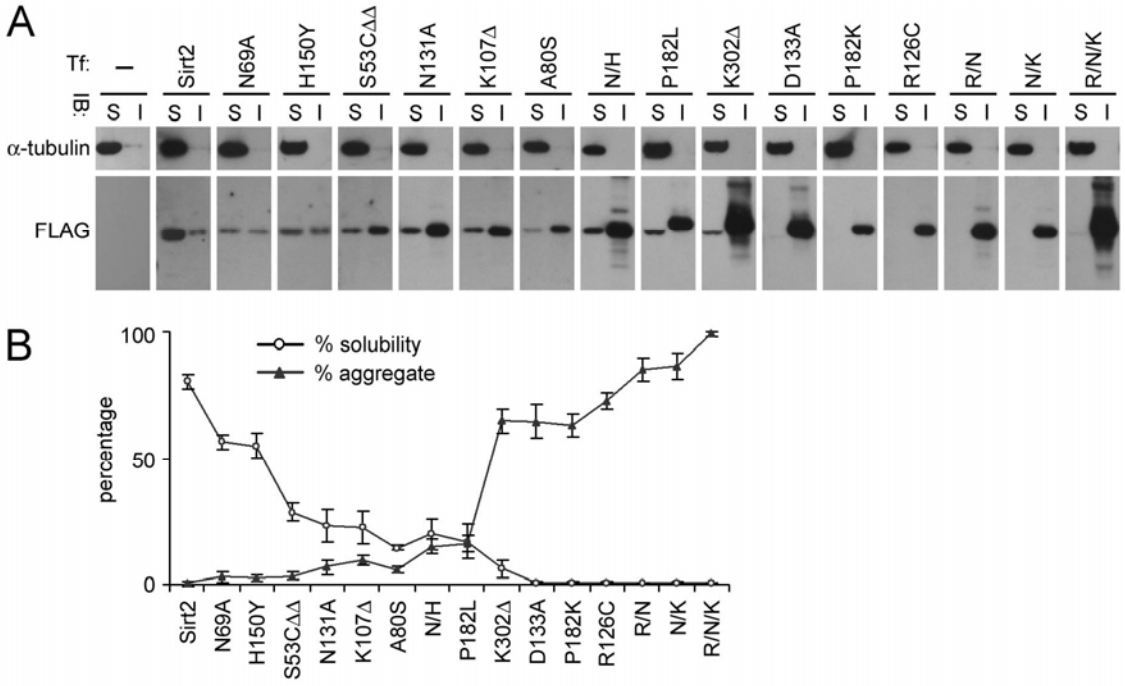

Figure 3.22 An inverse correlation between aggregate-triggering propensity and protein solubility of mutants

(A) Forty-eight hours after transfection, OLN-93 cells were lysed by RIPA buffer, and the distribution of wildtype or 15 mutated SIRT2 proteins in soluble supernatants (S) or insoluble pellets (I) of the cell lysates were examined by Western blots.

(B) Quantitative analysis of the solubility of 15 different SIRT2 mutants according to the Western blots immunoreactivities (as in panel D) and the corresponding aggregate-positive cell percentages after their transfection in OLN-93 cells. A trend of inverse correlation could be clearly observed between solubility and aggregate formation propensity of these mutants. Solubility decrease of SIRT2 mutants in comparison to wildtype may be correlated to aggregate formation.

Consistent with the speculation that solubility decrease contributed to aggregate formation, a portion of the transfected cells at early stages after overexpression were already aggregate-positive. At 12 hours after transfection, for example, aggregate-positive cells were 1.2±1.1% for rH150Y group, 5.2±1.1% for rP182L and 50±4.8% for rR/N. Accompanying the gradual decreases of solubility along the course of overexpression (**Fig. 3.21B**), the percentages of aggregate-positive cells, by contrast, increased gradually, and reached 2.9±1.3% for rSirt2H150Y, 16.1±3.3% for **rP182L** and 85.4±4.5% for rR/N at 48 hours after transfection. Overall, these data supports the notion that aggregate formation by rSIRT2 mutants rooted, at least in part, from solubility decreases of the mutated molecules. The kinetics of gradual but enhanced insolubilization as demonstrated by some of the mutants may implicate possibility of delayed or chronic aggregation by mutants of such type (**Fig. 3.21B**).

14. A protective role of the N-terminus domain of human SIRT2 against solubility loss and aggregation

As mentioned, different from rSirt2, mutations introduced into hSIRT2 only attenuate protein solubility but were incompetent to induce prominent aggregate formation (**Fig. 3.23B**). In addition, higher solubility was invariably detected for all overexpressed hSIRT2 and mutant proteins in comparison to rSIRT2 with mutations at corresponding positions (**Figs. 3.21, 3.22 and 3.23**). For example, the solubility of rK302Δ was 6.2±3.7% as compared to 66.2±1.5% of rSIRT2, whereas that of hK339Δ was found to be 32.0±1.6% as compared to 99.2±0.2% of hSIRT2. Similar results

were observed for all other 5 mutants (**Figs. 3.22B and 3.23B**). But the higher solubility of hSIRT2 and its mutants may not account for the absence of aggregates in OLN-93 overexpressors. The evidence is that some hSIRT2 mutant bears a solubility akin to that of rSIRT2 mutants (i.e. hR163C 17.8±4.5% versus **rP182L** 17.0±7.0%), but possesses significantly different ability to cause aggregate formation (hR163C ~0% versus **rP182L** 16.1±3.3%).

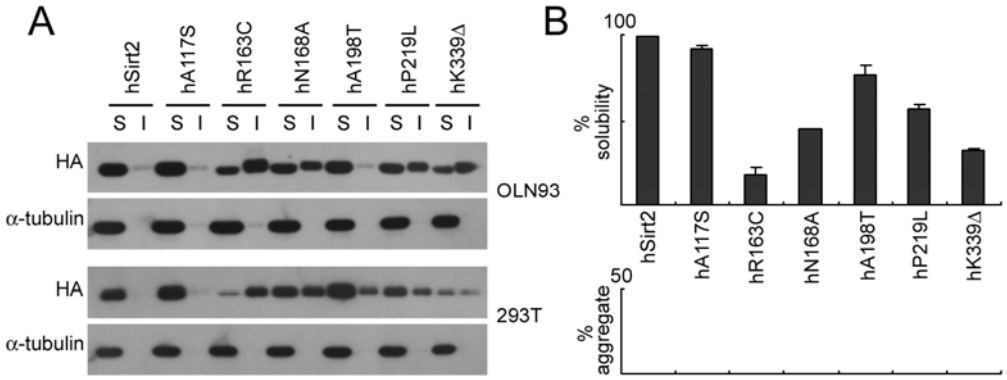

Fig 3.23 Upon overexpression, hSIRT2 mutants showed solubility decrease but did not cause aggregate formation

(A) OLN-93 or 293T cells transfected with wildtype hSirt2 and its mutants as indicated were lysed 48h after transfection in RIPA buffer, then divided into detergent-soluble (S) and -insoluble (I) fractions and probed with anti-HA or anti-α-tubulin.

(B) Bar graphs showing the mutant solubility and aggregate-positive cell percentages after transfection of different hSirt2 mutants in OLN-93 cells as described in panel A.

We thus sought to understand the mechanisms underlying such a discrepancy between these two SIRT2 homologues. Both rSIRT2 and hSIRT2 possesses NAD-dependent deacetylase activity and can be inactivated by specific mutations at correspondingly same positions (North et al., 2003; Li et al., 2007). The most significant structural difference between the two orthologs might be the 37-residue N terminus domain (hNter) which only present in hSIRT2 (**Fig. 3.16**). We questioned whether this hNter domain could be the player causing such difference. We firstly

tested the effects if this domain was deleted from hSIRT2 (**Fig. 3.24**). The hNter-deletion forms of wildtype and three hSIRT2 mutants (N^{Δ}hSIRT2, N^{Δ}hA117S, N^{Δ}hA198T and N^{Δ}hK339Δ) were constructed into HA-tagged pXJ40 vector and transfected into OLN-93 cells. As shown in **Figure 3.25A**, 24hrs after transfection, the solubility of overexpressed hSIRT2 and its mutants was greatly attenuated after hNter deletion. For example, the solubility of hSIRT2 is 95.1±1.0%, whereas that is 4.7±1.4% for N^{Δ}hSIRT2. Solubility of N^{Δ}hA117S, N^{Δ}hA198T and N^{Δ}hK339Δ are also significantly decreased in comparison to their counterparts bearing hNter (**Fig. 3.25 A, B**). Consistent with the notion that solubility is one of the determinants of aggregate formation, the solubility decrease after hNter deletion was accompanied by increases of aggregate percentages in transfected OLN-93 cells (**Fig. 3.25 B**).

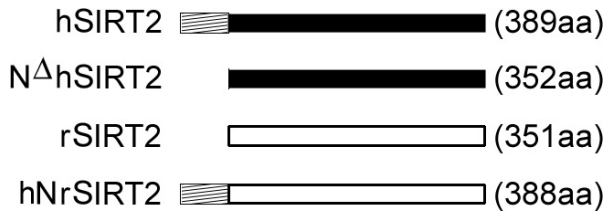

Fig 3.24 Schematic diagram showing four different kinds of human, rat or human-rat chimera SIRT2 used in this study

We next investigated if the addition of the hNter to rSIRT2 could change the biochemical and cellular properties of rSIRT2 and its mutants (**Fig. 3.24**). As shown in **Figure 3.25A** and **B**, 24hrs after transfection, the solubility of rSIRT2 and its mutants is 57.9±1.6% (rSIRT2), 48.9±0.7% (rA80S) and 24.6±3.3% (rK302Δ). By contrast, the solubility of chimera hNrSIRT2, hNrA80S and hNrK302Δ is greatly

improved and reached 95.8±1.1%, 89.6±4.3%, and 37.3±2.9%, respectively. This piece of result strongly suggested that hNter of hSIRT2 may prevent the solubility decrease of SIRT2 mutants. The aggregate formation percentages in the transfected OLN-93 cells were also assessed. The addition of hNter into rSIRT2 inhibited the aggregation of the later. Taking rK302Δ as an example, the aggregate percentages reduced from 14.7±2.1% to 3.6±0.5% after addition of hNter (data collected 24hrs after transfection) or from 61.3±6.2% to 5.4±1.2% (48hrs after transfection).

As presented above in **Figure 3.21B**, mutant rSIRT2 proteins exhibited kinetics of gradual insolubilization after overexpression. In this regard, the current experiments also indicated that the presence of hNter in the overexpressed proteins greatly inhibited the time-dependent progression of protein insolubilization. In between 24 and 48 hours post transfection, the solubility of rSIRT2 in RIPA buffer decreased from 90.4±2.0% to 57.9±1.6%, in sharp contrast to that of hNrSIRT2, the change of which is not statistically significant (96.0±0.4% to 95.8±1.1%). Similar trends are also observed for rA80S and rK302Δ as compared to their chimera counterparts (**Fig. 3.25 A, B**). Take together, all these results demonstrated that the 37aa N terminus domain of hSIRT2 may play a role to inhibit the insolubilization of proteins when mutations were introduced as well as prevent protein aggregation.

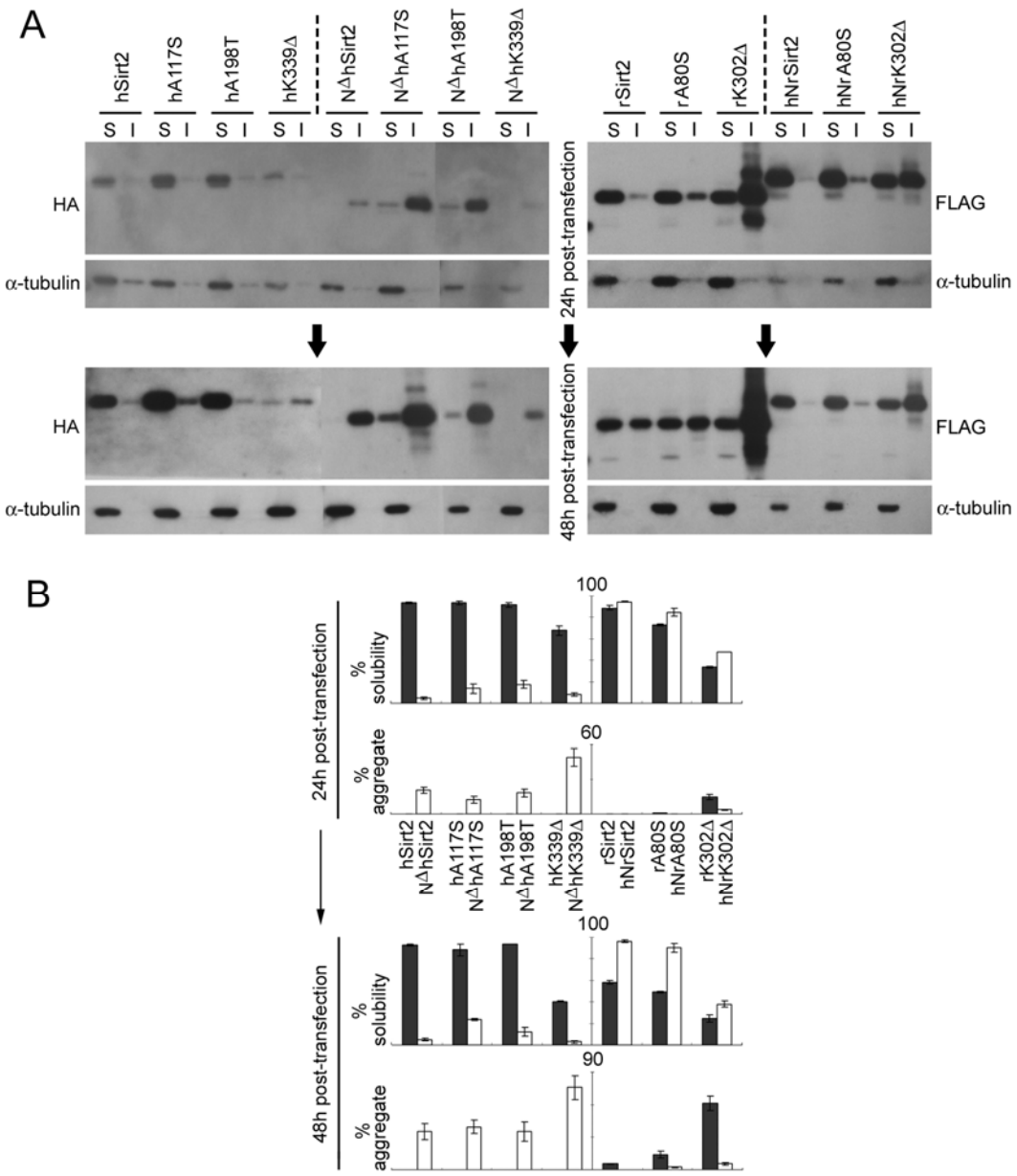

Fig 3.25 Protection of hSIRT2 N-terminus domain against solubility loss and protein aggregation

(A) OLN-93 cells were transfected with different kinds of human, rat or human-rat chimera SIRT2 plasmids as indicated. 24 or 48 hours post transfection, the cells were lysed and divided into RIPA detergent-soluble (S) and -insoluble (I) fractions and probed with anti-HA or anti-α-tubulin. Note the molecular weight difference between proteins with and without hNter is around 4kDa.

(B) Bar graphs showing the mutant solubility and aggregate-positive cell percentages after transfection of different kinds of human, rat or human-rat chimera SIRT2 plasmids as described in panel D. In each transfection time point, the solubility of hSIRT2 or its mutants was compared to corresponding hNter deletion forms; similarly, solubility of rSIRT2 or its mutants was compared to their respective forms with addition of the hNter domain. The aggregate-bearing transfection cell percentages were also assessed.

15. Microtubule and HDAC6 functions affect the aggregate formation induced by SIRT2 mutants

Several reports have implicated involvement of both microtubule network (MT) and HDAC6 in the formation (Johnston et al., 2002; Kawaguchi et al., 2003; Tanaka et al., 2004) or degradation of protein aggregates (Johnston et al., 1998). We hence investigated possible roles of MT and HDAC6 in the SIRT2 mutants-triggered aggregates formation. These experiments were carried out in 293T cells that bear endogenous HDAC6 expression. We first examined the effects of nocodazole and taxol, well-established microtubule destabilizing and stabilizing reagents, on SIRT2 mutants-related aggregates formation.

After wildtype Sirt2 transfection, both treatments did not cause aggregate formation. But as shown in **Figure 3.26 B**, in all three transfections by rR/N, **rK302Δ** and R126C, the addition of nocodazole significantly increased the aggregate-positive cell percentages in transfected cells, whereas taxol treatment exhibited the opposite effects (**Fig. 3.26 B**). In terms of the relative number of IB- and PA-positive cells, taxol treatment did not induce obvious change of the ratio between the two as compared to the control (**Fig. 3.26 C**), but nocodazole seemed promoting formation of PA aggregates and inhibiting that of IBs (**Fig. 3.26 C**). Neither of the two drugs significantly altered the detergent-solubility of FLAG-tagged SIRT2 mutants (**Fig. 3.26 A**). Put together, these results indicated that stabilization of MT may inhibit the aggregates formation, and MT destabilization by nocodazole preferably promoted the formation of PA aggregates in mutant SIRT2-transfected cells.

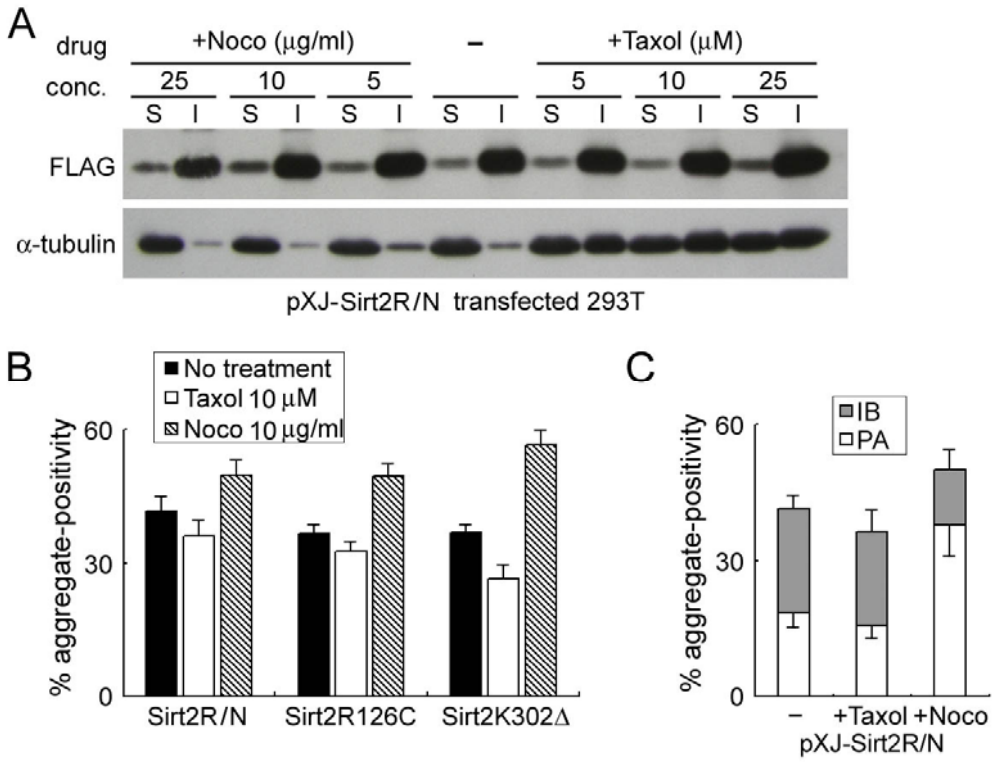

Figure 3.26 Stability of microtubule network influences the formation of aggregations but not protein solubility

(A) Thirty-six hours after transfection with Sirt2R/N, 293T cells were treated for 12 hours with various concentrations of taxol and nocodazole (Noco) as indicated before eventual cell lysis by RIPA buffer. Cell lysates were then divided into RIPA soluble (S) and insoluble (I) portion and subjected to Western blots analysis. The result indicated that treatment of these drugs, though changed the IB-to-PA ratio (panel C), did not significantly affect the solubility of rSIRT2 mutants. "conc.": concentration of drugs.
(B) 293T cells were transfected with rSirt2R/N, rR126C or **rK302Δ**, and treated with either taxol (10μM) or nocodazole (10μg/ml) in the culture medium 36 hours after transfection. The treatment persisted for 12h before the cells were fixed and subjected to immunofluorescent staining. Statistical analysis shows the percentages of aggregate-positive cells out of all transfected 293T cells in each transfection group.
(C) Statistical analysis of the percentages of IB-positive and PA-positive cells out of rSirt2R/N transfected cells after treatment by taxol (10μM) or nocodazole (10μg/ml) as described in panel B legend.

In 293T cells, when rSirt2R/N was cotransfected with an effective HDAC6 siRNA duplex that would knockdown endogenous HDAC6 expression of the cells (**Fig. 3.27 A**), the percentage of aggregate-positive cells was significantly reduced without obviously altering the IB-to-PA positivity ratio (**Fig. 3.27 B**), as compared

with the rSirt2R/N-JN siRNA cotransfection control group. HDAC6 did not co-pellet with FLAG-rSIRT2R/N in detergent-insoluble portion of cell lysates in RIPA buffer (**Fig. 3.27 C**).

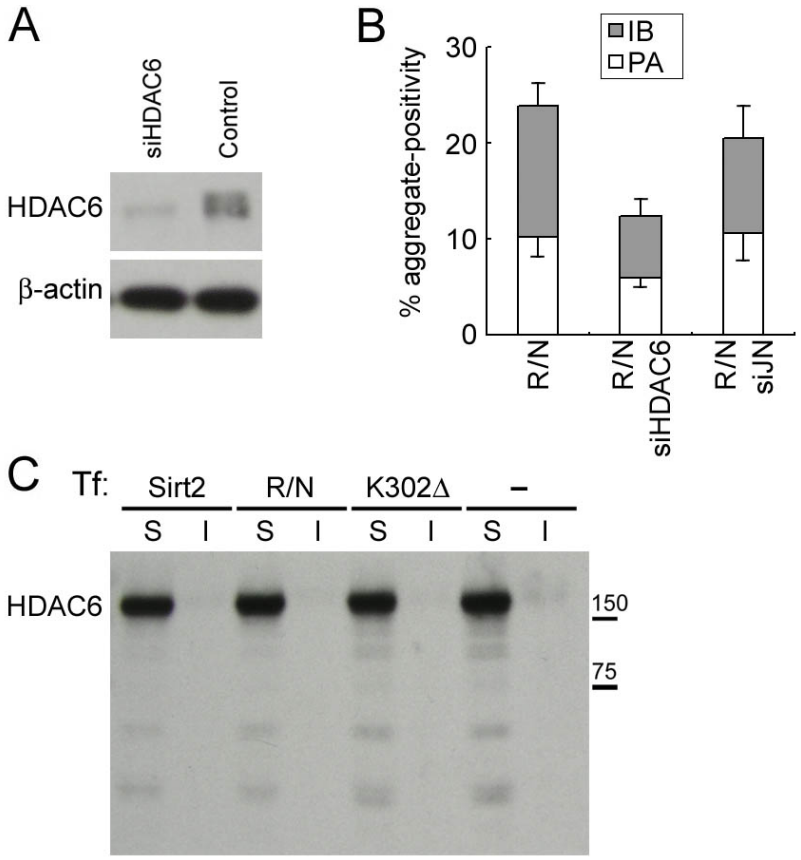

Figure 3.27 HDAC6 is required for the formation of aggregates triggered by rSIRT2 mutants

(A) Western blots showing endogenous HDAC6 was successfully knocked down in 293T cells; β-actin was used as the loading control.

(B) 293T cells were transfected with rSirt2R/N only, rSirt2R/N plus siHDAC6, or rSirt2R/N plus siJN. Thirty-six hours after transfection, cell counting based on immunofluorescent staining indicated percentages of aggregate-positive cells out of all transfected 293T cells.

(C) 293T cells transfected with rSirt2, rSirt2R/N and rK302Δ were lysed in RIPA buffer, the soluble (S) and insoluble (I) portions were subjected to Western blot analysis probed with an anti-HDAC6 antibody.

CHAPTER 4
DISCUSSION

1. SIRT2 as a protein preferentially expressed in oligodendrocytes

By means of ISH, IHC and double labeling, the present study identified SIRT2 was preferentially expressed by oligodendrocytes. This result agrees with previous proteomics studies that have identified SIRT2 in the myelin sheath (Vanrobaeys et al., 2005; Southwood et al., 2007). In comparison with various markers of developing and mature oligodendrocytes/myelin sheath, spatial and temporal profiles of SIRT2 expression closely matched those of CNP except in oligodendrocytic cell bodies where little SIRT2 was found. In **Figure 3.3**, SIRT2 and CNP expression levels were demonstrated to be co-variants along the progression of oligodendrocyte development *in vivo*. The two molecules colocalize in various regions of the CNS (**Fig. 3.6 A-D,K**). There is also *in vitro* evidence, such as those in **Figs. 3.11**, **3.14 and 3.15**. In this connection, it is noteworthy that CNP, like SIRT2, is also a tubulin-associated oligodendroglial protein in the CNS (Bifulco et al., 2002; Lee et al., 2005).

Unlike the absence of SIRT2 in the majority of oligodendroglial perikarya in the adult CNS, clear SIRT2 signals were observed in the cell bodies of cultured primary OLPs. This dissimilarity in subcellular distribution of the protein most likely reflected differences between mature oligodendrocytes in the adult CNS and oligodendrocyte precursors in the culture.

2. SIRT2 as a differentiation inhibitor of oligodendrocytes

Among others, cytoskeleton-associated oligodendroglial proteins such as CNP, JN and mayven, have been recently reported to regulate oligodendrocytic process

outgrowth, gene expression and/or myelin-axon interaction (Jiang et al., 2005; Lee et al., 2005; Zhang et al., 2005). The present results showed that SIRT2 is yet another member of the protein family, but probably functions as a "braking" mechanism in oligodendroglial development. Overexpression of SIRT2 significantly inhibited the oligodendroglial arborization and tubulin acetylation, indicating retardation of the cells' course of specialization, whereas siRNA knockdown of endogenous SIRT2 had the opposite effects. This inhibitory role of SIRT2 is further supported by our finding that overexpression of the protein counteracted the facilitatory effects of JN on arborization of OLN-93 oligodendrocyte cell line. Interestingly, SIRT2 has been implicated in regulating adipocyte differentiation (Jing et al., 2007). Its family homologue SIRT1 represses myocyte differentiation (Fulco et al., 2003).

Blockade of HDAC activities by TSA and valproic acid (VPA) was found to delay oligodendroglial differentiation (Marin-Husstege et al., 2002; Liu et al., 2003; Hsieh et al., 2004; Shen et al., 2005). The results were confirmed by our experiments (data not shown). Since SIRT2, as a member of class III HDACs, is not inhibited by TSA (North et al., 2003), these results clearly indicate the involvement of other HDACs in regulating oligodendroglial differentiation. HDAC6, another known tubulin deacetylase, was coimmunoprecipitated with SIRT2 when overexpressed together with SIRT2 (Hubbert et al., 2002; North et al., 2003). But expression pattern study seemed against the possibility that HDAC6 is involved in oligodendrocyte differentiation because this molecular predominantly presents in neurons (Southwood et al., 2007). Future studies are necessary to understand which HDAC members

mediate the effect of such inhibition.

Apart from regulating differentiation, the abundant SIRT2 immunoreactivity in adult oligodendrocytes (present results) entails functional roles of the protein in the mature CNS. Under the electron microscope, SIRT2 was mainly found in the non-compact outer and terminal loops of myelin sheath. This subcellular positioning and the tubulin deacetylation activity seemingly pointed to possible roles of the protein in subcytoarchitecture, molecular trafficking or myelin-axon signaling of oligodendroglia. Other cytoskeleton-related oligodendroglial proteins like CNP and JN have also been implicated in similar functions (Bifulco et al., 2002; Lappe-Siefke et al., 2003; Zhang et al., 2005).

3. SIRT2 expression, tubulin deacetylation and oligodendroglial differentiation

The present results demonstrated functional roles of tubulin acetylation in maturation of oligodendroglia, as well as SIRT2-mediated tubulin deacetylation in decelerating the differentiation/aging of the cell. Our data indicated that SIRT2 action in oligodendrocytes was most likely mediated through tubulin deacetylation. First, as revealed by our *in vivo* and cell culture results (**Figs.3.6 and 3.11**), SIRT2 was primarily an oligodendroglial cytoplasmic protein mainly localized to the cellular processes and non-compact cytoplasm-containing parts of myelin sheath, in agreement with previous data (Perrod et al., 2001; North et al., 2003; Vanrobaeys et al., 2005). Second, SIRT2 was colocalized with acetylated α-tubulin in cultured primary OLPs. Third, wildtype SIRT2 rather than SIRT2 mutants (SIRT2N131A and

SIRT2H150Y) simultaneously diminished its tubulin deacetylase activity and its inhibition of OLP morphological differentiation, and siRNA knockdown of SIRT2 gave rise to similar effects (**Figs. 3.9 and 3.15**). Finally, comparison of Western blotting results from the anti-acetylated lysine and the anti-acetylated α-tubulin antibodies identified α-tubulin as the main substrate for SIRT2 among OLN-93 cytoplasmic proteins (**Figs. 3.9 and 3.10**). In comparison to histones, tubulin has been demonstrated as a preferred substrate of SIRT2 (North et al., 2003). Our *in vitro* deacetylation test also indicated a NAD-dependent tubulin deacetylase activity of SIRT2. Hence tubulin deacetylation through SIRT2 probably represented yet another important mechanism in the complex cytoskeletal control of oligodendrogenesis and myelinogenesis, in parallel to those mediated through other cytoskeleton-related proteins such as MAP2, Tau, CNP and JN (LoPresti and Konat, 2001; Richter-Landsberg, 2001; Lee et al., 2005; Zhang et al., 2005).

It remains unclear how tubulin deacetylation by SIRT2 was translated into altered cytoplasmic extensions and delayed differentiation of oligodendrocytes. A plausible hypothesis might be that deacetylation lowered microtubule stability, reduced tubulin polymerization, increased depolymerization, or altered the binding of tubulin to associated proteins, as previously suggested in other cell types (Piperno et al., 1987; Robson and Burgoyne, 1989; Hubbert et al., 2002).

SIRT2 has also been shown to interact with histones H3, H4 (North et al., 2003; Vaquero et al., 2006) and transcription factor HoxA10 (Bae et al., 2004). Our electron microscopic observation also found SIRT2, albeit at lower levels than in the

cytoplasm, in the nuclei of a limited number of oligodendroglia. However, it seems that the acetylation levels of histone H3 (K14) and H4 (K16) were not altered in OLN-93 cells overexpressing SIRT2 (**Fig. 3.9**), suggesting the differentiation-inhibitory roles deciphered by the present data was not mediated through regulating histone acetylation. Future investigations are necessary to determine the circumstances/factors that govern the substrate selection (tubulin vs. histones, for example) and subcellular distribution (cytoplasmic vs. nuclear) of SIRT2.

4. Overexpression of mutated forms of rSIRT2 differentially induce aggregate formation

As illustrated by the current study and other reports, SIRT2 is an oligodendroglial protein in the CNS (Vanrobaeys et al., 2005; Li et al., 2007; Southwood et al., 2007). The current study identified that certain mutants of rSIRT2, when overexpressed, would trigger detergent solubility decreases of the proteins and cellular aggregates formation in a deacetylase activity-independent manner. At cellular level, similar characteristics could be found between rSIRT2 mutant aggregates as reported here and mutants aggregates of other proteins, such as parkin, α-synuclein, prion protein, peripheral myelin protein 22 (PMP22) and polyglutamine-containing proteins (Lee and Lee, 2002; Taylor et al., 2002; Ardley et al., 2003; Rajan and Kopito, 2005; Grenier et al., 2006). These similarities include that (1) formation of aggregates are related to solubility decreases of the protein mutants, and influenced by functions of MTs; (2) aggregates colocalized with ubiquitin; (3) affected cells exhibit

fragmentation of Golgi apparatus; and (4) aggregates appeared as either PAs dispersed throughout the cytoplasm or large IBs juxtanulearly localized.

5. Deacetylase activity loss is not the cause of aggregate formation

SIRT2 functions as NAD-dependent protein deacetylase using α-tubulin or histones as substrates (North et al., 2003; Li et al., 2007). Mutations of the enzyme cause variable loss of its deacetylase activity (Finnin et al., 2001; North et al., 2003). A possibility arises as whether the aggregation of SIRT2 mutants and endogenous oligodendroglial proteins (such as CNP in **Fig. 3.17**) was due to the loss of the deacetylase activity. Aggregation of the protein mutants would deplete availability and cause a further loss of the enzyme activity indirectly as has been suggested for mutants of other proteins, e.g., parkin (Sriram et al., 2005). Although theoretically conceivable, such a possibility was not supported by the present experimental data. siRNA knockdown of endogenous rSIRT2 in primary OLPs caused no obvious aggregates, and overexpression of other point-mutated deacetylase-defective rSIRT2 also did not resulted in pronounced aggregates formation in transfected cells. Three of the 12 mutated residues examined (rN131A, rH150Y and rD133A) in the present study are in adjoining regions of rSIRT2 (**Fig. 3.16**; Finnin et al., 2001), and are known to be deacetylase-defective *in vitro* and in cultured cells (North et al., 2003). But the insolubility and aggregate-forming propensity of the three differed drastically. rSIRT2N131A and rH150Y were similar to wildtype rSIRT2 in these two aspects whereas rSIRT2D133A was mostly insoluble and aggregation-prone (**Fig. 3.22**).

6. Determinant of aggregate formation

6.1 Insolubility, cytoplasmic aggregate formation and cytotoxicity of rSIRT2 mutants

Rather than activity loss, mutation-induced detergent insolubility was demonstrated to be related to aggregates formation in our current system. It is striking to note that in comparison with wildtype rSIRT2, all 15 rSIRT2 mutants tested in the present study showed lower solubility in the presence of 0.1% SDS, and their propensity to form aggregates in transfected cells was inversely correlated with their detergent solubility. Furthermore, complex rSIRT2 mutants combining two or three point mutations exhibited not only lower solubility but also accordingly higher aggregate formation propensity as compared to mutants harboring any of the single mutations (**Fig. 3.22**).

This conclusion is seemingly contradictory to our results that hSIRT2 mutants induced attenuated solubility in comparison to wildtype but no prominent aggregate formation (**Fig. 3.23**). We proposed that the reason for this discrepancy lay in the difference between rSIRT2 and hSIRT2. The 37aa hNter, as suggested by present data, protects hSIRT2 and its mutants from solubility decrease (see below). When this domain was deleted, the inverse correlation operates again (**Fig. 3.25**). Also, we proposed that the cell machinery might have different tolerance threshold to decreased solubility of different mutated proteins. For rSIRT2 proteins in OLN-93 cells, this threshold seemed to be somewhere between that of rSIRT2P182L (solubility 17±6.9%)

and rK302Δ (solubility 6.2±3.7%), because rSIRT2 mutants with solubility higher than ~17% only generated scarce aggregate-positive cells, but those lower than this threshold caused sharply increased number of aggregates (**Fig. 3.22**). In this regard, the difference between OLPs and OLN-93 cells in aggregate formation by some of the rSIRT2 mutants might also be partly attributed to the difference of the tolerance thresholds derived from variations in molecular trafficking, ubiquitin-proteasome system, binding partners and/or molecular chaperones across cell types. The microtubule-associated protein CNP, for example, is present in OLPs, but absent in OLN-93 cells (data not shown).

Factors affecting rSIRT2 solubility have not been well elucidated. The crystal structure of hSIRT2, however, has been reported (Finnin et al., 2001). As all the rSIRT2 residues subjected to point mutations in the current study are conserved between rat and human, detailed analyses and comparison of human and rat SIRT2 may provide some clues to the mutation-induced rSIRT2 solubility alterations. First, direct biophysical property change and conformational shifts may happen in response to point mutations (Garzon-Rodriguez et al., 2000; Ippel et al., 2002; Fasano et al., 2006). Investigations have shown that biophysical properties such as solvent accessibility (SA) significantly differ between soluble and amyloid forms of prion protein (Nazabal et al., 2003) (SA: the ratio of the solvent accessible surface area of an amino acid residue in a folded protein structure to that in the unfolded structure, which would be generally lower for hydrophobic residues than hydrophilic ones (Lee and Richards, 1971). R126 of rSIRT2, for example, is a residue predicted with low SA

and buried from solvent (Finnin et al., 2001), the substitution of which might compromise the overall or partial solvent accessibility of rSIRT2 protein, and resulted in the decreased solubility. Property of the substitute amino acid may bring in new modifications of the protein mutants, as is the case with phosphorylation of tau (Sahara et al., 2002). Properties and functions SIRT2 are also influenced by phosphorylation (Dryden et al., 2003).

Detergent insolubility has recently emerged as a common feature of many protein mutants involved in pathogenesis of diverse neurodegenerative diseases or in aggregation formation/cytotoxicity in cultured cells (Garcia-Mata et al., 1999; Wang et al., 1999; Johnston et al., 2000; Shinder et al., 2001; Sahara et al., 2002). Many studies connect aggregation of these disease-associated proteins to cell death or cellular toxicity in diseases. For example, the aggregation status of huntingtin protein is believed to determine neuronal loss in Huntingtin disease (Bates, 2003). Fibrillar α-synuclein aggregation into Lewy bodies is associated with nigrostriatral degeneration in PD (Lee and Trojanowski, 2006). One study suggested that, in protein misfolding diseases, the aggregates in host cells bearing them are inherently toxic (Bucciantini et al., 2002).A study on familial-associated mutations of parkin revealed that the aggregation of parkin might cause a sequestration of the enzymatic activity of this protein from its native substrates, which results in accumulation of toxic substrates of parkin and cellular toxicity (Sriram et al., 2005). On the contrary, inhibition of protein aggregation may prevent the cytotoxicity (Liu et al., 2004).

In terms of cytotoxicity or pathogenecity, aggregates may not only present as

mechanical barriers of molecular trafficking or as reservoirs of toxic mutant molecules, but also trap endogenous proteins of the cell and affect their normal functions. Previous studies showed that disease-associated mutants of PLP and PMP22, two integral membrane proteins of the myelin sheath, promoted formation of not only homodimers or oligomers of the mutants themselves, but also heterodimers or oligomers of the mutant molecules together with the wildtype proteins that were thus prevented from reaching the cytoplasmic membrane to perform normal functions (Yool et al., 2000; Suter and Scherer, 2003). These dimers/oligomers may accumulate later on and was considered as the direct cause of oligodendrocyte death (Tobler et al., 2002; Swanton et al., 2005).

6.2 Factors in addition to solubility decrease contributed to rSIRT2 mutation-induced aggregates formation

However, the current study indicated that solubility does not act as the unique regulating factor of aggregate formation. The present results support the notion as in previous reports that structural and functional status of intracellular trafficking or degradation affects aggregate formation (Kopito, 2000; Johnston et al., 2002; Riley et al., 2003; Bauer and Richter-Landsberg, 2006). First, the overall aggregate-positive cell numbers increased in the presence of nocodazole and decreased in the presence of taxol (**Fig. 3.26**), indicating that the formation of aggregates could be influenced by functional status of the microtubule trafficking or misfolding-cleaning mechanisms. In this regard, it is noteworthy that both nocodazole and taxol treatment were reportedly inhibiting in tau aggregate formation in OLN-t40 cells (Bauer and Richter-Landsberg,

2006). Second, overexpression of rSIRT2R/N or rK302Δ also resulted in aggregation of the cytoskeleton-related endogenous CNP of OLPs (**Fig. 3.17**) which indicates disruption of normal trafficking of oligodendroglial proteins.

Aggregation-inducing protein mutants have also been suggested to directly coaggregate with cytoskeleton (Refolo et al., 1991), or result in profound cytoskeletal elements reorganization or redistribution such as the intermediate filaments (IFs) protein, vimentin (Johnston et al., 1998). However, in oligodendrocytes which do not contain a cytoplasmic IF system, it is intriguing how the aggregates influence the cytoskeleton. Our current result showed no coaggregation between SIRT2 mutants and α-tubulin in both IBs and PAs (**Figs. 3.17 and 3.18**). Instead, the IBs were usually surrounded by bundles of tubulin staining (**Fig. 3.18 C,F**), which is consistent with a previous report about oligodendrocytic aggresomelike inclusions in cell line OLN-t40 (Bauer and Richter-Landsberg, 2006).

Another result from the current study is that HDAC6 activity influenced rSIRT2 mutants-induced aggregates formation, similar to a previous report in other cell models (Kawaguchi et al., 2003). However, HDAC6 was not pivotal for the transformation between PAs and IBs in our model, partly in contradiction to a previous report in which HDAC inhibition impaired the microaggregates transportation to MTOC to form large aggresomes (Corcoran et al., 2004). Overall, the current results on roles of MT network and HDAC6 in aggregate formation were mostly consistent with previous studies. Some of the discrepancies may be expected considering the heterogeneous nature of aggregate formation. The biochemical

properties of the aggregation-prone proteins themselves, for examples, would be crucial determinants. The specific environments of the host cells may also exert significant influences. Also, other future investigations are necessary to figure out the molecules playing the role of HDAC6 in oligodendrocytes.

Taken together, our current study suggested that solubility decrease was a direct result of protein mutations, which in turn only acts as a prerequisite for aggregate formation. The final extent to which aggregates formed are still determined by other factors, such as MT and HDAC6 mediated trafficking or degradation as implicated in current study (**Figs. 3.26** and **3.27**). But on the contrary, aggregate formation rooted from but was not solely determined by mutation-induced solubility attenuation. Aggregates to date almost invariably happened together with impaired protein solubility (Wang et al., 1999; Johnson, 2000; Shinder et al., 2001; Sahara et al., 2002; Sriram et al., 2005).

7. The extra N terminus domain endows hSIRT2 protection from mutation-induced insolubility and aggregation

Human SIRT2 is predicted to exist in two different isoforms as a result of alternative splicing (Voelter-Mahlknecht et al., 2005). But almost all studies about hSIRT2 are dedicated to the isoform bearing 389aa (hSIRT2_v1) rather than the other without the N-terminus 37-residue domain (352aa, hSIRT2_v2). The current study identified a role of this hNter domain in protecting the insolubilization and

aggregation of mutated SIRT2 proteins. The presence of hNter domain in hSIRT2 largely prevents the formation of mutation-induced aggregates and increased the detergent solubility of mutants as compared to rSIRT2 counterparts. The deletion of this domain from both wildtype and mutated hSIRT2 proteins resulted in their solubility attenuation as well as increased propensity to form cellular aggregates (**Fig. 3.25**). While the addition of this domain could help to prevent rSIRT2 from insolubilization and aggregation after being mutated or overexpression time was prolonged. These results raised a possibility that hNter domain plays a protective role against SIRT2 protein malformation and dysfunction.

Though brain-specific genes in mammals are reported to exhibit a lower rate of evolution than genes expressed in other tissues, the trend seems to be reversed in the human lineage (Dorus et al., 2004; Wang et al., 2007b). It is interesting to note that the hNter domain seems not to be detected in lower mammals such as rat, yeast or fruit fly, though one recent study tended to propose the presence of a longer form of mouse SIRT2 containing this domain (Werner et al., 2007). Therefore, it might be an interesting to know what kind of evolutionary pressure generating the difference from rSIRT2 to hSIRT2.

It is well-established that the age-dependent genomic instability and increase in protein mutations is an essential feature of aging, in which Sirtuins are important longevity regulators (Longo and Kennedy, 2006). Under the stress of SIRT2 mutations, this protective role the hNter may possibly represent an evolutionary improvement from rat to human, which at the molecular level guarantees more stable protein

properties in structure and function. This speculation is also supported by the greatly retarded insolubilization speed of rSIRT2 proteins adding with the hNter domain (**Fig. 3.25**). An interesting question could be what if rSIRT2 be engineered to bear such an hNTer *in vivo*, whether mutation-induced insolubilization of rat proteins and aggregation would be inhibited or even life span would be extended?

Further support of the crucial role of hNter came from a recent study which identified a disease-related mutated form of hSIRT2: SIRT2_v3mut (Lennerz et al., 2005). This isoform was found in a human melanoma sample, and its N terminus 37aa domain was replaced by a completely different 18aa domain, in the meantime, this isoform possesses a P199L mutation, which corresponds to P219L of hSIRT2_v1 (P182L of rSIRT2). These characters resulted in the recognition of the mutated protein by autologous T cells (Lennerz et al., 2005). This study suggested that in presence of mutations (i.e. P219L), hSIRT2 with deletion or substitution of the hNter domain could be particularly vulnerable to malfunction so that has to be cleared by immune system.

The mechanisms underlying the protective effects of hNter have yet to be clearly defined. But the possibility may include that the biophysical properties of the mutated protein are affected by the presence of this domain (e.g. SA) or that this fragment acts to recruit chaperones that would help proper trafficking or degradation of mutated proteins.

8. SIRT2, Brain Aging and Neurodegeneration?

SIR2 protein family extends lifespan or slows down aging in various species/cell types ranging from yeast, *Drosophila, C. elegans* to mouse and rat (Blander and Guarente, 2004). In view of the antagonistic effects of SIRT2 on oligodendrocyte differentiation, presence of the protein with normal functions in the adult CNS could presumably help prevent over-differentiation or premature senescence of oligodendrocytes or myelin sheaths. Alternatively, this negative influence of SIRT2 on oligodendroglial differentiation may help preserve an adequate pool of immature oligodendrocytes for remyelination or CNS self-repair when needed.

Meanwhile, the abnormality of the protein will inversely affect the function of oligodendrocytes. The mutation-induced aggregates will deform the Golgi apparatus and cause cell apoptosis (data not shown). Indirectly, the SIRT2 effects on oligodendroglia and myelin could also presumably influence neuronal survival or aging. It is well documented that structural/functional abnormality of oligodendroglia or myelin sheath may cause axon degeneration or neuronal death (Bifulco et al., 2002). Essential roles are illustrated of glial dysfunction in non-cell-autonomous neuron degeneration (Gong et al., 2000; Clement et al., 2003; Custer et al., 2006).

The results in this study that the mutated forms of SIRT2 are causing aggregates formation in both OLPs and cell lines make it intriguing to investigate the involvement of SIRT2 in CNS diseases or neurodegeneration. It remains unknown whether specific SIRT2 mutations in oligodendrocytes will affect normal functions and survival of neurons or through influencing myelin-axon interaction. We hope that

the present study could provide a cellular model to investigate aggregates formation related to myelinic or oligodendroglial diseases, and to help decipher the oligodendroglial roles in brain aging and non-cell-autonomous neurodegeneration.

CHAPTER 5
CONCLUSIONS AND FUTURE STUDIES

1. Conclusions

The present study comes to the following conclusions (**Figure 5.1**):

1) SIRT2 is preferentially an oligodendroglia protein which shows juxtanodal enrichments adjacent to nodes of Ranvier in the myelin sheath.

2) SIRT2 plays a role as NAD-dependent deacetylase with α-tubulin as its main substrate in oligodendrocytes. Also, this study established a correlation between CNP expression, α-tubulin acetylation levels and the degree of oligodendroglial differentiation.

3) SIRT2 inhibits the differentiation of oligodendrocytes via deacetylating α-tubulin: overexpression of SIRT2 inhibiting the differentiation of oligodendrocytes, whereas siRNA knockdown of endogenous SIRT2 expression in primary OLPs has opposite effects.

4) Overexpression of specific mutants of rat SIRT2 gene induces cellular aggregate formation in both OLPs and cell lines. The severity of aggregation formation is associated with the detergent insolubility of the mutants.

5) Different from rat SIRT2, the human ortholog of SIRT2 contains a 37-residue N terminus fragment, which protects the protein from mutation-induced solubility decrease and aggregation.

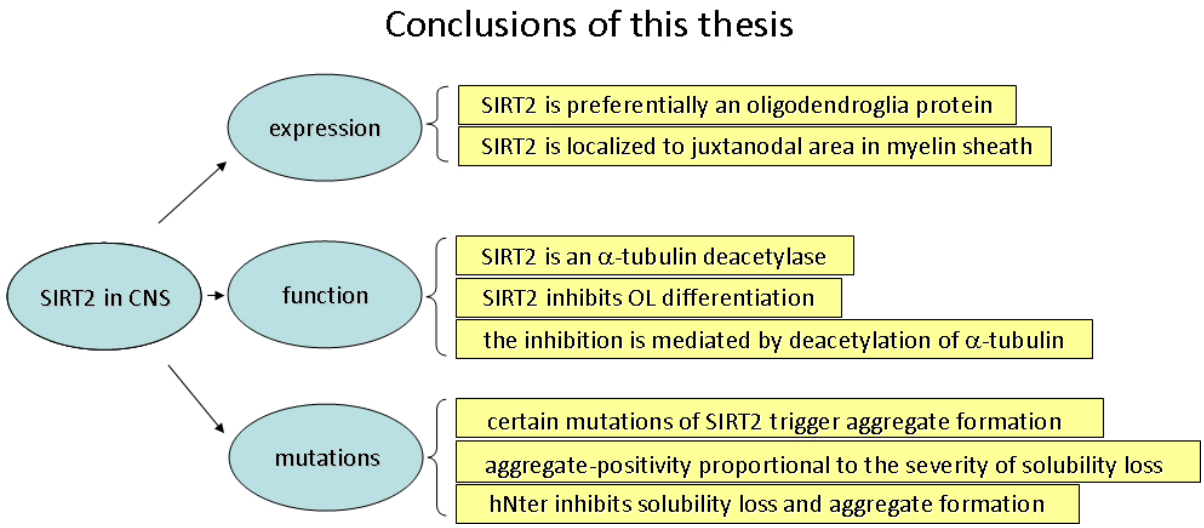

Figure 5.1 Summary of the conclusions reached in this thesis

2. Future studies

1) The current study revealed that the inhibitory role of SIRT2 on oligodendrocyte differentiation was mediated via deacetylating α-tubulin. However, there is still a lack of understanding about how the decrease of acetylation levels of α-tubulin is coupled to the morphological changes of the cell. Also, MBP expression is found to be upregulated when the endogenous SIRT2 expression was knockdown. This result seems to be consistent with other studies in which SIRT2 can translocate to nucleus or regulate transcription factors to modulate gene expression (North and Verdin, 2007; Jin et al., 2008), but the exact mechanisms behind such modulation in oligodendrocytes are still unclear.

2) In the present study, SIRT2 is found to be enriched in the juxtanodal region adjacent to nodes of Ranvier. This region as well as paranodal region is well-established area where essential axon-glia interactions take place. The role of

SIRT2 with regard to myelination or axon-glia interaction could be an interesting issue for further investigation.

3) Given the fact that several of the mutations examined in the current study (e.g. rS53CΔΔ, rA80S/hA117S, rK107Δ, hA198T, rP182L and rK302Δ) are either found in actual NCBI cDNA sequences or identified as single nucleotide polymorphism of Sirt2, our results imply potential involvement of SIRT2 mutations in certain CNS dys-/demyelinating or neurodegenerative diseases. Future studies are necessary to identify Sirt2 mutations in related diseases, and to establish animal models to test validity of this hypothesis.

4) The difference of solubility and aggregation properties between hSIRT2 and rSIRT2 are attributed, as least in part, to the 37 residue N terminus domain of hSIRT2. How exactly this domain protects the protein from solubility decrease and aggregation will be a crucial direction for future work.

5) HDAC6 and MT network are reported to be essential in forming aggresomes. Our present results indicated that the aggregates formed upon overexpression of SIRT2 mutants are affected by activity of HDAC6 and MT stability, but the exact pathways underlying these phenomena still await future investigations.

The functions of SIRT2 and the pathways how it exerts those functions are summarized in **Fig. 5.2**.

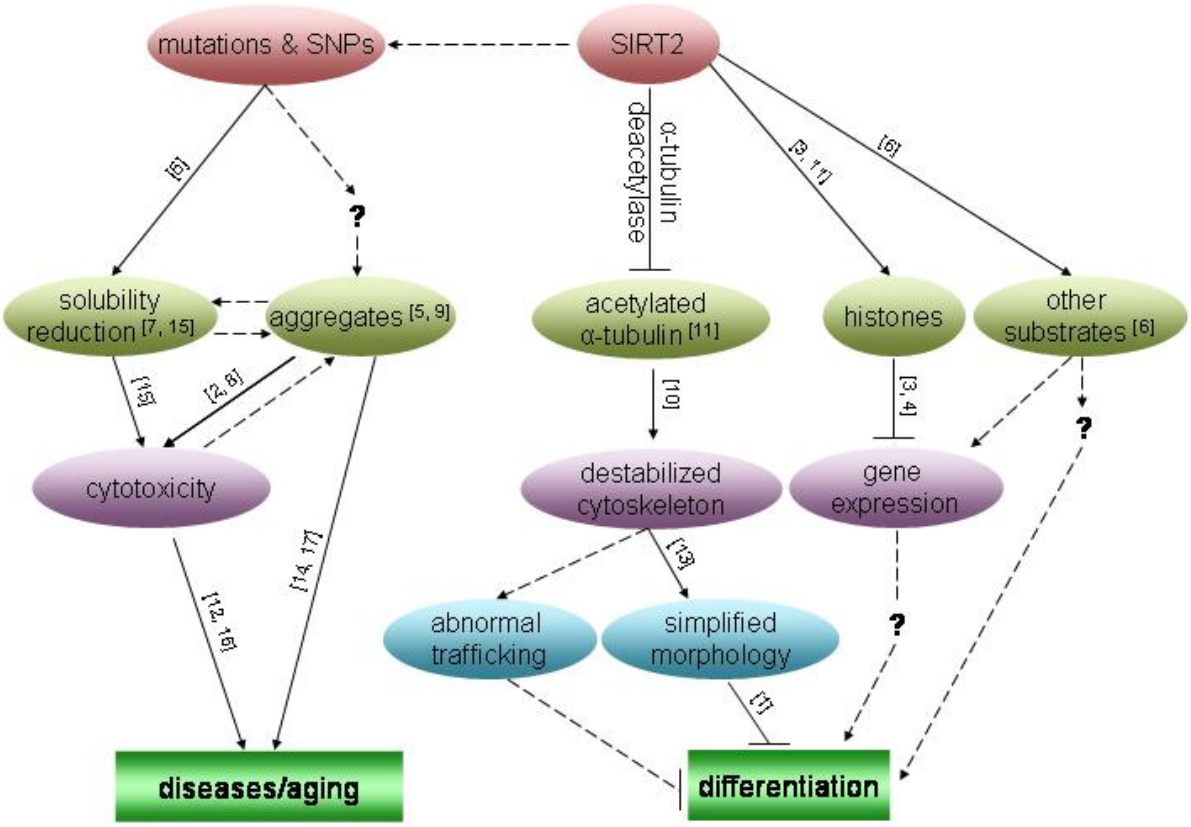

Figure 5.2 A diagram showing the functions and pathways associated with SIRT2

Solid lines represent pathways had been identified or reported by related studies. Dotted lines signify possible pathways implicated by previous studies or the current thesis. Question marks designate that the mechanisms or mediating molecules are not clear. "→" and "---|" are used to denote promotive and inhibitory pathways.

1. Baumann and Pham-Dinh, 2001
2. Bucciantini et al., 2002
3. Dryden et al., 2003
4. Gray and Ekstrom, 2001
5. Grenier et al., 2006
6. Jing et al., 2007
7. Johnson et al., 1999
8. Kristiansen et al., 2005
9. Lee and Lee, 2002
10. Matsuyama et al., 2002
11. North et al., 2003
12. Outeiro et al., 2007
13. Richter-Landsberg, 2008
14. Selkoe, 2003
15. Sriram et al., 2005
16. Suzuki and Koike, 2007
17. Taylor et al., 2002

REFERENCES

Agrawal,H.C., Randle,C.L., and Agrawal,D. (1982). In vivo acylation of rat brain myelin proteolipid protein. J. Biol. Chem. *257*, 4588-4592.

Ahlgren,S.C., Wallace,H., Bishop,J., Neophytou,C., and Raff,M.C. (1997). Effects of thyroid hormone on embryonic oligodendrocyte precursor cell development in vivo and in vitro. Mol. Cell Neurosci. *9*, 420-432.

Ahuja,N., Schwer,B., Carobbio,S., Waltregny,D., North,B.J., Castronovo,V., Maechler,P., and Verdin,E. (2007). Regulation of insulin secretion by SIRT4, a mitochondrial ADP-ribosyltransferase. J. Biol. Chem. *282*, 33583-33592.

Allfrey, V. G., Faulkner, R., and Mirsky, A.E. (1964). Acetylation and methylation of histones and their possible role in the regulation of RNA synthesis. Proc. Natl. Acad. Sci. U. S. A *51*, 786-794.

Allison,S.J., and Milner,J. (2007). SIRT3 is pro-apoptotic and participates in distinct basal apoptotic pathways. Cell Cycle *6*, 2669-2677.

Altschul,S.F., Madden,T.L., Schaffer,A.A., Zhang,J., Zhang,Z., Miller,W., and Lipman,D.J. (1997). Gapped BLAST and PSI-BLAST: a new generation of protein database search programs. Nucleic Acids Res. *25*, 3389-3402.

Anastasiou,D., and Krek,W. (2006). SIRT1: linking adaptive cellular responses to aging-associated changes in organismal physiology. Physiology. (Bethesda.) *21*, 404-410.

Anekonda,T.S. (2006). Resveratrol--a boon for treating Alzheimer's disease? Brain Res. Rev. *52*, 316-326.

Anekonda,T.S., and Reddy,P.H. (2006). Neuronal protection by Sirtuins in Alzheimer's disease. J. Neurochem. *96*, 305-313.

Anitei,M., Ifrim,M., Ewart,M.A., Cowan,A.E., Carson,J.H., Bansal,R., and Pfeiffer,S.E. (2006). A role for Sec8 in oligodendrocyte morphological differentiation. J. Cell Sci. *119*, 807-818.

Araki,T., Sasaki,Y., and Milbrandt,J. (2004). Increased nuclear NAD biosynthesis and SIRT1 activation prevent axonal degeneration. Science *305*, 1010-1013.

Ardley,H.C., Scott,G.B., Rose,S.A., Tan,N.G., Markham,A.F., and Robinson,P.A. (2003). Inhibition of proteasomal activity causes inclusion formation in neuronal and non-neuronal cells overexpressing Parkin. Mol. Biol. Cell *14*, 4541-4556.

Armstrong,R.C. (1998). Isolation and characterization of immature oligodendrocyte lineage cells. Methods *16*, 282-292.

Arnett,H.A., Fancy,S.P., Alberta,J.A., Zhao,C., Plant,S.R., Kaing,S., Raine,C.S.,

Rowitch,D.H., Franklin,R.J., and Stiles,C.D. (2004). bHLH transcription factor Olig1 is required to repair demyelinated lesions in the CNS. Science. *306*, 2111-2115.

Arroyo,E.J. and Scherer,S.S. (2000). On the molecular architecture of meylinated fibers. Histochem. Cell Biol. *113*, 1-18.

Ashburner,B.P., Westerheide,S.D., and Baldwin,A.S., Jr. (2001). The p65 (RelA) subunit of NF-kappaB interacts with the histone deacetylase (HDAC) corepressors HDAC1 and HDAC2 to negatively regulate gene expression. Mol. Cell Biol. *21*, 7065-7077.

Bae,N.S., Swanson,M.J., Vassilev,A., and Howard,B.H. (2004). Human histone deacetylase SIRT2 interacts with the homeobox transcription factor HOXA10. J. Biochem. (Tokyo) *135*, 695-700.

Baker,M., Mackenzie,I.R., Pickering-Brown,S.M., Gass,J., Rademakers,R., Lindholm,C., Snowden,J., Adamson,J., Sadovnick,A.D., Rollinson,S., Cannon,A., Dwosh,E., Neary,D., Melquist,S., Richardson,A., Dickson,D., Berger,Z., Eriksen,J., Robinson,T., Zehr,C., Dickey,C.A., Crook,R., McGowan,E., Mann,D., Boeve,B., Feldman,H., and Hutton,M. (2006). Mutations in progranulin cause tau-negative frontotemporal dementia linked to chromosome 17. Nature *442*, 916-919.

Ballas,N., Battaglioli,E., Atouf,F., Andres,M.E., Chenoweth,J., Anderson,M.E., Burger,C., Moniwa,M., Davie,J.R., Bowers,W.J., Federoff,H.J., Rose,D.W., Rosenfeld,M.G., Brehm,P., and Mandel,G. (2001). Regulation of neuronal traits by a novel transcriptional complex. Neuron *31*, 353-365.

Ballas,N., Grunseich,C., Lu,D.D., Speh,J.C., and Mandel,G. (2005). REST and its corepressors mediate plasticity of neuronal gene chromatin throughout neurogenesis. Cell *121*, 645-657.

Bardag-Gorce,F., Riley,N.E., Nan,L., Montgomery,R.O., Li,J., French,B.A., Lue,Y.H., and French,S.W. (2004). The proteasome inhibitor, PS-341, causes cytokeratin aggresome formation. Exp. Mol. Pathol. *76*, 9-16.

Barres,B.A., Lazar,M.A., and Raff,M.C. (1994). A novel role for thyroid hormone, glucocorticoids and retinoic acid in timing oligodendrocyte development. Development *120*, 1097-1108.

Barres,B.A., and Raff,M.C. (1994). Control of oligodendrocyte number in the developing rat optic nerve. Neuron *12*, 935-942.

Barry,C., Pearson,C., and Barbarese,E. (1996). Morphological organization of oligodendrocyte processes during development in culture and in vivo. Dev. Neurosci. *18*, 233-242.

Bates,G. (2003). Huntingtin aggregation and toxicity in Huntington's disease. Lancet

361, 1642-1644.

Bauer,N.G., and Richter-Landsberg,C. (2006). The dynamic instability of microtubules is required for aggresome formation in oligodendroglial cells after proteolytic stress. J. Mol. Neurosci. *29*, 153-168.

Baumann,N., and Pham-Dinh,D. (2001). Biology of Oligodendrocyte and Myelin in the Mammalian Central Nervous System. Physiol. Rev. *81*, 871-927.

Baur,J.A., Pearson,K.J., Price,N.L., Jamieson,H.A., Lerin,C., Kalra,A., Prabhu,V.V., Allard,J.S., Lopez-Lluch,G., Lewis,K., Pistell,P.J., Poosala,S., Becker,K.G., Boss,O., Gwinn,D., Wang,M., Ramaswamy,S., Fishbein,K.W., Spencer,R.G., Lakatta,E.G., Le,C.D., Shaw,R.J., Navas,P., Puigserver,P., Ingram,D.K., de,C.R., and Sinclair,D.A. (2006). Resveratrol improves health and survival of mice on a high-calorie diet. Nature *444*, 337-342.

Bence,N.F., Sampat,R.M., and Kopito,R.R. (2001). Impairment of the ubiquitin-proteasome system by protein aggregation. Science *292*, 1552-1555.

Bennett,E.J., Bence,N.F., Jayakumar,R., and Kopito,R.R. (2005). Global impairment of the ubiquitin-proteasome system by nuclear or cytoplasmic protein aggregates precedes inclusion body formation. Mol. Cell *17*, 351-365.

Benveniste,E.N., and Merrill,J.E. (1986). Stimulation of oligodendroglial proliferation and maturation by interleukin-2. Nature *321*, 610-613.

Berger,P., Niemann,A., and Suter,U. (2006). Schwann cells and the pathogenesis of inherited motor and sensory neuropathies (Charcot-Marie-Tooth disease). Glia *54*, 243-257.

Bermingham,J.R.Jr., Scherer,S.S., O'Connell,S., Arroyo,E., Kalla,K.A., Powell,F.L., and Rosenfeld,M.G. (1996). Tst-1/Oct-6/SCIP regulates a unique step in peripheral myelinatio nand is required for normal respiration. Genes Dev. *10*,1751-1762.

Berry,R.W., Quinn,B., Johnson,N., Cochran,E.J., Ghoshal,N., and Binder,L.I. (2001). Pathological glial tau accumulations in neurodegenerative disease: review and case report. Neurochem. Int. *39*, 469-479.

Bifulco,M., Laezza,C., Stingo,S., and Wolff,J. (2002). 2',3'-Cyclic nucleotide 3'-phosphodiesterase: a membrane-bound, microtubule-associated protein and membrane anchor for tubulin. Proc. Natl. Acad. Sci. U. S. A *99*, 1807-1812.

Billin,A.N., Thirlwell,H., and Ayer,D.E. (2000). Beta-catenin-histone deacetylase interactions regulate the transition of LEF1 from a transcriptional repressor to an activator. Mol. Cell Biol. *20*, 6882-6890.

Bjartmar,C., Karlsson,B., and Hildebrand,C. (1994). Cellular and extracellular

components at nodes of Ranvier in rat white matter. Brain Res. *667*, 111-114.

Blander,G., and Guarente,L. (2004). The Sir2 family of protein deacetylases. Annu. Rev. Biochem. *73*, 417-435.

Bogler,O., Wren,D., Barnett,S.C., Land,H., and Noble,M. (1990). Cooperation between two growth factors promotes extended self-renewal and inhibits differentiation of oligodendrocyte-type-2 astrocyte (O-2A) progenitor cells. Proc. Natl. Acad. Sci. U. S. A *87*, 6368-6372.

Boiko,T., and Winckler,B. (2006). Myelin under construction -- teamwork required. J. Cell Biol. *172*, 799-801.

Bone,J.R., Lavender,J., Richman,R., Palmer,M.J., Turner,B.M., and Kuroda,M.I. (1994). Acetylated histone H4 on the male X chromosome is associated with dosage compensation in Drosophila. Genes Dev. *8*, 96-104.

Borra,M.T., O'Neill,F.J., Jackson,M.D., Marshall,B., Verdin,E., Foltz,K.R., and Denu,J.M. (2002). Conserved enzymatic production and biological effect of O-acetyl-ADP-ribose by silent information regulator 2-like NAD+-dependent deacetylases. J. Biol. Chem. *277*, 12632-12641.

Braun,N. (2005). Biochemical and molecular studies of the prion protein. Dissertation, University of Zurich. pp. 69.

Brachmann,C.B., Sherman,J.M., Devine,S.E., Cameron,E.E., Pillus,L., and Boeke,J.D. (1995). The SIR2 gene family, conserved from bacteria to humans, functions in silencing, cell cycle progression, and chromosome stability. Genes Dev. *9*, 2888-2902.

Braunstein,M., Rose,A.B., Holmes,S.G., Allis,C.D., and Broach,J.R. (1993). Transcriptional silencing in yeast is associated with reduced nucleosome acetylation. Genes Dev. *7*, 592-604.

Braunstein,M., Sobel,R.E., Allis,C.D., Turner,B.M., and Broach,J.R. (1996). Efficient transcriptional silencing in Saccharomyces cerevisiae requires a heterochromatin histone acetylation pattern. Mol. Cell Biol. *16*, 4349-4356.

Brehm,A., Miska,E.A., McCance,D.J., Reid,J.L., Bannister,A.J., and Kouzarides,T. (1998). Retinoblastoma protein recruits histone deacetylase to repress transcription. Nature *391*, 597-601.

Brunet,A., Sweeney,L.B., Sturgill,J.F., Chua,K.F., Greer,P.L., Lin,Y., Tran,H., Ross,S.E., Mostoslavsky,R., Cohen,H.Y., Hu,L.S., Cheng,H.L., Jedrychowski,M.P., Gygi,S.P., Sinclair,D.A., Alt,F.W., and Greenberg,M.E. (2004). Stress-dependent regulation of FOXO transcription factors by the SIRT1 deacetylase. Science *303*, 2011-2015.

Bucciantini,M., Giannoni,E., Chiti,F., Baroni,F., Formigli,L., Zurdo,J., Taddei,N., Ramponi,G., Dobson,C.M., and Stefani,M. (2002). Inherent toxicity of aggregates implies a common mechanism for protein misfolding diseases. Nature *416*, 507-511.

Bunge,R.P. (1968). Glial cells and the central myelin sheath. Physiol Rev. *48*, 197-251.

Bunge,R.P. (1987). Tissue culture observations relevant to the study of axon-Schwann cell interactions during peripheral nerve development and repair. J. Exp. Biol. *132*, 21-34.

Bunge,R.P., Bunge,M.B., and Eldridge,C.F. (1986). Linkage between axonal ensheathment and basal lamina production by Schwann cells. Annu. Rev. Neurosci. *9*, 305-328.

Buss,A., and Schwab,M.E, (2003). Sequential loss of myelin proteins during Wallerian degeneration in the rat spinal cord. Glia. *42*,424-432.

Butt,A.M., Duncan,A., Hornby,M.F., Kirvell,S.L., Hunter,A., Levine,J.M., and Berry,M. (1999). Cells expressing the NG2 antigen contact nodes of Ranvier in adult CNS white matter. Glia. *26*,84-91.

Cai,R.L., Yan-Neale,Y., Cueto,M.A., Xu,H., and Cohen,D. (2000). HDAC1, a histone deacetylase, forms a complex with Hus1 and Rad9, two G2/M checkpoint Rad proteins. J. Biol. Chem. *275*, 27909-27916.

Canoll,P.D., Musacchio,J.M., Hardy,R., Reynolds,R., Marchionni,M.A., and Salzer,J.L. (1996). GGF/neuregulin is a neuronal signal that promotes the proliferation and survival and inhibits the differentiation of oligodendrocyte progenitors. Neuron *17*, 229-243.

Casaccia-Bonnefil,P., and Liu,A. (2003). Relationship between cell cycle molecules and onset of oligodendrocyte differentiation. J. Neurosci. Res. *72*, 1-11.

Chakraborty,G., Drivas,A., and Ledeen,R. (1999). The phosphoinositide signaling cycle in myelin requires cooperative interaction with the axon. Neurochem.Res. *24*,249-254.

Chandran,S., Svendsen,C., Compston,A., and Scolding,N. (1998). Regional potential for oligodendrocyte generation in the rodent embryonic spinal cord following exposure to EGF and FGF-2. Glia *24*, 382-389.

Chang,S., Young,B.D., Li,S., Qi,X., Richardson,J.A., and Olson,E.N. (2006). Histone deacetylase 7 maintains vascular integrity by repressing matrix metalloproteinase 10. Cell *126*, 321-334.

Chariot,A., van,L.C., Chapelier,M., Gielen,J., Merville,M.P., and Bours,V. (1999).

CBP and histone deacetylase inhibition enhance the transactivation potential of the HOXB7 homeodomain-containing protein. Oncogene *18*, 4007-4014.

Chen,Z.J., and Tian,L. (2007). Roles of dynamic and reversible histone acetylation in plant development and polyploidy. Biochim. Biophys. Acta *1769*, 295-307.

Cheng,H.L., Mostoslavsky,R., Saito,S., Manis,J.P., Gu,Y., Patel,P., Bronson,R., Appella,E., Alt,F.W., and Chua,K.F. (2003). Developmental defects and p53 hyperacetylation in Sir2 homolog (SIRT1)-deficient mice. Proc. Natl. Acad. Sci. U. S. A *100*, 10794-10799.

Chin,S.S., and Goldman,J.E. (1996). Glial inclusions in CNS degenerative diseases. J. Neuropathol. Exp. Neurol. *55*, 499-508.

Chinnadurai,G. (2002). CtBP, an unconventional transcriptional corepressor in development and oncogenesis. Mol. Cell *9*, 213-224.

Choi,C.Y., Kim,Y.H., Kwon,H.J., and Kim,Y. (1999). The homeodomain protein NK-3 recruits Groucho and a histone deacetylase complex to repress transcription. J. Biol. Chem. *274*, 33194-33197.

Chowdari,K.V., Northup,A., Pless,L., Wood,J., Joo,Y.H., Mirnics,K., Lewis,D.A., Levitt,P.R., Bacanu,S.A., and Nimgaonkar,V.L. (2007). DNA pooling: a comprehensive, multi-stage association analysis of ACSL6 and SIRT5 polymorphisms in schizophrenia. Genes Brain Behav. *6*, 229-239.

Clayton,A.L., Hazzalin,C.A., and Mahadevan,L.C. (2006). Enhanced histone acetylation and transcription: a dynamic perspective. Mol. Cell *23*, 289-296.

Clayton,A.L., Hebbes,T.R., Thorne,A.W., and Crane-Robinson,C. (1993). Histone acetylation and gene induction in human cells. FEBS Letters *336*, 23-26.

Clement,A.M., Nguyen,M.D., Roberts,E.A., Garcia,M.L., Boillee,S., Rule,M., McMahon,A.P., Doucette,W., Siwek,D., Ferrante,R.J., Brown,R.H., Jr., Julien,J.P., Goldstein,L.S., and Cleveland,D.W. (2003). Wild-type nonneuronal cells extend survival of SOD1 mutant motor neurons in ALS mice. Science *302*, 113-117.

Cohen,H.Y., Lavu,S., Bitterman,K.J., Hekking,B., Imahiyerobo,T.A., Miller,C., Frye,R., Ploegh,H., Kessler,B.M., and Sinclair,D.A. (2004). Acetylation of the C terminus of Ku70 by CBP and PCAF controls Bax-mediated apoptosis. Mol. Cell *13*, 627-638.

Corcoran,L.J., Mitchison,T.J., and Liu,Q. (2004). A novel action of histone deacetylase inhibitors in a protein aggresome disease model. Curr. Biol. *14*, 488-492.

Cunningham,J.J., and Roussel,M.F. (2001). Cyclin-dependent kinase inhibitors in the development of the central nervous system. Cell Growth Differ. *12*, 387-396.

Custer,S.K., Garden,G.A., Gill,N., Rueb,U., Libby,R.T., Schultz,C., Guyenet,S.J., Deller,T., Westrum,L.E., Sopher,B.L., and La Spada,A.R. (2006). Bergmann glia expression of polyglutamine-expanded ataxin-7 produces neurodegeneration by impairing glutamate transport. Nat. Neurosci. *9*, 1302-1311.

Davis,T., Kennedy,C., Chiew,Y.E., Clarke,C.L., and deFazio,A. (2000). Histone deacetylase inhibitors decrease proliferation and modulate cell cycle gene expression in normal mammary epithelial cells. Clin. Cancer Res. *6*, 4334-4342.

Dorus,S., Vallender,E.J., Evans,P.D., Anderson,J.R., Gilbert,S.L., Mahowald,M., Wyckoff,G.J., Malcom,C.M., and Lahn,B.T. (2004). Accelerated evolution of nervous system genes in the origin of Homo sapiens. Cell *119*, 1027-1040.

Dryden,S.C., Nahhas,F.A., Nowak,J.E., Goustin,A.S., and Tainsky,M.A. (2003). Role for human SIRT2 NAD-dependent deacetylase activity in control of mitotic exit in the cell cycle. Mol. Cell Biol. *23*, 3173-3185.

Dryja,T.P., McGee,T.L., Reichel,E., Hahn,L.B., Cowley,G.S., Yandell,D.W., Sandberg,M.A., and Berson,E.L. (1990). A point mutation of the rhodopsin gene in one form of retinitis pigmentosa. Nature *343*, 364-366.

Duan,W., and Mattson,M.P. (1999). Dietary restriction and 2-deoxyglucose administration improve behavioral outcome and reduce degeneration of dopaminergic neurons in models of Parkinson's disease. J. Neurosci. Res. *57*, 195-206.

Dugas,J.C., Ibrahim,A., and Barres,B.A. (2007). A crucial role for p57(Kip2) in the intracellular timer that controls oligodendrocyte differentiation. J. Neurosci. *27*, 6185-6196.

Edgar,J.M., McLaughlin,M., Yool,D., Zhang,S.C., Fowler,J.H., Montague,P., Barrie,J.A., McCulloh,M.C., Duncan,I.D., Garbern,J., Nave,K.A., Griffiths,I.R. (2004). Oligodendroglial modulation of fast axonal transport in a mouse model of hereditary spastic paraplegia. J. Cell. Biol. *166*, 121-131

MclEisenbarth,G.S., Walsh,F.S., and Nirenberg,M. (1979). Monoclonal antibody to a plasma membrane antigen of neurons. Proc. Natl. Acad. Sci. U. S. A *76*, 4913-4917.

Fasano,C., Campana,V., and Zurzolo,C. (2006). Prions: protein only or something more? Overview of potential prion cofactors. J. Mol. Neurosci. *29*, 195-214.

Finnin,M.S., Donigian,J.R., and Pavletich,N.P. (2001). Structure of the histone deacetylase SIRT2. Nat. Struct. Biol. *8*, 621-625.

Finzer,P., Kuntzen,C., Soto,U., zur,H.H., and Rosl,F. (2001). Inhibitors of histone deacetylase arrest cell cycle and induce apoptosis in cervical carcinoma cells circumventing human papillomavirus oncogene expression. Oncogene *20*, 4768-4776.

Folch,J., and Lees,M. (1951). Proteolipides, a new type of tissue lipoproteins; their isolation from brain. J. Biol. Chem. *191*, 807-817.

Ford,E., Voit,R., Liszt,G., Magin,C., Grummt,I., and Guarente,L. (2006). Mammalian Sir2 homolog SIRT7 is an activator of RNA polymerase I transcription. Genes Dev. *20*, 1075-1080.

Franklin,R.J. (2002). Why does remyelination fail in multiple sclerosis? Nat. Rev. Neurosci. *3*, 705-714.

Fratta,P., Engel,W.K., McFerrin,J., Davies,K.J., Lin,S.W., and Askanas,V. (2005). Proteasome inhibition and aggresome formation in sporadic inclusion-body myositis and in amyloid-beta precursor protein-overexpressing cultured human muscle fibers. Am. J. Pathol. *167*, 517-526.

Fredman,P., Magnani,J.L., Nirenberg,M., and Ginsburg,V. (1984). Monoclonal antibody A2B5 reacts with many gangliosides in neuronal tissue. Arch. Biochem. Biophys. *233*, 661-666.

Friedrich,V.L.Jr, and Mugnaini,E. (1983). Myelin sheath thickness in the CNS is regulated near the axon. Brain Res. *274*, 329-331

Frye,R.A. (1999). Characterization of five human cDNAs with homology to the yeast SIR2 gene: Sir2-like proteins (Sirtuins) metabolize NAD and may have protein ADP-ribosyltransferase activity. Biochem. Biophys. Res. Commun. *260*, 273-279.

Frye,R.A. (2000). Phylogenetic classification of prokaryotic and eukaryotic Sir2-like proteins. Biochem. Biophys. Res. Commun. *273*, 793-798.

Fuchs,J., Demidov,D., Houben,A., and Schubert,I. (2006). Chromosomal histone modification patterns--from conservation to diversity. Trends Plant Sci. *11*, 199-208.

Fujita,Y., Okamoto,K., Sakurai,A., Kusaka,H., Aizawa,H., Mihara,B., and Gonatas,N.K. (2002). The Golgi apparatus is fragmented in spinal cord motor neurons of amyotrophic lateral sclerosis with basophilic inclusions. Acta Neuropathol. (Berl) *103*, 243-247.

Fulco,M., Schiltz,R.L., Iezzi,S., King,M.T., Zhao,P., Kashiwaya,Y., Hoffman,E., Veech,R.L., and Sartorelli,V. (2003). Sir2 Regulates Skeletal Muscle Differentiation as a Potential Sensor of the Redox State. Molecular Cell *12*, 51-62.

Gao,L., Cueto,M.A., Asselbergs,F., and Atadja,P. (2002). Cloning and functional characterization of HDAC11, a novel member of the human histone deacetylase family. J. Biol. Chem. *277*, 25748-25755.

Garcia-Mata,R., Bebok,Z., Sorscher,E.J., and Sztul,E.S. (1999). Characterization and dynamics of aggresome formation by a cytosolic GFP-chimera. J. Cell Biol. *146*,

1239-1254.

Garzon-Rodriguez,W., Vega,A., Sepulveda-Becerra,M., Milton,S., Johnson,D.A., Yatsimirsky,A.K., and Glabe,C.G. (2000). A conformation change in the carboxyl terminus of Alzheimer's Abeta (1-40) accompanies the transition from dimer to fibril as revealed by fluorescence quenching analysis. J. Biol. Chem. *275*, 22645-22649.

Ghazvini,M., Mandemakers,W., Jaegle,M., Piirsoo,M., Driegen,S., Koutsourakis,M., Smit,X., Grosveld,F., and Meijer,D. (2002). A cell type-specific allele of the POU gene Oct-6 reveals Schwann cell autonomous function in nerve development and regeneration. EMBO J. *21*, 4162-4120.

Ghiani,C., and Gallo,V. (2001). Inhibition of cyclin E-cyclin-dependent kinase 2 complex formation and activity is associated with cell cycle arrest and withdrawal in oligodendrocyte progenitor cells. J. Neurosci. *21*, 1274-1282.

Ghiani,C.A., Eisen,A.M., Yuan,X., DePinho,R.A., McBain,C.J., and Gallo,V. (1999). Neurotransmitter receptor activation triggers p27(Kip1)and p21(CIP1) accumulation and G1 cell cycle arrest in oligodendrocyte progenitors. Development *126*, 1077-1090.

Ghosh,A.K., Steele,R., and Ray,R.B. (1999). MBP-1 physically associates with histone deacetylase for transcriptional repression. Biochem. Biophys. Res. Commun. *260*, 405-409.

Girault,J.A. and Peles,E. (2002). Development of nodes of Ranvier. Curr. Opin. Neurobiol. *12*, 476-485.

Goedert,M., Spillantini,M.G., and Davies,S.W. (1998). Filamentous nerve cell inclusions in neurodegenerative diseases. Curr. Opin. Neurobiol. *8*, 619-632.

Gong,Y.H., Parsadanian,A.S., Andreeva,A., Snider,W.D., and Elliott,J.L. (2000). Restricted expression of G86R Cu/Zn superoxide dismutase in astrocytes results in astrocytosis but does not cause motoneuron degeneration. J. Neurosci. *20*, 660-665.

Gosavi,N., Lee,H.J., Lee,J.S., Patel,S., and Lee,S.J. (2002). Golgi fragmentation occurs in the cells with prefibrillar alpha-synuclein aggregates and precedes the formation of fibrillar inclusion. J. Biol. Chem. *277*, 48984-48992.

Gray,S.G., and Ekstrom,T.J. (2001). The human histone deacetylase family. Exp. Cell Res. *262*, 75-83.

Grenier,C., Bissonnette,C., Volkov,L., and Roucou,X. (2006). Molecular morphology and toxicity of cytoplasmic prion protein aggregates in neuronal and non-neuronal cells. J. Neurochem. *97*, 1456-1466.

Grewal,S.I., and Elgin,S.C. (2002). Heterochromatin: new possibilities for the

inheritance of structure. Curr. Opin. Genet. Dev. *12*, 178-187.

Grubisha,O., Rafty,L.A., Takanishi,C.L., Xu,X., Tong,L., Perraud,A.L., Scharenberg,A.M., and Denu,J.M. (2006). Metabolite of SIR2 reaction modulates TRPM2 ion channel. J. Biol. Chem. *281*, 14057-14065.

Haigis,M.C., and Guarente,L.P. (2006). Mammalian Sirtuins--emerging roles in physiology, aging, and calorie restriction. Genes Dev. *20*, 2913-2921.

Haigis,M.C., Mostoslavsky,R., Haigis,K.M., Fahie,K., Christodoulou,D.C., Murphy,A.J., Valenzuela,D.M., Yancopoulos,G.D., Karow,M., Blander,G., Wolberger,C., Prolla,T.A., Weindruch,R., Alt,F.W., and Guarente,L. (2006). SIRT4 inhibits glutamate dehydrogenase and opposes the effects of calorie restriction in pancreatic beta cells. Cell *126*, 941-954.

Hall,A., Giese,N.A., and Richardson,W.D. (1996). Spinal cord oligodendrocytes develop from ventrally derived progenitor cells that express PDGF alpha-receptors. Development *122*, 4085-4094.

Hallows,W.C., Lee,S., and Denu,J.M. (2006). Sirtuins deacetylate and activate mammalian acetyl-CoA synthetases. Proc. Natl. Acad. Sci. U. S. A *103*, 10230-10235.

Hebbes,T.R., Thorne,A.W., Clayton,A.L., and Crane-Robinson,C. (1992). Histone acetylation and globin gene switching. Nucleic Acids Res. *20*, 1017-1022.

Hiratsuka,M., Inoue,T., Toda,T., Kimura,N., Shirayoshi,Y., Kamitani,H., Watanabe,T., Ohama,E., Tahimic,C.G., Kurimasa,A., and Oshimura,M. (2003). Proteomics-based identification of differentially expressed genes in human gliomas: down-regulation of SIRT2 gene. Biochem. Biophys. Res. Commun. *309*, 558-566.

Hsieh,J., Nakashima,K., Kuwabara,T., Mejia,E., and Gage,F.H. (2004). Histone deacetylase inhibition-mediated neuronal differentiation of multipotent adult neural progenitor cells. Proc. Natl. Acad. Sci. U. S. A *101*, 16659-16664.

Hu,E., Chen,Z., Fredrickson,T., Zhu,Y., Kirkpatrick,R., Zhang,G.F., Johanson,K., Sung,C.M., Liu,R., and Winkler,J. (2000). Cloning and characterization of a novel human class I histone deacetylase that functions as a transcription repressor. J. Biol. Chem. *275*, 15254-15264.

Hu,Q.D., Ang,B.T., Karsak,M., Hu,W.P., Cui,X.Y., Duka,T., Takeda,Y., Chia,W., Sankar,N., Ng,Y.K., Ling,E.A., Maciag,T., Small,D., Trifonova,R., Kopan,R., Okano,H., Nakafuku,M., Chiba,S., Hirai,H., Aster,J.C., Schachner,M., Pallen,C.J., Watanabe,K., and Xiao,Z.C. (2003). F3/contactin acts as a functional ligand for Notch during oligodendrocyte maturation. Cell *115*, 163-175.

Hubbert,C., Guardiola,A., Shao,R., Kawaguchi,Y., Ito,A., Nixon,A., Yoshida,M., Wang,X.F., and Yao,T.P. (2002). HDAC6 is a microtubule-associated deacetylase.

Nature *417*, 455-458.

Huynh,K.D., and Bardwell,V.J. (1998). The BCL-6 POZ domain and other POZ domains interact with the co-repressors N-CoR and SMRT. Oncogene *17*, 2473-2484.

Imai,S., Armstrong,C.M., Kaeberlein,M., and Guarente,L. (2000). Transcriptional silencing and longevity protein Sir2 is an NAD-dependent histone deacetylase. Nature *403*, 795-800.

Ippel,J.H., Olofsson,A., Schleucher,J., Lundgren,E., and Wijmenga,S.S. (2002). Probing solvent accessibility of amyloid fibrils by solution NMR spectroscopy. Proc. Natl. Acad. Sci. U. S. A *99*, 8648-8653.

Ito,K., Barnes,P.J., and Adcock,I.M. (2000). Glucocorticoid receptor recruitment of histone deacetylase 2 inhibits interleukin-1beta-induced histone H4 acetylation on lysines 8 and 12. Mol. Cell Biol. *20*, 6891-6903.

Iwata,A., Riley,B.E., Johnston,J.A., and Kopito,R.R. (2005). HDAC6 and microtubules are required for autophagic degradation of aggregated huntingtin. J. Biol. Chem. *280*, 40282-40292.

Jeppesen,P., and Turner,B.M. (1993). The inactive X chromosome in female mammals is distinguished by a lack of histone H4 acetylation, a cytogenetic marker for gene expression. Cell *74*, 281-289.

Jiang,S., Avraham,H.K., Park,S.Y., Kim,T.A., Bu,X., Seng,S., and Avraham,S. (2005). Process elongation of oligodendrocytes is promoted by the Kelch-related actin-binding protein Mayven. J. Neurochem. *92*, 1191-1203.

Jin,Y.H., Kim,Y.J., Kim,D.W., Baek,K.H., Kang,B.Y., Yeo,C.Y., and Lee,K.Y. (2008). Sirt2 interacts with 14-3-3 beta/gamma and down-regulates the activity of p53. Biochem. Biophys. Res. Commun. *368*, 690-695.

Jing,E., Gesta,S., and Kahn,C.R. (2007). SIRT2 Regulates Adipocyte Differentiation through FoxO1 Acetylation/Deacetylation. Cell Metab *6*, 105-114.

Johnston,J.A., Dalton,M.J., Gurney,M.E., and Kopito,R.R. (2000). Formation of high molecular weight complexes of mutant Cu, Zn-superoxide dismutase in a mouse model for familial amyotrophic lateral sclerosis. Proc. Natl. Acad. Sci. U. S. A *97*, 12571-12576.

Johnston,J.A., Illing,M.E., and Kopito,R.R. (2002). Cytoplasmic dynein/dynactin mediates the assembly of aggresomes. Cell Motil. Cytoskeleton *53*, 26-38.

Johnston,J.A., Ward,C.L., and Kopito,R.R. (1998). Aggresomes: a cellular response to misfolded proteins. J. Cell Biol. *143*, 1883-1898.

Junn,E., Lee,S.S., Suhr,U.T., and Mouradian,M.M. (2002). Parkin accumulation in aggresomes due to proteasome impairment. J. Biol. Chem. *277*, 47870-47877.

Kandel,E.R. (2001a) Nerve cells and behavior. In: Principles of Neural Science, 4th edition, edited by Kandel,E.R., Schwartz,J.H., and Jessell,T.M. New York: McGraw-Hill, pp. 19-35.

Kawaguchi,Y., Kovacs,J.J., McLaurin,A., Vance,J.M., Ito,A., and Yao,T.P. (2003). The deacetylase HDAC6 regulates aggresome formation and cell viability in response to misfolded protein stress. Cell *115*, 727-738.

Kies,M.W., Murphy, J.B., and Alvord, E.C. (1965) Fractionation of guinea-pig proteins with encephalitogenic activity (Abstract). Federation Proc. *19*, 207.

Kim,D., Nguyen,M.D., Dobbin,M.M., Fischer,A., Sananbenesi,F., Rodgers,J.T., Delalle,I., Baur,J.A., Sui,G., Armour,S.M., Puigserver,P., Sinclair,D.A., and Tsai,L.H. (2007). SIRT1 deacetylase protects against neurodegeneration in models for Alzheimer's disease and amyotrophic lateral sclerosis. EMBO J. *26*, 3169-3179.

Kim,T.Y., Bang,Y.J., and Robertson,K.D. (2006). Histone deacetylase inhibitors for cancer therapy. Epigenetics. *1*, 14-23.

Kirsh,O., Seeler,J.S., Pichler,A., Gast,A., Muller,S., Miska,E., Mathieu,M., Harel-Bellan,A., Kouzarides,T., Melchior,F., and Dejean,A. (2002). The SUMO E3 ligase RanBP2 promotes modification of the HDAC4 deacetylase. EMBO J. *21*, 2682-2691.

Kitamura,Y.I., Kitamura,T., Kruse,J.P., Raum,J.C., Stein,R., Gu,W., and Accili,D. (2005). FoxO1 protects against pancreatic beta cell failure through NeuroD and MafA induction. Cell Metab *2*, 153-163.

Knoepfler,P.S., and Eisenman,R.N. (1999). Sin meets NuRD and other tails of repression. Cell *99*, 447-450.

Komori,T. (1999). Tau-positive glial inclusions in progressive supranuclear palsy, corticobasal degeneration and Pick's disease. Brain Pathol. *9*, 663-679.

Kopito,R.R. (2000). Aggresomes, inclusion bodies and protein aggregation. Trends Cell Biol. *10*, 524-530.

Kornberg,R.D. (1977). Structure of chromatin. Annu. Rev. Biochem. *46*, 931-954.

Kristiansen, M., Messenger, M.J., Klohn, P., Brandner, S., et al. (2005). isease-related prion protein forms aggresomes in neuronal cells leading to caspase activation and apoptosis. J. Biol. Chem. *280 (46)*, 38851–38861.

Kuhlbrodt,K., Herbarth,B., Sock,E., Hermans-Borgmeyer,I., and Wegner,M. (1998).

Sox10, a novel transcriptional modulator in glial cells. J. Neurosci. *18*, 237-250.

Kuo,M.H., and Allis,C.D. (1998). Roles of histone acetyltransferases and deacetylases in gene regulation. Bioessays *20*, 615-626.

Lagace,D.C., and Nachtigal,M.W. (2004). Inhibition of histone deacetylase activity by valproic acid blocks adipogenesis. J. Biol. Chem. *279*, 18851-18860.

Lagouge,M., Argmann,C., Gerhart-Hines,Z., Meziane,H., Lerin,C., Daussin,F., Messadeq,N., Milne,J., Lambert,P., Elliott,P., Geny,B., Laakso,M., Puigserver,P., and Auwerx,J. (2006). Resveratrol improves mitochondrial function and protects against metabolic disease by activating SIRT1 and PGC-1alpha. Cell *127*, 1109-1122.

Landry,J., Sutton,A., Tafrov,S.T., Heller,R.C., Stebbins,J., Pillus,L., and Sternglanz,R. (2000). The silencing protein SIR2 and its homologs are NAD-dependent protein deacetylases. PNAS *97*, 5807-5811.

Langley,E., Pearson,M., Faretta,M., Bauer,U.M., Frye,R.A., Minucci,S., Pelicci,P.G., and Kouzarides,T. (2002). Human SIR2 deacetylates p53 and antagonizes PML/p53-induced cellular senescence. EMBO J. *21*, 2383-2396.

Lappe-Siefke,C., Goebbels,S., Gravel,M., Nicksch,E., Lee,J., Braun,P.E., Griffiths,I.R., and Nave,K.A. (2003). Disruption of Cnp1 uncouples oligodendroglial functions in axonal support and myelination. Nat. Genet. *33*, 366-374.

Lee,B., and Richards,F.M. (1971). The interpretation of protein structures: estimation of static accessibility. J. Mol. Biol. *55*, 379-400.

Lee,H.J., and Lee,S.J. (2002). Characterization of cytoplasmic alpha-synuclein aggregates. Fibril formation is tightly linked to the inclusion-forming process in cells. J. Biol. Chem. *277*, 48976-48983.

Lee,J., Gravel,M., Zhang,R., Thibault,P., and Braun,P.E. (2005). Process outgrowth in oligodendrocytes is mediated by CNP, a novel microtubule assembly myelin protein. J. Cell Biol. *170*, 661-673.

Lee,V.M., and Trojanowski,J.Q. (2006). Mechanisms of Parkinson's disease linked to pathological alpha-synuclein: new targets for drug discovery. Neuron *52*, 33-38.

Lelouard,H., Ferrand,V., Marguet,D., Bania,J., Camosseto,V., David,A., Gatti,E., and Pierre,P. (2004). Dendritic cell aggresome-like induced structures are dedicated areas for ubiquitination and storage of newly synthesized defective proteins. J. Cell Biol. *164*, 667-675.

Lelouard,H., Gatti,E., Cappello,F., Gresser,O., Camosseto,V., and Pierre,P. (2002). Transient aggregation of ubiquitinated proteins during dendritic cell maturation. Nature *417*, 177-182.

Lennerz,V., Fatho,M., Gentilini,C., Frye,R.A., Lifke,A., Ferel,D., Wolfel,C., Huber,C., and Wolfel,T. (2005). The response of autologous T cells to a human melanoma is dominated by mutated neoantigens. Proc. Natl. Acad. Sci. U. S. A *102*, 16013-16018.

Li,J., Wang,J., Wang,J., Nawaz,Z., Liu,J.M., Qin,J., and Wong,J. (2000). Both corepressor proteins SMRT and N-CoR exist in large protein complexes containing HDAC3. EMBO J. *19*, 4342-4350.

Li,W., Zhang,B., Tang,J., Cao,Q., Wu,Y., Wu,C., Guo,J., Ling,E.A., and Liang,F. (2007). Sirtuin 2, a mammalian homolog of yeast silent information regulator-2 longevity regulator, is an oligodendroglial protein that decelerates cell differentiation through deacetylating alpha-tubulin. J. Neurosci. *27*, 2606-2616.

li-Youcef,N., Lagouge,M., Froelich,S., Koehl,C., Schoonjans,K., and Auwerx,J. (2007). Sirtuins: the 'magnificent seven', function, metabolism and longevity. Ann. Med. *39*, 335-345.

Liang,F., Hatanaka,Y., Saito,H., Yamamori,T., and Hashikawa,T. (2000). Differential expression of gamma-aminobutyric acid type B receptor-1a and -1b mRNA variants in GABA and non-GABAergic neurons of the rat brain. J. Comp Neurol. *416*, 475-495.

Lin,S.J., Kaeberlein,M., Andalis,A.A., Sturtz,L.A., Defossez,P.A., Culotta,V.C., Fink,G.R., and Guarente,L. (2002). Calorie restriction extends Saccharomyces cerevisiae lifespan by increasing respiration. Nature *418*, 344-348.

Ling,E.A., Kaur,C., and Wong,W.C. (1992). Expression of major histocompatibility complex antigens and CR3 complement receptors in activated microglia following an injection of ricin into the sciatic nerve in rats. Histol. Histopathol. *7*, 93-100.

Liszt,G., Ford,E., Kurtev,M., and Guarente,L. (2005). Mouse Sir2 homolog SIRT6 is a nuclear ADP-ribosyltransferase. J. Biol. Chem. *280*, 21313-21320.

Liu,A., Muggironi,M., Marin-Husstege,M., and Casaccia-Bonnefil,P. (2003). Oligodendrocyte process outgrowth in vitro is modulated by epigenetic regulation of cytoskeletal severing proteins. Glia *44*, 264-274.

Liu,R., McAllister,C., Lyubchenko,Y., and Sierks,M.R. (2004). Proteolytic antibody light chains alter beta-amyloid aggregation and prevent cytotoxicity. Biochemistry *43*, 9999-10007.

Longo,V.D., and Kennedy,B.K. (2006). Sirtuins in aging and age-related disease. Cell *126*, 257-268.

LoPresti,P., and Konat,G.W. (2001). Hydrogen peroxide induces transient dephosphorylation of tau protein in cultured rat oligodendrocytes. Neurosci. Lett. *311*, 142-144.

LoPrestic,P., Muma,N.A., and De Vries,G.H. (2001). Neu differentiation factor regulaters tau protein and mRNA in cultured neonatal oligodendrocytes. Glia. *35*, 147-155

Lu,Q.R., Sun,T., Zhu,Z., Ma,N., Garcia,M., Stiles,C.D., and Rowitch,D.H. (2002). Common developmental requirement for Olig function indicates a motor neuron/oligodendrocyte connection. Cell *109*, 75-86.

Luo,J., Nikolaev,A.Y., Imai,S., Chen,D., Su,F., Shiloh,A., Guarente,L., and Gu,W. (2001). Negative control of p53 by Sir2alpha promotes cell survival under stress. Cell *107*, 137-148.

Lusser,A., Brosch,G., Loidl,A., Haas,H., and Loidl,P. (1997). Identification of maize histone deacetylase HD2 as an acidic nucleolar phosphoprotein. Science *277*, 88-91.

Manser,E., Huang,H.Y., Loo,T.H., Chen,X.Q., Dong,J.M., Leung,T., and Lim,L. (1997). Expression of constitutively active alpha-PAK reveals effects of the kinase on actin and focal complexes. Mol. Cell Biol. *17*, 1129-1143.

Marin-Husstege,M., Muggironi,M., Liu,A., and Casaccia-Bonnefil,P. (2002). Histone deacetylase activity is necessary for oligodendrocyte lineage progression. J. Neurosci. *22*, 10333-10345.

Matsuyama,A., Shimazu,T., Sumida,Y., Saito,A., Yoshimatsu,Y., Seigneurin-Berny,D., Osada,H., Komatsu,Y., Nishino,N., Khochbin,S., Horinouchi,S., and Yoshida,M. (2002). In vivo destabilization of dynamic microtubules by HDAC6-mediated deacetylation. EMBO J. *21*, 6820-6831.

Mattson,M.P., and Cheng,A. (2006). Neurohormetic phytochemicals: Low-dose toxins that induce adaptive neuronal stress responses. Trends Neurosci. *29*, 632-639.

Melendez-Vasquez,C.V., Einheber,S., and Salzer,J.L. (2004). Rho kinase regulates schwann cell myelination and formation of associaterd axonal domains. J. Neurosci. *24*,3953-3963.

McCarthy,K.D., and de,V.J. (1980). Preparation of separate astroglial and oligodendroglial cell cultures from rat cerebral tissue. J. Cell Biol. *85*, 890-902.

McKinnon,R.D., Matsui,T., Dubois-Dalcq,M., and Aaronson,S.A. (1990). FGF modulates the PDGF-driven pathway of oligodendrocyte development. Neuron *5*, 603-614.

McKinnon,R.D., Piras,G., Ida,J.A., Jr., and Dubois-Dalcq,M. (1993). A role for TGF-beta in oligodendrocyte differentiation. J. Cell Biol. *121*, 1397-1407.

McKinsey,T.A., Zhang,C.L., and Olson,E.N. (2001). Control of muscle development by dueling HATs and HDACs. Curr. Opin. Genet. Dev. *11*, 497-504.

McNaught,K.S., Shashidharan,P., Perl,D.P., Jenner,P., and Olanow,C.W. (2002). Aggresome-related biogenesis of Lewy bodies. Eur. J. Neurosci. *16*, 2136-2148.

Mi,S., Miller,R.H., Lee,X., Scott,M.L., Shulag-Morskaya,S., Shao,Z., Chang,J., Thill,G., Levesque,M., Zhang,M., Hession,C., Sah,D., Trapp,B., He,Z., Jung,V., McCoy,J.M., and Pepinsky,R.B. (2005). LINGO-1 negatively regulates myelination by oligodendrocytes. Nat. Neurosci. *8*, 745-751.

Michailov,G.V., Sereda,M.W., Brinkmann,B.G., Fischer,T.M., Haug,B., Birchmeier,C., Role,L., Lai,C., Schwab,M.H. and Nave,K.A. (2004). Axonal neuregulin-1 regulates myelin sheath thickness. Science. *304*, 700-703.

Milne,J.C., Lambert,P.D., Schenk,S., Carney,D.P., Smith,J.J., Gagne,D.J., Jin,L., Boss,O., Perni,R.B., Vu,C.B., Bemis,J.E., Xie,R., Disch,J.S., Ng,P.Y., Nunes,J.J., Lynch,A.V., Yang,H., Galonek,H., Israelian,K., Choy,W., Iffland,A., Lavu,S., Medvedik,O., Sinclair,D.A., Olefsky,J.M., Jirousek,M.R., Elliott,P.J., and Westphal,C.H. (2007). Small molecule activators of SIRT1 as therapeutics for the treatment of type 2 diabetes. Nature *450*, 712-716.

Montgomery,R.L., Davis,C.A., Potthoff,M.J., Haberland,M., Fielitz,J., Qi,X., Hill,J.A., Richardson,J.A., and Olson,E.N. (2007). Histone deacetylases 1 and 2 redundantly regulate cardiac morphogenesis, growth, and contractility. Genes Dev. *21*, 1790-1802.

Morell,P., Quarles,R.H., and Norton,W.T. (1994). Myelin formation, structure and biochemistry. In: Basic Neurochemistry, edited by Siegel,G.J., Agranoff, B.W., Albers, R.W., and Molinoff, P.B. New York: Raven, pp.117-143.

Mostoslavsky,R., Chua,K.F., Lombard,D.B., Pang,W.W., Fischer,M.R., Gellon,L., Liu,P., Mostoslavsky,G., Franco,S., Murphy,M.M., Mills,K.D., Patel,P., Hsu,J.T., Hong,A.L., Ford,E., Cheng,H.L., Kennedy,C., Nunez,N., Bronson,R., Frendewey,D., Auerbach,W., Valenzuela,D., Karow,M., Hottiger,M.O., Hursting,S., Barrett,J.C., Guarente,L., Mulligan,R., Demple,B., Yancopoulos,G.D., and Alt,F.W. (2006). Genomic instability and aging-like phenotype in the absence of mammalian SIRT6. Cell *124*, 315-329.

Motta,M.C., Divecha,N., Lemieux,M., Kamel,C., Chen,D., Gu,W., Bultsma,Y., McBurney,M., and Guarente,L. (2004). Mammalian SIRT1 represses forkhead transcription factors. Cell *116*, 551-563.

Moynihan,K.A., Grimm,A.A., Plueger,M.M., Bernal-Mizrachi,E., Ford,E., Cras-Meneur,C., Permutt,M.A., and Imai,S. (2005). Increased dosage of mammalian Sir2 in pancreatic beta cells enhances glucose-stimulated insulin secretion in mice. Cell Metab *2*, 105-117.

Nakamura,Y., Ogura,M., Tanaka,D., and Inagaki,N. (2008). Localization of mouse mitochondrial SIRT proteins: Shift of SIRT3 to nucleus by co-expression with SIRT5.

Biochem. Biophys. Res. Commun. *366*, 174-179.

Nawrocki,S.T., Carew,J.S., Pino,M.S., Highshaw,R.A., Andtbacka,R.H., Dunner,K., Jr., Pal,A., Bornmann,W.G., Chiao,P.J., Huang,P., Xiong,H., Abbruzzese,J.L., and McConkey,D.J. (2006). Aggresome disruption: a novel strategy to enhance bortezomib-induced apoptosis in pancreatic cancer cells. Cancer Res. *66*, 3773-3781.

Nazabal,A., Dos,R.S., Bonneu,M., Saupe,S.J., and Schmitter,J.M. (2003). Conformational transition occurring upon amyloid aggregation of the HET-s prion protein of Podospora anserina analyzed by hydrogen/deuterium exchange and mass spectrometry. Biochemistry *42*, 8852-8861.

Nishiyama,A., Lin,X.H., Giese,N., Heldin,C.H., and Stallcup,W.B. (1996). Co-localization of NG2 proteoglycan and PDGF alpha-receptor on O2A progenitor cells in the developing rat brain. J. Neurosci. Res. *43*, 299-314.

North,B.J., and Verdin,E. (2007). Interphase nucleo-cytoplasmic shuttling and localization of SIRT2 during mitosis. PLoS. ONE. *2*, e784.

North,B.J., Marshall,B.L., Borra,M.T., Denu,J.M., and Verdin,E. (2003). The Human Sir2 Ortholog, SIRT2, Is an NAD+-Dependent Tubulin Deacetylase. Molecular Cell *11*, 437-444.

Oh,L.Y., Larsen,P.H., Krekoski,C.A., Edwards,D.R., Donovan,F., Werb,Z., and Yong,V.W. (1999). Matrix metalloproteinase-9/gelatinase B is required for process outgrowth by oligodendrocytes. J. Neurosci. *19*, 8464-8475.

Onyango,P., Celic,I., McCaffery,J.M., Boeke,J.D., and Feinberg,A.P. (2002). SIRT3, a human SIR2 homologue, is an NAD-dependent deacetylase localized to mitochondria. Proc. Natl. Acad. Sci. U. S. A *99*, 13653-13658.

Osterhout,D.J., Wolven,A., Wolf,R.M., Resh,M.D., and Chao,M.V. (1999). Morphological Differentiation of Oligodendrocytes Requires Activation of Fyn Tyrosine Kinase. J. Cell Biol. *145*, 1209-1218.

Outeiro,T.F., Kontopoulos,E., Altmann,S.M., Kufareva,I., Strathearn,K.E., Amore,A.M., Volk,C.B., Maxwell,M.M., Rochet,J.C., McLean,P.J., Young,A.B., Abagyan,R., Feany,M.B., Hyman,B.T., and Kazantsev,A.G. (2007). Sirtuin 2 inhibitors rescue alpha-synuclein-mediated toxicity in models of Parkinson's disease. Science *317*, 516-519.

Park,B.L., Kim,Y.J., Cheong,H.S., Lee,S.O., Han,C.S., Yoon,J.H., Park,J.H., Chang,H.S., Park,C.S., Lee,H.S., and Shin,H.D. (2007). HDAC10 promoter polymorphism associated with development of HCC among chronic HBV patients. Biochem. Biophys. Res. Commun. *363*, 776-781.

Parker,J.A., Arango,M., Abderrahmane,S., Lambert,E., Tourette,C., Catoire,H., and

Neri,C. (2005). Resveratrol rescues mutant polyglutamine cytotoxicity in nematode and mammalian neurons. Nat. Genet. *37*, 349-350.

Patel,N.V., Gordon,M.N., Connor,K.E., Good,R.A., Engelman,R.W., Mason,J., Morgan,D.G., Morgan,T.E., and Finch,C.E. (2005). Caloric restriction attenuates Abeta-deposition in Alzheimer transgenic models. Neurobiol. Aging *26*, 995-1000.

Peinado,H., Ballestar,E., Esteller,M., and Cano,A. (2004). Snail mediates E-cadherin repression by the recruitment of the Sin3A/histone deacetylase 1 (HDAC1)/HDAC2 complex. Mol. Cell Biol. *24*, 306-319.

Peles,E. and Salzer,J.L. (2000). Molecular domains of myelinated axons. Curr. Opin. Neurobiol. *10*, 558-565.

Perrod,S., Cockell,M.M., Laroche,T., Renauld,H., Ducrest,A.L., Bonnard,C., and Gasser,S.M. (2001). A cytosolic NAD-dependent deacetylase, Hst2p, can modulate nucleolar and telomeric silencing in yeast. EMBO J. *20*, 197-209.

Pfeiffer,S.E., Warrington,A.E., and Bansal,R. (1993). The oligodendrocyte and its many cellular processes. Trends in Cell Biology *3*, 191-197.

Piperno,G., LeDizet,M., and Chang,X.J. (1987). Microtubules containing acetylated alpha-tubulin in mammalian cells in culture. J. Cell Biol. *104*, 289-302.

Poncet,C., Soula,C., Trousse,F., Kan,P., Hirsinger,E., Pourquie,O., Duprat,A.M., and Cochard,P. (1996). Induction of oligodendrocyte progenitors in the trunk neural tube by ventralizing signals: effects of notochord and floor plate grafts, and of sonic hedgehog. Mech. Dev. *60*, 13-32.

Pringle,N.P., Yu,W.P., Guthrie,S., Roelink,H., Lumsden,A., Peterson,A.C., and Richardson,W.D. (1996). Determination of neuroepithelial cell fate: induction of the oligodendrocyte lineage by ventral midline cells and sonic hedgehog. Dev. Biol. *177*, 30-42.

Qi,Y., Cai,J., Wu,Y., Wu,R., Lee,J., Fu,H., Rao,M., Sussel,L., Rubenstein,J., and Qiu,M. (2001). Control of oligodendrocyte differentiation by the Nkx2.2 homeodomain transcription factor. Development *128*, 2723-2733.

Qin,W., Yang,T., Ho,L., Zhao,Z., Wang,J., Chen,L., Zhao,W., Thiyagarajan,M., MacGrogan,D., Rodgers,J.T., Puigserver,P., Sadoshima,J., Deng,H., Pedrini,S., Gandy,S., Sauve,A.A., and Pasinetti,G.M. (2006). Neuronal SIRT1 activation as a novel mechanism underlying the prevention of Alzheimer disease amyloid neuropathology by calorie restriction. J. Biol. Chem. *281*, 21745-21754.

Quarles,R.H. (1997). Glycoproteins of myelin sheaths. J. Mol. Neurosci. *8*, 1-12.

Raff,M., Apperly,J., Kondo,T., Tokumoto,Y., and Tang,D. (2001). Timing cell-cycle

exit and differentiation in oligodendrocyte development. Novartis. Found. Symp. *237*, 100-107.

Rajan,R.S., and Kopito,R.R. (2005). Suppression of wild-type rhodopsin maturation by mutants linked to autosomal dominant retinitis pigmentosa. J. Biol. Chem. *280*, 1284-1291.

Rasband,M.N., and Trimmer,J.S. (2001). Developmental clustering of ion channels at and near the node of Ranvier. Dev. Biol. *236*, 5-16.

Rasouri,S., Lagouge,M., and Auwerx,J. (2007). [SIRT1/PGC-1: a neuroprotective axis?]. Med. Sci. (Paris) *23*, 840-844.

Refolo,L.M., Wittenberg,I.S., Friedrich,V.L., Jr., and Robakis,N.K. (1991). The Alzheimer amyloid precursor is associated with the detergent-insoluble cytoskeleton. J. Neurosci. *11*, 3888-3897.

Richter-Landsberg,C. (2001). Organization and functional roles of the cytoskeleton in oligodendrocytes. Microsc. Res. Tech. *52*, 628-636.

Richter-Landsberg,C. (2008). The cytoskeleton in oligodendrocytes. Microtubule dynamics in health and disease. J. Mol. Neurosci. *35*, 55-63.

Richter-Landsberg,C., and Heinrich,M. (1996). OLN-93: a new permanent oligodendroglia cell line derived from primary rat brain glial cultures. J. Neurosci. Res. *45*, 161-173.

Riley,N.E., Bardag-Gorce,F., Montgomery,R.O., Li,J., Lungo,W., Lue,Y.H., and French,S.W. (2003). Microtubules are required for cytokeratin aggresome (Mallory body) formation in hepatocytes: an in vitro study. Exp. Mol. Pathol. *74*, 173-179.

Rio Hortega, D.P. (1921). Histogenesis y evolucion normal; exodo y distribucion sregional de la microglia. Memor. Real. Soc. Esp. Hist. Nat. *11*, 213-268.

Robertson,K.D., it-Si-Ali,S., Yokochi,T., Wade,P.A., Jones,P.L., and Wolffe,A.P. (2000). DNMT1 forms a complex with Rb, E2F1 and HDAC1 and represses transcription from E2F-responsive promoters. Nat. Genet. *25*, 338-342.

Robinson,S., Tani,M., Strieter,R.M., Ransohoff,R.M., and Miller,R.H. (1998). The chemokine growth-regulated oncogene-alpha promotes spinal cord oligodendrocyte precursor proliferation. J. Neurosci. *18*, 10457-10463.

Robson,S.J., and Burgoyne,R.D. (1989). Differential localisation of tyrosinated, detyrosinated, and acetylated alpha-tubulins in neurites and growth cones of dorsal root ganglion neurons. Cell Motil. Cytoskeleton *12*, 273-282.

Rodgers,J.T., Lerin,C., Haas,W., Gygi,S.P., Spiegelman,B.M., and Puigserver,P.

(2005). Nutrient control of glucose homeostasis through a complex of PGC-1alpha and SIRT1. Nature *434*, 113-118.

Rundlett,S.E., Carmen,A.A., Kobayashi,R., Bavykin,S., Turner,B.M., and Grunstein,M. (1996). HDA1 and RPD3 are members of distinct yeast histone deacetylase complexes that regulate silencing and transcription. Proc. Natl. Acad. Sci. U. S. A *93*, 14503-14508.

Ryan,M.C., Shooter,E.M., and Notterpek,L. (2002). Aggresome formation in neuropathy models based on peripheral myelin protein 22 mutations. Neurobiol. Dis. *10*, 109-118.

Ryu,J.K., Lee,W.J., Lee,K.H., Hwang,J.H., Kim,Y.T., Yoon,Y.B., and Kim,C.Y. (2006). SK-7041, a new histone deacetylase inhibitor, induces G2-M cell cycle arrest and apoptosis in pancreatic cancer cell lines. Cancer Lett. *237*, 143-154.

Sahara,N., Lewis,J., DeTure,M., McGowan,E., Dickson,D.W., Hutton,M., and Yen,S.H. (2002). Assembly of tau in transgenic animals expressing P301L tau: alteration of phosphorylation and solubility. J. Neurochem. *83*, 1498-1508.

Sakurai,A., Okamoto,K., Fujita,Y., Nakazato,Y., Wakabayashi,K., Takahashi,H., and Gonatas,N.K. (2000). Fragmentation of the Golgi apparatus of the ballooned neurons in patients with corticobasal degeneration and Creutzfeldt-Jakob disease. Acta Neuropathol. (Berl) *100*, 270-274.

Salzer,J.L. (1995). Mechanisms of adhesion between axons and glial cells. In The Axon, Waxman,S., Kocsis,J., and Stys,P, eds. New York: Oxford University press, pp.164-184.

Salzer,J.L. (2003). Polarized domains of myelinated axons. Neuron. *40*, 297-318.

Sanchez,I., Hassinger,L., Paskevich,P.A., Shine,H.D., and Nixon,R.A. (1996). Oligodendroglia regulate the regional expansion of axon caliber and local accumulation of neurofilaments during development independently of myelin formation. J. Neurosci. *16*, 5095-5105.

Scher,M.B., Vaquero,A., and Reinberg,D. (2007). SirT3 is a nuclear NAD+-dependent histone deacetylase that translocates to the mitochondria upon cellular stress. Genes Dev. *21*, 920-928.

Schlierf,B., Werner,T., Glaser,G., Wegner,M.(2006). Expression of connexin47 in oligodendrocytes is regulated by the Sox10 transcription factor. J. Mol. Biol. *361*:11-21.

Schnell,R., and Rine,J. (1986). A position effect on the expression of a tRNA gene mediated by the SIR genes in Saccharomyces cerevisiae. Mol. Cell Biol. *6*, 494-501.

Schuetz,A., Min,J., Antoshenko,T., Wang,C.L., lali-Hassani,A., Dong,A., Loppnau,P., Vedadi,M., Bochkarev,A., Sternglanz,R., and Plotnikov,A.N. (2007). Structural basis of inhibition of the human NAD+-dependent deacetylase SIRT5 by suramin. Structure. *15*, 377-389.

Seeler,J.S., and Dejean,A. (1999). The PML nuclear bodies: actors or extras? Curr. Opin. Genet. Dev. *9*, 362-367.

Seigneurin-Berny,D., Verdel,A., Curtet,S., Lemercier,C., Garin,J., Rousseaux,S., and Khochbin,S. (2001). Identification of components of the murine histone deacetylase 6 complex: link between acetylation and ubiquitination signaling pathways. Mol. Cell Biol. *21*, 8035-8044.

Selkoe,D.J. (2003). Folding proteins in fatal ways. Nature *426*, 900-904.

Shahbazian,M.D., and Grunstein,M. (2007). Functions of site-specific histone acetylation and deacetylation. Annu. Rev. Biochem. *76*, 75-100.

Shen,S., Li,J., and Casaccia-Bonnefil,P. (2005). Histone modifications affect timing of oligodendrocyte progenitor differentiation in the developing rat brain. J. Cell Biol. *169*, 577-589.

Shi,T., Wang,F., Stieren,E., and Tong,Q. (2005). SIRT3, a mitochondrial Sirtuin deacetylase, regulates mitochondrial function and thermogenesis in brown adipocytes. J. Biol. Chem. *280*, 13560-13567.

Shimazu,T., Horinouchi,S., and Yoshida,M. (2007). Multiple histone deacetylases and the CREB-binding protein regulate pre-mRNA 3'-end processing. J. Biol. Chem. *282*, 4470-4478.

Shinder,G.A., Lacourse,M.C., Minotti,S., and Durham,H.D. (2001). Mutant Cu/Zn-superoxide dismutase proteins have altered solubility and interact with heat shock/stress proteins in models of amyotrophic lateral sclerosis. J. Biol. Chem. *276*, 12791-12796.

Shindler,K.S., Ventura,E., Rex,T.S., Elliott,P., and Rostami,A. (2007). SIRT1 activation confers neuroprotection in experimental optic neuritis. Invest Ophthalmol. Vis. Sci. *48*, 3602-3609.

Shogren-Knaak,M., Ishii,H., Sun,J.M., Pazin,M.J., Davie,J.R., and Peterson,C.L. (2006). Histone H4-K16 acetylation controls chromatin structure and protein interactions. Science *311*, 844-847.

Shore,D., Squire,M., and Nasmyth,K.A. (1984). Characterization of two genes required for the position-effect control of yeast mating-type genes. EMBO J. *3*, 2817-2823.

Sinclair,D.A., and Guarente,L. (1997). Extrachromosomal rDNA circles--a cause of aging in yeast. Cell *91*, 1033-1042.

Smith,J.S., and Boeke,J.D. (1997). An unusual form of transcriptional silencing in yeast ribosomal DNA. Genes Dev. *11*, 241-254.

Smith,J.S., Brachmann,C.B., Celic,I., Kenna,M.A., Muhammad,S., Starai,V.J., Avalos,J.L., Escalante-Semerena,J.C., Grubmeyer,C., Wolberger,C., and Boeke,J.D. (2000). A phylogenetically conserved NAD+-dependent protein deacetylase activity in the Sir2 protein family. Proc. Natl. Acad. Sci. U. S. A *97*, 6658-6663.

Smith,K.J., Blakemore,W.F., Murray,J.A., and Patterson,R.C. (1982). Internodal myelin volume and axon surface area: A relationship determining myelin thickness? J. Neurol. Sci. *55*, 231-246.

Sohn,J., Natale,J., Chew,L.J., Belachew,S., Cheng,Y., Aguirre,A., Lytle,J., Nait-Oumesmar,B., Kerninon,C., Kanai-Azuma,M., Kanai,Y., and Gallo,V. (2006). Identification of Sox17 as a transcription factor that regulates oligodendrocyte development. J. Neurosci. *26*, 9722-9735.

Sommer,I., and Schachner,M. (1981). Monoclonal antibodies (O1 to O4) to oligodendrocyte cell surfaces: an immunocytological study in the central nervous system. Dev. Biol. *83*, 311-327.

Southwood,C.M., Garbern,J., Jiang,W., and Gow,A. (2002). The unfolded protein response modulates disease severity in Pelizaeus-Merzbacher disease. Neuron *36*, 585-596.

Southwood,C.M., He,C., Garbern,J., Kamholz,J., Arroyo,E., and Gow,A. (2004). CNS myelin paranodes require Nkx6-2 homeoprotein transcriptional activity for normal structure. J. Neurosci. *24*, 11215-11225.

Southwood,C.M., Peppi,M., Dryden,S., Tainsky,M.A., and Gow,A. (2007). Microtubule deacetylases, SirT2 and HDAC6, in the nervous system. Neurochem. Res. *32*, 187-195.

Sprinkle,T.J. (1989). 2',3'-cyclic nucleotide 3'-phosphodiesterase, an oligodendrocyte-Schwann cell and myelin-associated enzyme of the nervous system. Crit Rev. Neurobiol. *4*, 235-301.

Sriram,S.R., Li,X., Ko,H.S., Chung,K.K., Wong,E., Lim,K.L., Dawson,V.L., and Dawson,T.M. (2005). Familial-associated mutations differentially disrupt the solubility, localization, binding and ubiquitination properties of parkin. Hum. Mol. Genet. *14*, 2571-2586.

Stolt,C.C., Rehberg,S., Ader,M., Lommes,P., Riethmacher,D., Schachner,M., Bartsch,U., Wegner,M.(2002). Terminal differentiation of myelin-forming

oligodendrocytes depends on the transcription factor Sox10.Genes Dev. *16*,165-70.

Stolt,C.C., Lommes,P., Sock,E., Chaboissier,M.C., Schedl,A., and Wegner,M. (2003). The Sox9 transcription factor determines glial fate choice in the developing spinal cord. Genes Dev. *17*, 1677-1689.

Stolt,C.C., Lommes,P., Friedrich,R.P., and Wegner,M. (2004). Transcription factors Sox8 and Sox10 perform non-equivalent roles during oligodendrocyte development despite functional redundancy. Development *131*, 2349-2358.

Stolt,C.C., Schmitt,S., Lommes,P., Sock,E., Wegner, M. (2005). Impact of transcription factor Sox8 on oligodendrocyte specification in the mouse embryonic spinal cord. Dev Biol. *15*, 309-17.

Strahl,B.D., and Allis,C.D. (2000). The language of covalent histone modifications. Nature *403*, 41-45.

Suter,U., and Scherer,S.S. (2003). Disease mechanisms in inherited neuropathies. Nat. Rev. Neurosci. *4*, 714-726.

Suzuki,K., and Koike,T. (2007). Resveratrol abolishes resistance to axonal degeneration in slow Wallerian degeneration (WldS) mice: activation of SIRT2, an NAD-dependent tubulin deacetylase. Biochem. Biophys. Res. Commun. *359*, 665-671.

Swanton,E., Holland,A., High,S., and Woodman,P. (2005). Disease-associated mutations cause premature oligomerization of myelin proteolipid protein in the endoplasmic reticulum. Proc. Natl. Acad. Sci. U. S. A *102*, 4342-4347.

Tanaka,M., Kim,Y.M., Lee,G., Junn,E., Iwatsubo,T., and Mouradian,M.M. (2004). Aggresomes formed by alpha-synuclein and synphilin-1 are cytoprotective. J. Biol. Chem. *279*, 4625-4631.

Tang,D.G., Tokumoto,Y.M., Apperly,J.A., Lloyd,A.C., and Raff,M.C. (2001). Lack of replicative senescence in cultured rat oligodendrocyte precursor cells. Science *291*, 868-871.

Tanner,K.G., Landry,J., Sternglanz,R., and Denu,J.M. (2000). Silent information regulator 2 family of NAD- dependent histone/protein deacetylases generates a unique product, 1-O-acetyl-ADP-ribose. Proc. Natl. Acad. Sci. U. S. A *97*, 14178-14182.

Tanny,J.C., Dowd,G.J., Huang,J., Hilz,H., and Moazed,D. (1999). An enzymatic activity in the yeast Sir2 protein that is essential for gene silencing. Cell *99*, 735-745.

Taunton,J., Hassig,C.A., and Schreiber,S.L. (1996). A mammalian histone deacetylase related to the yeast transcriptional regulator Rpd3p. Science *272*, 408-411.

Taylor,J.P., Hardy,J., and Fischbeck,K.H. (2002). Toxic proteins in neurodegenerative disease. Science *296*, 1991-1995.

Temple,S., and Raff,M.C. (1986). Clonal analysis of oligodendrocyte development in culture: evidence for a developmental clock that counts cell divisions. Cell *44*, 773-779.

Thompson,J.S., Ling,X., and Grunstein,M. (1994). Histone H3 amino terminus is required for telomeric and silent mating locus repression in yeast. Nature *369*, 245-247.

Timsit,S., Martinez,S., Allinquant,B., Peyron,F., Puelles,L., and Zalc,B. (1995). Oligodendrocytes originate in a restricted zone of the embryonic ventral neural tube defined by DM-20 mRNA expression. J. Neurosci. *15*, 1012-1024.

Tissenbaum,H.A., and Guarente,L. (2001). Increased dosage of a sir-2 gene extends lifespan in Caenorhabditis elegans. Nature *410*, 227-230.

Tobler,A.R., Liu,N., Mueller,L., and Shooter,E.M. (2002). Differential aggregation of the Trembler and Trembler J mutants of peripheral myelin protein 22. Proc. Natl. Acad. Sci. U. S. A *99*, 483-488.

Trousse,F., Giess,M.C., Soula,C., Ghandour,S., Duprat,A.M., and Cochard,P. (1995). Notochord and floor plate stimulate oligodendrocyte differentiation in cultures of the chick dorsal neural tube. J. Neurosci. Res. *41*, 552-560.

Turner,B.M., Birley,A.J., and Lavender,J. (1992). Histone H4 isoforms acetylated at specific lysine residues define individual chromosomes and chromatin domains in Drosophila polytene nuclei. Cell *69*, 375-384.

Uhm,J.H., Dooley,N.P., Oh,L.Y., and Yong,V.W. (1998). Oligodendrocytes utilize a matrix metalloproteinase, MMP-9, to extend processes along an astrocyte extracellular matrix. Glia *22*, 53-63.

Ursell,M.R., McLaurin,J., Wood,D.D., Ackerley,C.A., and Moscarello,M.A. (1995). Localization and partial characterization of a 60 kDa citrulline-containing transport form of myelin basic protein from MO3-13 cells and human white matter. J. Neurosci. Res. *42*, 41-53.

Umemori,H., Sato,S., Yagi,T., Aizawa,S., and Yamamoto,T. (1994). Initial events of myelination involve Fyn tyrosine kinase signaling. Nature. *367*, 572-576.

Vanrobaeys,F., Van,C.R., Dhondt,G., Devreese,B., and Van,B.J. (2005). Profiling of myelin proteins by 2D-gel electrophoresis and multidimensional liquid chromatography coupled to MALDI TOF-TOF mass spectrometry. J. Proteome. Res. *4*, 2283-2293.

Vaquero,A., Scher,M.B., Lee,D.H., Sutton,A., Cheng,H.L., Alt,F.W., Serrano,L., Sternglanz,R., and Reinberg,D. (2006). SirT2 is a histone deacetylase with preference for histone H4 Lys 16 during mitosis. Genes Dev. *20*, 1256-1261.

Vaziri,H., Dessain,S.K., Ng,E.E., Imai,S.I., Frye,R.A., Pandita,T.K., Guarente,L., and Weinberg,R.A. (2001). hSIR2(SIRT1) functions as an NAD-dependent p53 deacetylase. Cell *107*, 149-159.

Verdin,E., Dequiedt,F., and Kasler,H. (2004). HDAC7 regulates apoptosis in developing thymocytes. Novartis. Found. Symp. *259*, 115-129.

Verdin,E., Dequiedt,F., and Kasler,H.G. (2003). Class II histone deacetylases: versatile regulators. Trends Genet. *19*, 286-293.

Vidal,M., and Gaber,R.F. (1991). RPD3 encodes a second factor required to achieve maximum positive and negative transcriptional states in Saccharomyces cerevisiae. Mol. Cell Biol. *11*, 6317-6327.

Vidal,M., Strich,R., Esposito,R.E., and Gaber,R.F. (1991). RPD1 (SIN3/UME4) is required for maximal activation and repression of diverse yeast genes. Mol. Cell Biol. *11*, 6306-6316.

Voelter-Mahlknecht,S., Ho,A.D., and Mahlknecht,U. (2005). FISH-mapping and genomic organization of the NAD-dependent histone deacetylase gene, Sirtuin 2 (Sirt2). Int. J. Oncol. *27*, 1187-1196.

Wang,A.H., Kruhlak,M.J., Wu,J., Bertos,N.R., Vezmar,M., Posner,B.I., Bazett-Jones,D.P., and Yang,X.J. (2000). Regulation of histone deacetylase 4 by binding of 14-3-3 proteins. Mol. Cell Biol. *20*, 6904-6912.

Wang,F., Nguyen,M., Qin,F.X., and Tong,Q. (2007a). SIRT2 deacetylates FOXO3a in response to oxidative stress and caloric restriction. Aging Cell *6*, 505-514.

Wang,H.Y., Chien,H.C., Osada,N., Hashimoto,K., Sugano,S., Gojobori,T., Chou,C.K., Tsai,S.F., Wu,C.I., and Shen,C.K. (2007b). Rate of evolution in brain-expressed genes in humans and other primates. PLoS. Biol. *5*, e13.

Wang,J., Dickson,D.W., Trojanowski,J.Q., and Lee,V.M. (1999). The levels of soluble versus insoluble brain Abeta distinguish Alzheimer's disease from normal and pathologic aging. Exp. Neurol. *158*, 328-337.

Wang,J., Zhai,Q., Chen,Y., Lin,E., Gu,W., McBurney,M.W., and He,Z. (2005). A local mechanism mediates NAD-dependent protection of axon degeneration. J. Cell Biol. *170*, 349-355.

Ward,C.L., Omura,S., and Kopito,R.R. (1995). Degradation of CFTR by the ubiquitin-proteasome pathway. Cell *83*, 121-127.

Wegner,M. (2000). Transcriptional control in myelinating glia: the basic recipe. Glia. *29*,118-123.

Weindruch,R. (1996). The retardation of aging by caloric restriction: studies in rodents and primates. Toxicol. Pathol. *24*, 742-745.

Werner,H.B., Kuhlmann,K., Shen,S., Uecker,M., Schardt,A., Dimova,K., Orfaniotou,F., Dhaunchak,A., Brinkmann,B.G., Mobius,W., Guarente,L., Casaccia-Bonnefil,P., Jahn,O., and Nave,K.A. (2007). Proteolipid protein is required for transport of Sirtuin 2 into CNS myelin. J. Neurosci. *27*, 7717-7730.

Wilson,A.J., Byun,D.S., Popova,N., Murray,L.B., L'Italien,K., Sowa,Y., Arango,D., Velcich,A., Augenlicht,L.H., and Mariadason,J.M. (2006). Histone deacetylase 3 (HDAC3) and other class I HDACs regulate colon cell maturation and p21 expression and are deregulated in human colon cancer. J. Biol. Chem. *281*, 13548-13558.

Wiper-Bergeron,N., Wu,D., Pope,L., Schild-Poulter,C., and Hache,R.J. (2003). Stimulation of preadipocyte differentiation by steroid through targeting of an HDAC1 complex. EMBO J. *22*, 2135-2145.

Wotton,D., Lo,R.S., Lee,S., and Massague,J. (1999). A Smad transcriptional corepressor. Cell *97*, 29-39.

Yamashita,Y., Shimada,M., Harimoto,N., Rikimaru,T., Shirabe,K., Tanaka,S., and Sugimachi,K. (2003). Histone deacetylase inhibitor trichostatin A induces cell-cycle arrest/apoptosis and hepatocyte differentiation in human hepatoma cells. Int. J. Cancer *103*, 572-576.

Yang,W.M., Yao,Y.L., Sun,J.M., Davie,J.R., and Seto,E. (1997). Isolation and characterization of cDNAs corresponding to an additional member of the human histone deacetylase gene family. J. Biol. Chem. *272*, 28001-28007.

Yang,X.J. (2004). Lysine acetylation and the bromodomain: a new partnership for signaling. Bioessays *26*, 1076-1087.

Yeung,F., Hoberg,J.E., Ramsey,C.S., Keller,M.D., Jones,D.R., Frye,R.A., and Mayo,M.W. (2004). Modulation of NF-kappaB-dependent transcription and cell survival by the SIRT1 deacetylase. EMBO J. *23*, 2369-2380.

Yool,D.A., Edgar,J.M., Montague,P., and Malcolm,S. (2000). The proteolipid protein gene and myelin disorders in man and animal models. Hum. Mol. Genet. *9*, 987-992.

Youn,H.D., Grozinger,C.M., and Liu,J.O. (2000). Calcium regulates transcriptional repression of myocyte enhancer factor 2 by histone deacetylase 4. J. Biol. Chem. *275*, 22563-22567.

Zeng,L., and Zhou,M.M. (2002). Bromodomain: an acetyl-lysine binding domain.

FEBS Lett. *513*, 124-128.

Zeng,Y., Tang,C.M., Yao,Y.L., Yang,W.M., and Seto,E. (1998). Cloning and characterization of the mouse histone deacetylase-2 gene. J. Biol. Chem. *273*, 28921-28930.

Zhang,B., Cao,Q., Guo,A., Chu,H., Chan,Y.G., Buschdorf,J.P., Low,B.C., Ling,E.A., and Liang,F. (2005). Juxtanodin: An oligodendroglial protein that promotes cellular arborization and 2',3'-cyclic nucleotide-3'-phosphodiesterase trafficking. PNAS *102*, 11527-11532.

Zhang,C.L., McKinsey,T.A., and Olson,E.N. (2002). Association of class II histone deacetylases with heterochromatin protein 1: potential role for histone methylation in control of muscle differentiation. Mol. Cell Biol. *22*, 7302-7312.

Zhao,X.H., Jin,W.L., and Ju,G. (2007). An in vitro study on the involvement of LINGO-1 and Rho GTPases in Nogo-A regulated differentiation of oligodendrocyte precursor cells. Mol. Cell Neurosci. *36*, 260-269.

Zhou,Q., Choi,G., and Anderson,D.J. (2001). The bHLH transcription factor Olig2 promotes oligodendrocyte differentiation in collaboration with Nkx2.2. Neuron. *31*,791-807.

Zhou,Q., and Anderson,D.J. (2002). The bHLH transcription factors OLIG2 and OLIG1 couple neuronal and glial subtype specification. Cell *109*, 61-73.

Zhu,H., Guo,Q., and Mattson,M.P. (1999). Dietary restriction protects hippocampal neurons against the death-promoting action of a presenilin-1 mutation. Brain Res. *842*, 224-229.

Zhuang,H., Kim,Y.S., Koehler,R.C., and Dore,S. (2003). Potential mechanism by which resveratrol, a red wine constituent, protects neurons. Ann. N. Y. Acad. Sci. *993*, 276-286.